AUTOMATIC OIL PALM DETECTION AND IDENTIFICATION FROM AERIAL IMAGES USING MULTI-SCALE CLUSTERING AND NORMALIZED CROSS CORRELATION

Mr. Teerawut Wong-in

A Thesis Submitted in Partial Fulfillment of the Requirements
for the Degree of Master of Science Program in Computer Science and Information Technology
Department of Mathematics and Computer Science
Faculty of Science
Chulalongkorn University
Academic Year 2015

การตรวจหาและการระบุต้นปาล์มน้ำมันโดยอัตโนมัติจากภาพถ่ายทางอากาศด้วยเทคนิคการจัดกลุ่มที่หลากหลายเชิงมาตราส่วนและสหสัมพันธ์ไขว้ดัดแปร

นายธีรวุฒิ วงศ์อินทร์

วิทยานิพนธ์นี้เป็นส่วนหนึ่งของการศึกษาตามหลักสูตรปริญญาวิทยาศาสตรมหาบัณฑิต
สาขาวิชาวิทยาการคอมพิวเตอร์และเทคโนโลยีสารสนเทศ ภาควิชาคณิตศาสตร์และวิทยาการคอมพิวเตอร์
คณะวิทยาศาสตร์ จุฬาลงกรณ์มหาวิทยาลัย
ปีการศึกษา 2558

Thesis Title	AUTOMATIC OIL PALM DETECTION AND IDENTIFICATION FROM AERIAL IMAGES USING MULTI-SCALE CLUSTERING AND NORMALIZED CROSS CORRELATION
By	Mr. Teerawut Wong-in
Field of Study	Computer Science and Information Technology
Thesis Advisor	Associate Professor Rajalida Lipikorn, Ph.D.
Thesis Co-Advisor	Assistant Professor Tonphong Kaewkongka, Ph.D.

Accepted by the Faculty of Science, Chulalongkorn University in Partial Fulfillment of the Requirements for the Master's Degree

.....Dean of the Faculty of Science
(Associate Professor Polkit Sangvanich, Ph.D.)

THESIS COMMITTEE

.....Chairman
(Associate Professor Nagul Cooharojananone, Ph.D.)

.....Thesis Advisor
(Associate Professor Rajalida Lipikorn, Ph.D.)

.....Thesis Co-Advisor
(Assistant Professor Tonphong Kaewkongka, Ph.D.)

.....External Examiner
(Assistant Professor Gun Srijuntongsiri, Ph.D.)

ธีรวุฒิ วงศ์อินทร์ : การตรวจหาและการระบุต้นปาล์มน้ำมันโดยอัตโนมัติจากภาพถ่ายทางอากาศด้วยเทคนิคการจัดกลุ่มที่หลากหลายเชิงมาตราส่วนและสหสัมพันธ์ไขว้ดัดแปร (AUTOMATIC OIL PALM DETECTION AND IDENTIFICATION FROM AERIAL IMAGES USING MULTI-SCALE CLUSTERING AND NORMALIZED CROSS CORRELATION) อ.ที่ปรึกษาวิทยานิพนธ์หลัก: รศ. ดร.รัชลิดา ลิปิกรณ์, อ.ที่ปรึกษาวิทยานิพนธ์ร่วม: ผศ. ดร.ต้นพงศ์ แก้วคงคา, 141 หน้า.

การปลูกปาล์มน้ำมันเป็นหนึ่งในอาชีพที่สำคัญที่สุดในประเทศที่ตั้งอยู่ในแถบเอเชียตะวันออกเฉียงใต้.เนื่องจากการปลูกปาล์มน้ำมันครอบคลุมบริเวณกว้างบนพื้นที่ของสวนปาล์มน้ำมัน ซึ่งทำให้ยากต่อการนับจำนวนประชากรของปาล์มน้ำมันด้วยวิธีการนับแบบลงพื้นที่ งานวิจัยนี้จึงนำเสนอวิธีการใหม่ในการตรวจหาและระบุปาล์มน้ำมันบนพื้นที่เพาะปลูกจากภาพถ่ายทางอากาศโดยไม่คำนึงถึงขนาดของต้นปาล์มด้วยการใช้ลักษณะที่หลากหลาย เช่น รูปร่าง และ พื้นผิว วิธีการที่นำเสนอสามารถจัดการปัญหาของการระบุปาล์มน้ำมันจากภาพถ่ายทางอากาศเมื่อปาล์มน้ำมันหลาย ๆ ต้นติดกันมากซึ่งเป็นสาเหตุให้ต้นปาล์มเหล่านั้นถูกตรวจหาว่าเป็นต้นปาล์มเพียงต้นเดียว วิธีการตรวจหาและระบุปาล์มน้ำมันประกอบด้วย การกำจัดวัตถุที่ไม่ใช่ต้นปาล์มออกจากภาพ การจำแนกความแตกต่างของต้นปาล์มน้ำมันจากส่วนประกอบอื่นที่ไม่ใช่ปาล์มน้ำมัน (เช่น หญ้า วัชพืช ถนน สระ และ คลอง) การระบุปาล์มน้ำมันต้นเดี่ยว และ การนับจำนวนของปาล์มน้ำมันทั้งหมด ในงานวิจัยนี้ปาล์มน้ำมันสามารถถูกตรวจหาและถูกจำแนกความแตกต่างจากส่วนประกอบอื่นที่ไม่ใช่ต้นปาล์มด้วยการใช้การกรองความถี่ต่ำแบบบัตเตอร์เวิร์ธบนภาพโดเมนเชิงความถี่ที่อยู่ในรูปของฟูเรียร์สเปกตรัม และ การใช้วิธีจับคู่รูปภาพ หรือ วิธีสหสัมพันธ์ไขว้ดัดแปรระหว่างส่วนประกอบที่ใช่และไม่ใช่ต้นปาล์ม กับ รูปแบบของส่วนประกอบ (เช่น หนองน้ำ สระน้ำ และ พุ่มไม้) ต่อจากนั้นวิธีการจัดกลุ่มหลากหลายขนาดและวิธีการกร่อนส่วนประกอบซึ่งทำให้ส่วนประกอบมีขนาดเล็กลงและขาดออกจากกันถูกนำมาใช้ในการระบุปาล์มน้ำมันต้นเดี่ยวจากพื้นที่ ๆ ประกอบไปด้วยปาล์มน้ำมันหลาย ๆ ต้นติดกัน วิธีการการตรวจหาและระบุปาล์มน้ำมันจากภาพถ่ายทางอากาศถูกใช้ในการคำนวณจำนวนประชากรปาล์มน้ำมันบนเซตของภาพทั้งหมด 21 ภาพที่ถูกนำมาจากพื้นที่เพาะปลูกปาล์มน้ำมันจากบริเวณที่แตกต่างกันของสวนปาล์มน้ำมันซึ่งตั้งอยู่ในจังหวัดทางตอนใต้ของประเทศไทยโดยภาพทั้งหมดถูกถ่ายด้วยกล้องดิจิทัลที่ถูกผูกติดกับเครื่องบินบังคับและถูกควบคุมให้บินรอบ ๆ บริเวณของสวนปาล์ม จากผลการทดลองพบว่างานวิจัยฉบับนี้สามารถตรวจหาและระบุปาล์มน้ำมันด้วยความถูกต้องและแม่นยำ 96.34%

ภาควิชา	คณิตศาสตร์และวิทยาการคอมพิวเตอร์	ลายมือชื่อนิสิต .....
สาขาวิชา	วิทยาการคอมพิวเตอร์และเทคโนโลยีสารสนเทศ	ลายมือชื่อ อ.ที่ปรึกษาหลัก .....
		ลายมือชื่อ อ.ที่ปรึกษาร่วม .....
ปีการศึกษา	2558	

5472628823 : MAJOR COMPUTER SCIENCE AND INFORMATION TECHNOLOGY
KEYWORDS: NORMALIZED CROSS CORRELATION / MULTI-SCALE CLUSTERING / OIL PALM IDENTIFICATION / TEMPLATE MATCHING

TEERAWUT WONG-IN: AUTOMATIC OIL PALM DETECTION AND IDENTIFICATION FROM AERIAL IMAGES USING MULTI-SCALE CLUSTERING AND NORMALIZED CROSS CORRELATION. ADVISOR: ASSOC. PROF.RAJALIDA LIPIKORN, Ph.D., CO-ADVISOR: ASST. PROF.TONPHONG KAEWKONGKA, Ph.D., 141 pp.

Oil palm cultivation is one of the most important occupation in South East Asia. Since oil palm plantation covers the wide range of areas, it is very difficult to count the numbers of oil palms manually. This thesis presents the new methods to detect and identify an individual of oil palms in plantation areas from aerial images regardless of their sizes using features including shape and texture. The proposed methods can handle the problem of oil palm identification from aerial image when oil palms are too close to each other such that they are identified as single oil palm. The processes of oil pam detection and identification consist of non-oil palm components and noise filtering, distinguishing oil palms from non-oil palm components (e.g., grass, weed, road, pond or swamp), identifying individual oil palms and counting the numbers of oil palms. In this thesis, oil palms can be detected and distinguished from non-oil palm components by using Butterworth low-pass filter on Fourier spectrum in frequency domain and template matching based on normalized cross correlation. Then the multi-scale clustering method is used to separate the oil palm stand into individual oil palms. The proposed method is used to estimate the population of oil palms on a set of 21 aerial images. All the aerial images were captured by mounting a digital camera on the model airplane that was controlled to fly over the plantation areas. Each image was taken from different view and location. The experimental results show that the proposed methods can detect and identify oil palms correctly with the recognition rate at 96.34%

Department:	Mathematics and Computer Science	Student's Signature .....
		Advisor's Signature .....
Field of Study:	Computer Science and Information Technology	Co-Advisor's Signature .....
Academic Year:	2015	

ACKNOWLEDGEMENTS

I would like to thank my thesis advisor, Associate Professor Dr. Rajalida Lipikorn, who supports and helps me in numerous ways with her guidance and encouragement throughout the development of my thesis. She gives me many useful suggestions and helps me go through the problems by asking me questions that lead me to discover the methodology for solving the problems. She spends time to proofread and edit the thesis before publishing. I feel honor having a chance to work with her and learn from her for 4 years and I will always keep all I have learnt from her. I also want to thank Assistant Professor Dr. Tonphong Kaewkongka from department of Physics, who provides me aerial images of oil palm plantation that I use in the experiments and gives me very helpful suggestions. He was the one who controlled the model airplane to fly over the plantation areas.

Finally, I would like to thank my family for their support especially my mom and dad who have supported me throughout my education.

CONTENTS

Page

THAI ABSTRACT iv

ENGLISH ABSTRACT v

ACKNOWLEDGEMENTS vi

CONTENTS vii

LIST OF TABLES 9

LIST OF FIGURES 10

CHAPTER I Introduction 18

1.1 Objectives 23

1.2 Scope of the work 24

1.3 Problem Formulation 24

1.4 Expected Outcomes 25

CHAPTER II Related Work and Theoretical Background 26

2.1 Related work 26

2.2 Background 29

2.3 Gaussian filter and Butterworth low-pass filter 30

2.3.1 Gaussian filter in spatial domain 31

2.3.2 Fourier transform 33

2.3.3 Butterworth low-pass filter 34

2.4 Adaptive local thresholding method 38

2.5 Connected component labeling 39

2.6 Erosion 43

2.7 Normalized cross correlation for template matching 48

Page

Chapter III Proposed Method and Implementation 53
3.1 Preprocessing 54
3.2 Non-oil palm and noise filtering 56
3.2.1 Elevation Determination 58
3.2.2 Filtering in Frequency Domain 60
3.3 Oil palm detection 64
3.4 Individual oil palm identification 80
Chapter IV Experimental Results and Discussion 90
Chapter V Conclusion 113
REFERENCES 116
APPENDIX 118
VITA 141

LIST OF TABLES

Table 1: the median sizes of oil palms obtained from 21 aerial images 90

Table 2: The results for oil palm detection and identification using multi-scale clustering 108

LIST OF FIGURES

Figure 1 (a) a cluster of oil palm fruit and (b) oil palm fruit 19

Figure 2 The planting pattern 20

Figure 3 Aerial image of oil palm planting 20

Figure 4 An aerial image of plantations from low elevation 21

Figure 5 An aerial image of plantations from high elevation 22

Figure 6 An aerial image of plantations including 3 – 4 years 23

Figure 7 There are oil palms and non-oil palm components, such as pond, ... 23

Figure 8 24-bit color image of oil palms on the left and zoomed image 29

Figure 9 8-bit gray scale image on the left and zoomed image 30

Figure 10 An example of a convolution process with a kernel of size 3 x 3 31

Figure 11 2D Gaussian distribution with mean (0, 0) and σ =1 32

Figure 12 The effect of smoothing with various filter sizes and σ 32

Figure 13 Butterworth low-pass filter, High frequencies correspond to abrupt changed regions (edges) whereas low frequencies correspond to slow change regions (smooth regions) 35

Figure 14 The perspective plot of a Butterworth low-pass filter 35

Figure 15 Filter radial cross sections of orders 1 through 4 36

Figure 16 The images after applying Butterworth low-pass filter to Figure 8 with n=3 37

Figure 17 Binary image of an aerial image that was captured from far distance 39

Figure 18 Binary image of an aerial image that was captured from near distance 39

Figure 19 A graph with six vertices or nodes and seven edges 40

Figure 20 A graph with three connected components 40

Figure 21 4 –connected connectivity 41

Figure 22 8 – connected connectivity 41

Figure 23 The result of connected component labeling performed on the 42

Figure 24 The result of connected component labeling performed on the 42

Figure 25 5 x 5 square structuring element 43

Figure 26 5 x 5 diamond-shaped structuring element 43

Figure 27 5 x 5 cross-shaped structuring element 44

Figure 28 Probing an image with three structuring elements 44

Figure 29 Original image and binary image 45

Figure 30 Result from using 5 x 5 square structuring element 46

Figure 31 Result from using 5 x 5 diamond-shaped structuring element 46

Figure 32 Result from using 5 x 5 cross-shaped structuring element 46

Figure 33 Original image and binary image 47

Figure 34 Result from using 5 x 5 square structuring element 47

Figure 35 Result from using 5 x 5 diamond-shaped structuring element 48

Figure 36 Result from using 5 x 5 cross-shaped structuring element 48

Figure 37 The process of template matching using cross correlation to find the region in an image I that matches a template t which pictures (a) – (e) has the 3 × 3 template that placed over a region of an image and (f) is the final result 50

Figure 38 An example of template matching by cross correlation 52

Figure 39 The best match region after performing template matching using 52

Figure 40 The process of oil palm detection and identification 53

Figure 41 The operation of image pre-processing 54

Figure 42 (a) the original image, (b) the gray scale image of (a), (c)-(e) the histograms of red, green, and blue channels, respectively, (f) the histogram of a gray scale image 55

Figure 43 (a) the result image from histogram equalization and (b) the histogram of the equalized image 56

Figure 44 The operation of non-oil palm and noise filtering 57

Figure 45 The aerial image including all individual oil palms (green) and 59

Figure 46 The aerial image including all individual oil palms (green) and 59

Figure 47 Original aerial image 61

Figure 48 The output of equalized image 61

Figure 49 The output of Fourier spectrum image 62

Figure 50 The Butterworth low pass filter 62

Figure 51 The result of Fourier spectrum image after filtering 63

Figure 52 The final output of filtered image on spatial domain 63

Figure 53 The result of detected oil palms from filtered image 63

Figure 54 The result of detected oil palms from enhanced image 64

Figure 55 The operation of oil palm detection 65

Figure 56 Examples of aerial images from different view 66

Figure 57 The results of binary images after applying adaptive local thresholding method on images in Figures 56 (a) – (d) 67

Figure 58 The detection results from using the proposed oil palm detection method on a set of binary images in Figures 57 (a)-(d) 68

Figure 59 An example of mask with 8-connected connectivity 69

Figure 60 An example of a binary image containing foreground and 70

Figure 61 (a) all pixels under the mask of current pixel at (x, y) of the second and the sixth columns in the first row have intensities equal to 0. Then, those pixels are labeled by the new number, e.g., 2 and 3 as the output image shown in (b) 72

Figure 62 (a) the current pixel at (x, y) in the second row of the first column contains some pixels under the mask whose intensities are not equal to 0, so that pixel is labeled by the same number as its neighbor pixel, e.g., 2 as shown in Figure (b) 73

Figure 63 The process of first scanning is repeated until all the first pixels are scanned 74

Figure 64 During the second scanning, if there are different labeling numbers of the pixels under the mask, they should belong to the same component as shown in picture (b) 75

Figure 65 There are two different labeling numbers in the same component 75

Figure 66 The result of the second scanning of two-scan algorithm 76

Figure 67 The result images from 8-neighbor connected component labeling using the two-scan algorithm on binary images in Figures 57 (a) – (d) 76

Figure 68 Some components of non-oil palm have been detected during the process of oil palm detection, such as pond, swamp, thick grass and weed. These components are marked by red color 78

Figure 69 the results of removing the components of none oil palm from an image in Figures 68 (a) – (d) 79

Figure 70 The process of individual oil palm identification 80

Figure 71 The results from applying K-means clustering to separate oil palms into three clusters of small trees (green), big trees (yellow), and tree stands (red) 81

Figure 72 An example of tree stands obtained from Figure 71 (a) 83

Figure 73 The process of erosion and identification in multi-scale clustering from Figure 72(a)..... 84

Figure 74 K-means clustering result of an aerial image 85

Figure 75 Example of tree stands obtained from K-means clustering and its regions obtained from a binary image, f 85

Figure 76 The process of erosion and identification in multi-scale clustering from Figure 75(a)..... 87

Figure 77 The result of multi-scale clustering from Figure 74 87

Figure 78 The results of multi-scale clustering from Figures 71 (a)-(d) 89

Figure 79 The far-distance aerial image with median-size oil palm 92

Figure 80 The far-distance aerial image with median-size oil palm 92

Figure 81 The far-distance aerial image with median-size oil palm 92

Figure 82 The far-distance aerial image with median-size oil palm 93

Figure 83 The far-distance aerial image with median-size oil palm 93

Figure 84 The far-distance aerial image with median-size oil palm 93

Figure 85 The far-distance aerial image with median-size oil palm 94

Figure 86 The far-distance aerial image with median-size oil palm 94

Figure 87 The far-distance aerial image with median-size oil palm 94

Figure 88 The far-distance aerial image with median-size oil palm 95

Figure 89 The far-distance aerial image with median-size oil palm 95

Figure 90 The far-distance aerial image with median-size oil palm 95

Figure 91 The far-distance aerial image with median-size oil palm..... 96

Figure 92 The far-distance aerial image with median-size oil palm..... 96

Figure 93 The far-distance aerial image with median-size oil palm..... 96

Figure 94 The far-distance aerial image with median-size oil palm..... 97

Figure 95 The near-distance aerial image with median-size oil palm..... 97

Figure 96 The near-distance aerial image with median-size oil palm..... 97

Figure 97 The near-distance aerial image with median-size oil palm..... 98

Figure 98 The near-distance aerial image with median-size oil palm..... 98

Figure 99 The near-distance aerial image with median-size oil palm..... 98

Figure 100 The appearance of all kinds of components in plantation areas..... 99

Figure 101 The results from oil palm identification: (a) the result of using K means clustering to classify small tree, big tree and tree stands; (b) enlarged region where false detection occurs from non-removable non-oil palm components..... 101

Figure 102 The results from oil palm identification: (a) the result of using K means clustering to classify small tree, big tree and tree stands; (b) enlarged region where false detection occurs from non-removable non-oil palm components..... 101

Figure 103 The results from oil palm identification: (a) the result of using K means clustering to classify small tree, big tree and tree stands; (b) enlarged region where false detection occurs from non-removable non-oil palm components..... 102

Figure 104 The results from oil palm identification: (a) the result of using K means clustering to classify small tree, big tree and tree stands; (b) enlarged region where false detection occurs from non-removable non-oil palm components..... 102

Figure 105 The results from oil palm identification: (a) the result of using K means clustering to classify small tree, big tree and tree stands; (b) enlarged region where false detection occurs from non-removable non-oil palm component**s**..... 103

Figure 106 (a) The result from using multi-scale clustering to separate individual oil palms from tree stands..... 103

Figure 107 (a) The result from using multi-scale clustering to separate individual oil palms from tree stands..... 104

Figure 108 (a) The result from using multi-scale clustering to separate individual oil palms from tree stands 104

Figure 109 (a) The result from using multi-scale clustering to separate individual oil palms from tree stands 105

Figure 110 (a) The result from using multi-scale clustering to separate individual oil palms from tree stands 105

Figure 111 Manually counted oil palms: (a) counted oil palms and 106

Figure 112 An example of false detection from K-means clustering 109

Figure 113 An example of false identification from multi-scale clustering 109

Figure 114 Examples of multi-scale clustering results of tree stands from Figure 113 (blue circle) 112

Figure 115 (a) original aerial image and (b) the result from applying K-means clustering 120

Figure 116 The result of multi-scale clustering from Figure 115 (b) including 272 small trees, 285 big trees, and 74 tree stands consist of 330 individual oil palms 120

Figure 117 (a) original aerial image and (b) the result from applying K-means clustering 122

Figure 118 The result of multi-scale clustering from Figure 117 (b) including 403 small trees, 302 big trees, and 113 tree stands consist of 468 individual oil palms 122

Figure 119 (a) original aerial image and (b) the result from applying K-means clustering 123

Figure 120 The result of multi-scale clustering from Figure 119 (b) including 428 small trees, 414 big trees, and 91 tree stands consist of 314 individual oil palms 123

Figure 121 (a) original aerial image and (b) the result from applying K-means clustering 124

Figure 122 The result of multi-scale clustering from Figure 121 (b) including 241 small trees, 224 big trees, and 63 tree stands consist of 228 individual oil palms 124

Figure 123 (a) original aerial image and (b) the result from applying K-means clustering 125

Figure 124 The result of multi-scale clustering from Figure 123 (b) including 382 small trees, 443 big trees, and 91 tree stands consist of 285 individual oil palms 125

Figure 125 (a) original aerial image and (b) the result from applying K-means clustering 126

Figure 126 The result of multi-scale clustering from Figure 125 (b) including 373 small trees, 402 big trees, and 71 tree stands consist of 241 individual oil palms 126

Figure 127 (a) original aerial image and (b) the result from applying K-means clustering..... 127

Figure 128 The result of multi-scale clustering from Figure 127 (b) including 328 small trees, 302 big trees, and 79 tree stands consist of 352 individual oil palms..... 127

Figure 129 (a) original aerial image and (b) the result from applying K-means clustering..... 128

Figure 130 The result of multi-scale clustering from Figure 129 (b) including 322 small trees, 308 big trees, and 81 tree stands consist of 243 individual oil palms..... 128

Figure 131 (a) original aerial image and (b) the result from applying K-means clustering..... 129

Figure 132 The result of multi-scale clustering from Figure 131 (b) including 335 small trees, 313 big trees, and 66 tree stands consist of 213 individual oil palms..... 129

Figure 133 (a) original aerial image and (b) the result from applying K-means clustering..... 130

Figure 134 The result of multi-scale clustering from Figure 133 (b) including 313 small trees, 287 big trees, and 84 tree stands consist of 235 individual oil palms..... 130

Figure 135 (a) original aerial image and (b) the result from applying K-means clustering..... 131

Figure 136 The result of multi-scale clustering from Figure 135 (b) including 525 small trees, 413 big trees, and 117 tree stands consist of 476 individual oil palms..... 131

Figure 137 (a) original aerial image and (b) the result from applying K-means clustering..... 132

Figure 138 The result of multi-scale clustering from Figure 135 (b) including 358 small trees, 455 big trees, and 97 tree stands consist of 428 individual oil palms..... 132

Figure 139 (a) original aerial image and (b) the result from applying K-means clustering..... 133

Figure 140 The result of multi-scale clustering from Figure 139 (b) including 307 small trees, 224 big trees, and 84 tree stands consist of 222 individual oil palms..... 133

Figure 141 (a) original aerial image and (b) the result from applying K-means clustering..... 134

Figure 142 The result of multi-scale clustering from Figure 141 (b) including 498 small trees, 21 big trees, and 66 tree stands consist of 277 individual oil palms..... 134

Figure 143 (a) original aerial image and (b) the result from applying K-means clustering..... 135

Figure 144 The result of multi-scale clustering from Figure 143 (b) including 550 small trees, 14 big trees, and 80 tree stands consist of 362 individual oil palms..... 135

Figure 145 (a) original aerial image and (b) the result from applying K-means clustering..... 136

Figure 146 The result of multi-scale clustering from Figure 145 (b) including 344 small trees, 314 big trees, and 90 tree stands consist of 397 individual oil palms 136

Figure 147 (a) original aerial image and (b) the result from applying K-means clustering..... 137

Figure 148 The result of multi-scale clustering from Figure 147 (b) including 354 small trees, 313 big trees, and 97 tree stands consist of 379 individual oil palms 137

Figure 149 (a) original aerial image and (b) the result from applying K-means clustering..... 138

Figure 150 The result of multi-scale clustering from Figure 149 (b) including 281 small trees, 227 big trees, and 75 tree stands consist of 271 individual oil palms 138

Figure 151 (a) original aerial image and (b) the result from applying K-means clustering..... 139

Figure 152 The result of multi-scale clustering from Figure 151 (b) including 133 small trees, 294 big trees, and 30 tree stands consist of 167 individual oil palms 139

Figure 153 (a) original aerial image and (b) the result from applying K-means clustering..... 140

Figure 154 The result of multi-scale clustering from Figure 153 (b) including 132 small trees, 227 big trees, and 36 tree stands consist of 97 individual oil palms 140

CHAPTER I

Introduction

Oil palms are economic plants that are cultivated in tropical regions of West Africa, South America, and Asia. They grow well and give lots of product in regions where the weather is hot and humid with the conditions of well drained, deep fertile loamy to loam clay soil.

An oil palm is a plant with semisperical shape that has only trunk and leaves without any branches. Its trunk is the stem of the palm, at the tip of the stem there is one bud that is the growing point. The growing point of an adult oil palm produces 20 – 25 leaves every year. An oil palm yields the first harvest after it has been planted for 3 – 4 years. Once an oil palm has begun to bear fruits (as shown in Figure 1), the fruits must be harvest at the right moment, otherwise they become too rip and many clusters will fall, which cause the quality of fruits to decline.

A spacing and method of planting for oil palms is commonly done in triangular form with 9 meters between trees to achieve a plant density of approximately 100 – 150 trees per hectare as shown in Figure 2. It is recommended that 143 oil palms per hectare is the best density but many plantations may plant at more or less density. The planting density is very important to ensure that oil palms have sufficient space to grow and to receive adequate sunlight.

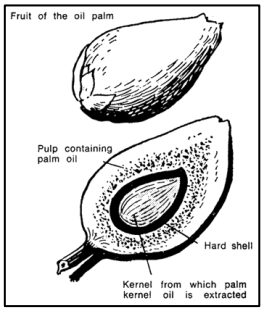

(a) (b)

Figure 1 (a) a cluster of oil palm fruit and (b) oil palm fruit

Palm oil is vegetable oil derived from the oil palms, which was left in the pulp and kernels. It has become a raw material in many products such as cooking oil, margarine, oil for the cosmetic industry and production of bio diesel. It has become the world's leading vegetable oil concern and is needed in great demand. This situation leads farmers to turn to cultivate oil palm. From the past decades, the number of oil palm plantations has been increased tremendously which results in supply over demand. Moreover, the planting areas have been spread all over the country, thus it is difficult to explore the population of oil palms.

In Thailand, most of oil palm plantations are located in the southern provinces of Thailand, where the farmers cultivate oil palms on small to medium size farms while the large oil palm plantations are normally owned by companies.

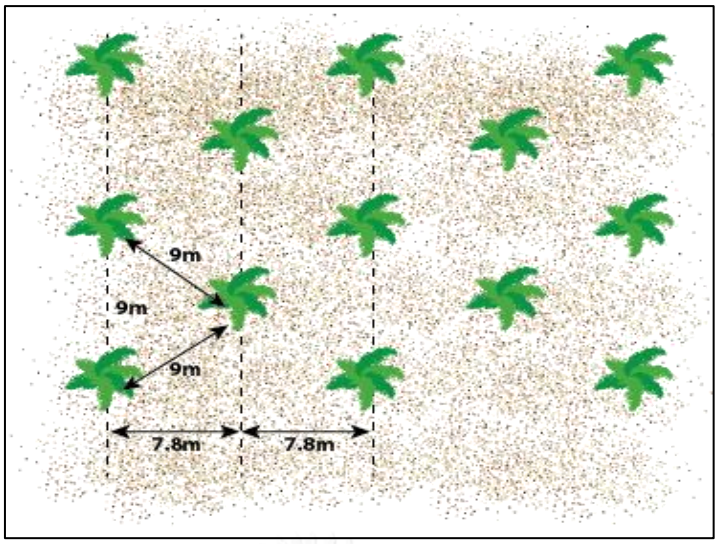

Figure 2 The planting pattern

Figure 3 Aerial image of oil palm planting

The maintenance capability of young oil palms is essential in order to achieve a great number of crop yield. For the plantation management system, farmers try to ensure that the area surrounding each young oil palm is free from any vegetation that may compete with the oil palms for fertilizer, water and sunlight. An exploration of oil palm population in planting area is valuable information that can be used to estimate total numbers of oil palms and to observe the growth rate. It can be very helpful in forecasting of supply and demand.

However, the planting areas for oil palm are spread all over and some areas are located in the rainforest that is difficult to be explored. Thus, we propose a method to detect and identify oil palms from aerial imagery using special features of oil palms and the planting pattern. The images are photographed in top-down view by a digital camera that is mounted on the remote-control airplane as shown in Figure 3. The airplane is controlled to fly over the planting areas from the ground. However, the elevation of the airplane is not constant, thus some images are taken from near distance as shown in Figure 4 and some images are taken from far distance as shown in Figure 5.

Figure 4 An aerial image of plantations from low elevation

Figure 5 An aerial image of plantations from high elevation

In this paper, we are interested in the planting areas that are located in the southern part of Thailand where the plantations cover large area and are difficult to explore on foot. Even though the cultivation of oil palms has a standard pattern of planting as mentioned above, the growth rate of each oil palm is different and there might be other trees and weeds that grow unexpectedly.

Figure 6 shows the image that contains only oil palms while Figure 7 shows the image that contains oil palm and non-oil palm components, such as other trees, weed, shrubs, pond, swamp, footpath, and road. In order to estimate the population of oil palms from aerial images, we have to first remove all non-oil palm components from the image. Then we need to filter all the noise and finally we have to detect and count the number of oil palms. However, there is one more problem that must be handled before we can count the number of oil palms. The problem occurs when an image contains one or more stands of oil palms. A stand of oil palm refers to a group of oil palms that are very close to each other such that we see them as a single oil palm from an aerial image as shown in Figure 6. Thus, we need to separate them into individual oil palms before we can count them.

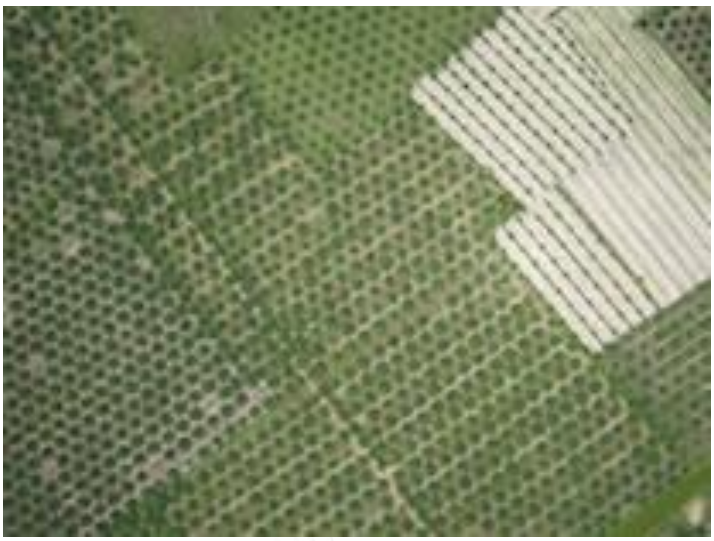

Figure 6 An aerial image of plantations including 3 – 4 years

Figure 7 There are oil palms and non-oil palm components, such as pond, road, shrub, thick grass and weed

1.1 Objectives

To develop an algorithm that can remove all non-oil palm components, then detect and identify oil palms from an aerial image in order to estimate the population of oil palms per hectare in planting areas.

1.2 Scope of the work

In this study, the oil palm detection and identification algorithm is constrained as follows:

1. An exploration of the oil palm population in planting areas is applied to estimate the total number of oil palms and the growth rate.
2. An aerial image of oil palms must be captured in top-down view by digital camera that is mounted on the airplane and is controlled to fly over planting area in the Southern part of Thailand.
3. The elevation of the airplane should be in the range that oil palms must be countable by human eyes.
4. The proposed method accepts color aerial images with .jpg format.
5. The size of each color image should be no larger than 912 x 684 pixels.
6. There are two types of aerial images: near-distance and far-distance images where most of the regions in each image contain 80 – 99% oil palms.
7. The algorithm can determine near- or far-distance image automatically.
8. Oil palm plantation may include oil palms of various sizes.
9. The algorithm can distinguish oil palms from non-oil palm components.
10. Oil palms should be 3-4 years old or big enough and have many leaves.
11. The algorithm can separate individual oil palms from oil palm stands.

1.3 Problem Formulation

It is not that easy to detect and identify oil palms from aerial images because there are many problems that have to be solved. First, the remote-control airplane does not fly at the constant level above the ground, thus the sizes of oil palms will be different. Second, different plantations start cultivating oil palms at different period of time; therefore, the sizes of oil palms from different plantations will be different. Third, there are non-oil palm components included in aerial images. The non-oil palm components are, for example, road, swamp, pond, grass, and other

kinds of trees. Thus we need to distinguish these objects from oil palms and remove them from aerial images. These are the processes that our proposed algorithm needs to handle before oil palms can be detected. Once, we can identify and remove all non-oil palm components, then the last step is to estimate the oil palm population by counting the number of oil palms from each image. However, some oil palms are very close to each other such that they form a single stand. Therefore, our proposed algorithm needs to separate them into individual trees before they can be counted.

1.4 Expected Outcomes

- Non-oil palm components in the plantation can be distinguished from oil palms.
- The proposed method can detect and identify individual oil palms with 90 – 95% accuracy from aerial images that contain only oil palms.
- The proposed method can detect and identify individual oil palms with 80 – 90% accuracy from aerial images that contain oil palms and non-oil palm components such as other trees, road, swamp, and weed.
- The proposed method should be able to estimate the oil palm population accurately.

CHAPTER II

Related Work and Theoretical Background

This chapter discusses about related work including existing techniques used in object detection and identification for all types of images which are studied during the time of doing the research. Preliminary knowledge and theoretical background of all techniques related to tree detection and identification, which have been used in this thesis, are described in detail.

2.1 Related work

From the past decades, several methods on tree detection have been proposed in the literatures. [1] proposed a scalable approach to tree detection based on segmentation followed by classification in large urban and landscape using aerial LiDAR data by projecting 3D point cloud onto a 2.5D depth image with fixed-size pixels in the $(\mathbf{x}, \mathbf{y})$ plane. LiDAR points are used to compute the average, $\mathbf{z_{mean}}$, and maximum height, $\mathbf{z_{max}}$, in order to form 2.5D depth images. The edges were detected by applying Robert cross gradient operator. They performed two separate segmentations on the maximum height and the edges. This technique is similar to [2]. The results are under segmentation and over-segmentation. For example, buildings and trees are fragmented into many segments which can be classified into groups of trees and non-trees by using statistical machine learning technique. In order to apply this approach to large regions, they used the seed-based region growing segmentation and merged segments that are smaller than a pre-specified threshold with neighboring segments. Their precision and recall rates are over 95%. Their tree detection did not use color imagery or colored LiDAR returns or image intensity. This proposed method works well on urban regions with a few tree, there is substantial performance degradation in suburban regions with a large number of trees.

Luciana Satiko, et al. [3] identified individual palm trees using high spatial resolution images from videography that were recorded by remote sensors on board of airplanes and controlled to fly over the Brazilian amazon rainforest. The image data acquired from sensor systems of high spatial resolution can provide more information about the structure of large areas of rainforest. Techniques of image segmentation and classification were used to identify individual crown of palm trees. Region growing segmentation and three classification methods were applied to test the classification of videography images with two different image contrasts. As the segmentation results, region-growing segmentation is effective to separate some palm treetops in canopy of the amazon rainforest for all images. The segmentation results of both positive and negative contrasts are similar. However, the image with negative contrast shows better enhancement of the tree crowns of palm trees and some other species than the positive contrast for visual analysis. A classification based on visual analysis with K-means classification for some negative images presents the best results in identifying tree crowns and palm trees, but there are some negative images in segmentation procedure that leaves were identified instead of tree crowns and the classification procedure did not identify individual trees. The videography images were used to identify individual palm trees from large area of Amazon.

Amin P. Charaniya, et al. [4] used a supervised parametric classification algorithm on the raw LiDAR point cloud acquired from 3D aerial LiDAR or Light Detection and Ranging, to classify the LiDAR dataset and group them into four disjoint classes: trees, grass, roads, and building roofs. In addition to the given height information of 3D aerial LiDAR, the authors used the following types of information for classifying LiDAR dataset: height texture, intensity, multiple two returns from LiDAR, and the use of luminance derived from aerial imagery as the fifth feature for classification. They defined five features to be used for data classification: the normalized height, the height variation, the multiple returns, the luminance, and the intensity. There were several combinations of the features for testing and the classification results show that the height feature is effective in overall classification

and the height variation is effective in tree classification, whereas the luminance and intensity together are effective in grass and road classification. Using more features can produce better results sometimes but not always. However, some of the combinations seem to be better than others, for examples, the height feature is an important classifier for the terrain, the height variation plays an important role in classifying high vegetation areas, and the light features – luminance and intensity are useful for separating the low vegetation (grass) and roads.

Lin Yang, et al. [5] proposed an automatic approach to tree detection from aerial imagery by segmenting the aerial image into tree and non-tree regions and then applying a pixel level classification based on a set of visual features followed by a partitioning algorithm for refinement. All visual features, which can be used to distinguish the properties of trees, were selected at the pixel level. These visual features are: color, texture, and entropy. The results of pixel level classification were noisy (e.g., shadowed tree leaves are labeled as non-tree; sparse points on a grass filed are labeled as tree; etc.), therefore, the authors refined the pixel-level classification results by considering the local smoothness of pixel labeling to generate a clean segmentation of tree and non-tree regions. During the refinement stage, a set of tree templates were used to correlate with the classification results and to locate candidate tree crowns. The tree crowns were then selected in a greedy manner to maximize correlation scores while minimizing the overlap. The proposed method only requires the RGB channels of aerial imagery and it achieves greater than 90% accuracy in pixel level tree classification.

Salim Malek, et al. [6] used the technology of unmanned aerial vehicles (UAVs) associated with the remote sensing system for automatic detection of palm trees by first extracting a set of candidate keypoints from a given 3.5 cm spatial resolution of UAV images using the Scale-Invariant Feature Transform (SIFT) [7]. A set of candidate keypoints were then analyzed with a recent kernel-based classification method that was termed as extreme learning machine (ELM) [8-10]. The ELM classifier marked each detected palm tree by several keypoints, which were merged together in order to capture the shape of each tree by active contour method based

on level sets (LSs). There were side-effects appeared at the end of grouping process because the keypoints were classified incorrectly as palm trees by ELM classifier, such as merging very close trees and the creation of regions related to other green vegetation. The authors then applied mathematical morphology to separate the large connected components that may contain more than one palm tree. In order to distinguish palm trees from other vegetation, the local spatial structure of the obtained regions was described with local binary patterns (LBPs).

2.2 Background

All the image data used in this research are 24-bit color images in .JPG format. An example of aerial image of oil palms and its zoom-in version is shown in Figure 8 while Figure 9 shows an 8-bit gray scale image of oil palms. The methods that are used in oil palm detection and identification include fundamental methods in image processing and our proposed method. Fundamental methods that will be described in this chapter are Gaussian filter, Butterworth low-pass filter, adaptive local thresholding method, connected component labeling, morphological operation, normalized cross correlation, and color-based segmentation using K-means clustering.

(a) (b)

Figure 8 24-bit color image of oil palms on the left and zoomed image

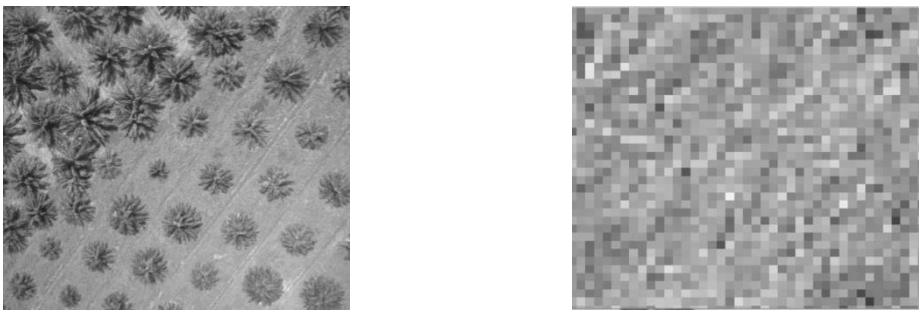

(a) (b)

Figure 9 8-bit gray scale image on the left and zoomed image

2.3 Gaussian filter and Butterworth low-pass filter

Noise in a digital image is considered undesirable. It is usually represented by speckled pixels of color in an image. Some certain types of noise can be removed by using linear filters, such as Gaussian filter and Butterworth filter. The ways to remove noise can be performed by either removing it or blurring an image. Some linear filters are the smoothing operations that can be applied to an image in order to reduce noise. It modifies and enhances an image to emphasize certain features and to remove some features in an image. Smoothing operation is carried out by convolution operator that convolves an image by using a kernel. The procedure is carried out by sliding the kernel across all pixels on the source image and calculating the value of new pixel based on the summation of local neighborhood pixels as shown in Figure 10. The output image appears blurry with less defined edges. Let f_{input} be an image and H be a kernel of size $k \times k$. The output of convolving f_{input} with H is denoted by Eq. (1),

$$f_{output}(x,y) = \sum_{i=-k/2}^{k/2} \sum_{j=-k/2}^{k/2} H(i,j) \times f_{input}(x+i, y+j) \quad (1)$$

where (x, y) are coordinates of each pixel, (i, j) are coordinates of a kernel.

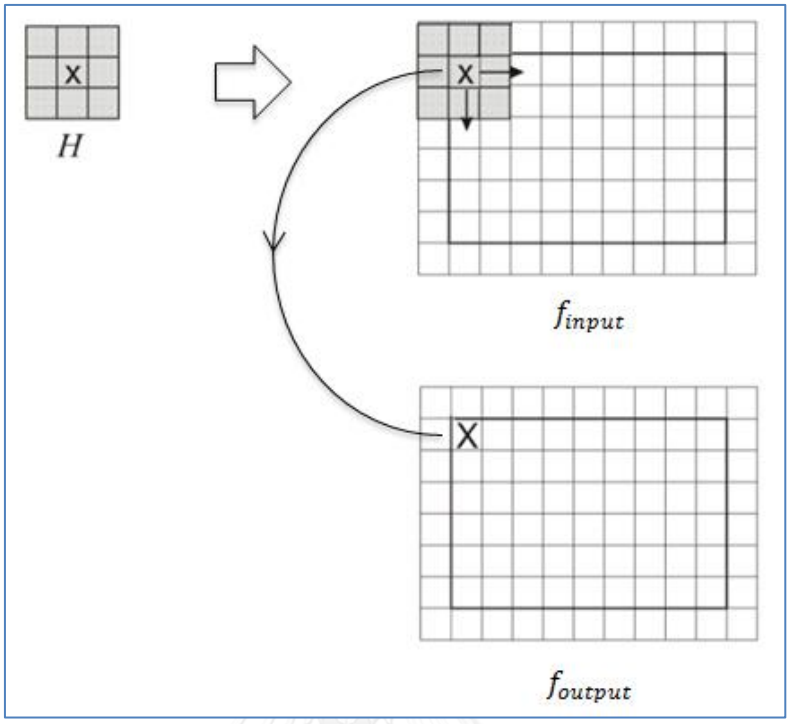

Figure 10 An example of a convolution process with a kernel of size 3 x 3

2.3.1 Gaussian filter in spatial domain

Gaussian filter has the weight higher than those pixels on the periphery. The filter does not preserve image brightness. Gaussian filter is represented by a shape of Gaussian hump as shown in Figure 11. The two dimensional Gaussian function has the form as follows

$$G(x,y) = \frac{1}{2\pi\sigma^2} e^{-\frac{x^2+y^2}{2\sigma^2}} \quad (2)$$

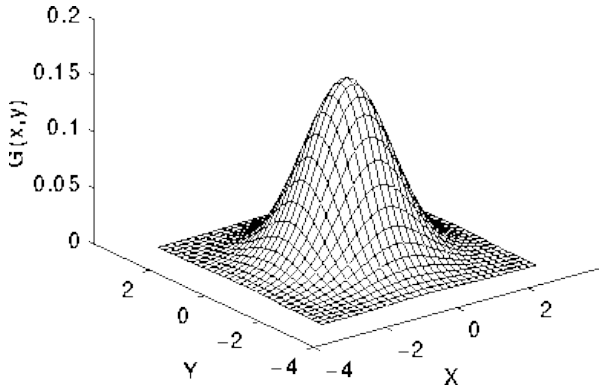

Figure 11 2D Gaussian distribution with mean (0, 0) and σ =1
(http://homepages.inf.ed.ac.uk/rbf/HIPR2/gsmooth.htm. 2015:Online)

Figures 12(a) - (d) illustrate the results from using Gaussian filter with different sizes and different values of σ.

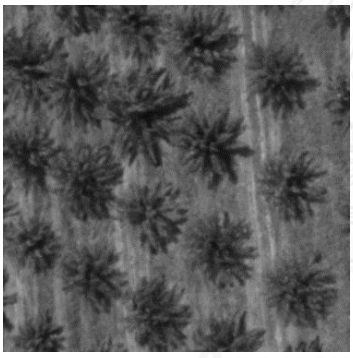

(a) 3 x 3 filter size with $\sigma = 1$

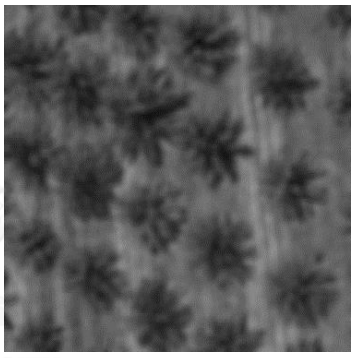

(b) 5 x 5 filter size with $\sigma = 10$

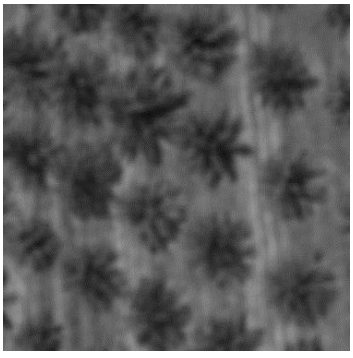

(c) 7 x 7 filter size with $\sigma = 20$

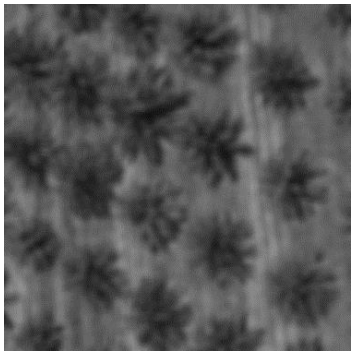

(d) 9 x 9 filter size with $\sigma = 30$

Figure 12 The effect of smoothing with various filter sizes and σ

2.3.2 Fourier transform

Fourier spectrum is a waveform that can be used to represent an image in frequency domain. It is constructed from using the sum of sine and cosine waves with different frequencies which can be determined by the exponential in discrete Fourier transform (DFT). It can be expanded into sines and cosines by variables u and v. An image $f(x,y)$ of size $M \times N$ is represented in the frequency domain $F(u,v)$ by using 2D Discrete Fourier transform (DFT) as given by the following equation:

$$F(u,v) = \frac{1}{MN} \sum_{x=0}^{M-1} \sum_{y=0}^{N-1} f(x,y) e^{-2\pi i(\frac{ux}{M} + \frac{vy}{N})} \tag{3}$$

where $u = 0,1,\dots,M-1$ and $v = 0,1,\dots,N-1$

The inverse of the Discrete Fourier transform (DFT) is given by the following equation:

$$f(x,y) = \sum_{u=0}^{M-1} \sum_{v=0}^{N-1} F(u,v) e^{2\pi i(\frac{ux}{M} + \frac{vy}{N})} \tag{4}$$

where $x = 0,1,\dots,M-1$ and $y = 0,1,\dots,N-1$

2.3.3 Butterworth low-pass filter

Butterworth low-pass filter can be used to reduce the effects of noise by blocking high frequency spectrum which represents abrupt changes in an image. In order to apply low-pass filter, an image has to be transformed to spectrum in frequency domain. When an image is transformed to spectrum in frequency domain, the areas near the origin represent low frequencies while the areas further away from the origin represent high frequencies as shown in Figure 13. Butterworth low-pass filter is suitable for noise that appears as random spots in an image. A filter is applied on spectrum in frequency domain. Low-pass filter always retains low frequency information within an image while reducing the high frequency information. Butterworth low pass filter of order n with cutoff frequency D_0 as shown in Figure 14 and Figure 15, is given by the following equation:

$$H(u,v) = \frac{1}{1 + [D(u,v)/D_0]^{2n}} \tag{5}$$

where $D(u,v) = [u^2 + v^2]^{1/2}$, is the distance from point (u,v) to the center of the filter, and D_0 is a specified nonnegative number.

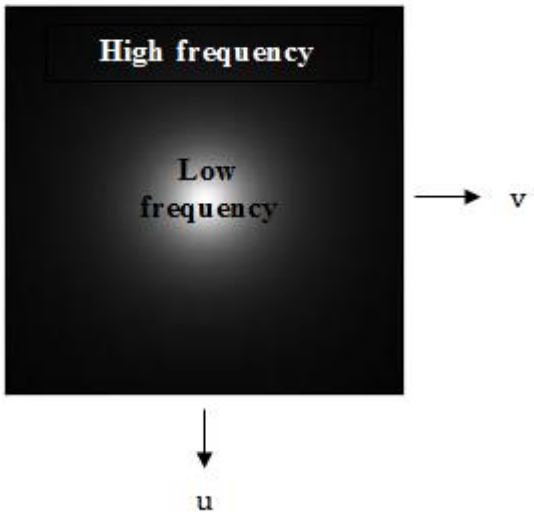

Figure 13 Butterworth low-pass filter, High frequencies correspond to abrupt changed regions (edges) whereas low frequencies correspond to slow change regions (smooth regions)

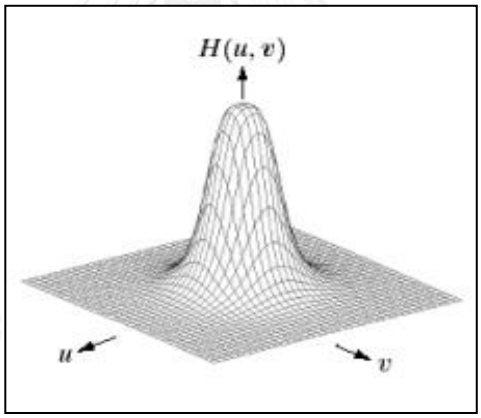

Figure 14 The perspective plot of a Butterworth low-pass filter (http://mipav.cit.nih.gov/pubwiki/index.php/Filters_(Frequency). 2015:Online)

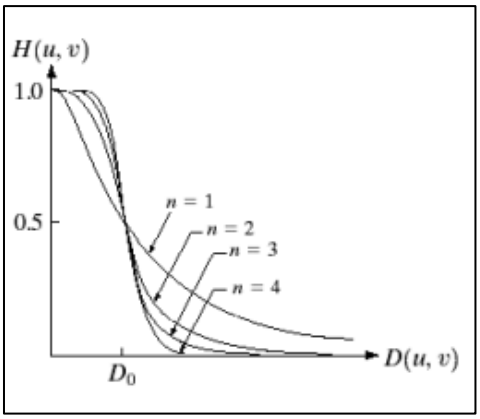

Figure 15 Filter radial cross sections of orders 1 through 4 (http://mipav.cit.nih.gov/pubwiki/index.php/Filters_(Frequency). 2015:Online)

The procedure is carried out by using low-pass filter to perform point-wise multiplication with the spectrum of an image. Then, the spectrum is transformed back to an image in spatial domain by inverse discrete Fourier transform. Examples of filtered images with different degrees and different cut off values are shown in figure 16.

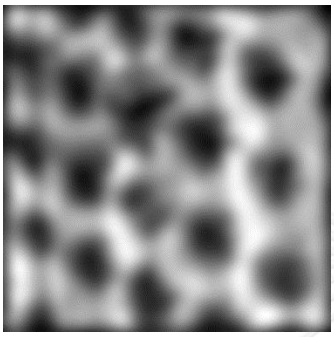

(a) $D_0 = 10$

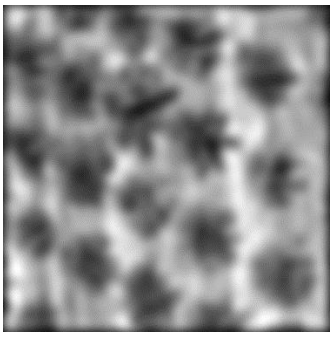

(b) $D_0 = 15$

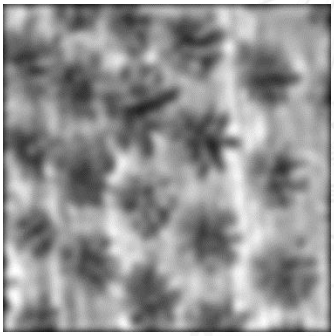

(e) $D_0 = 40$

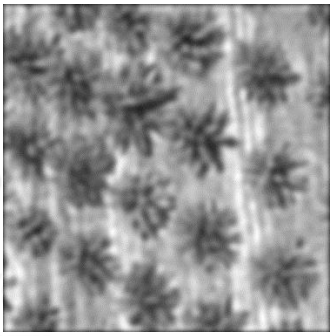

(f) $D_0 = 60$

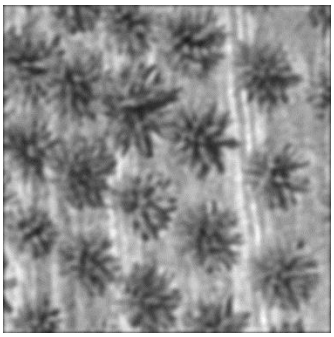

(e) $D_0 = 40$

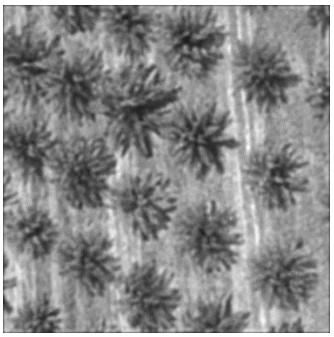

(f) $D_0 = 60$

Figure 16 The images after applying Butterworth low-pass filter to Figure 8 with n=3

2.4 Adaptive local thresholding method

Thresholding is the segmentation method that has been widely used. Thresholding operation maps a gray scale image to a binary image by using an appropriate threshold T defined by:

$$\hat{f}(x,y) = \begin{cases} 1, & if\ f(x,y) > T \\ 0, & if\ f(x,y) \leq T \end{cases} \quad (6)$$

where $\hat{f}(x,y)$ is a result image in binary format, $f(x,y)$ is the original gray scale image. The adaptive local thresholding method calculates the threshold value, T, from the average intensity of the pixels under the kernel. The size of the kernel depends on each problem. Figures 17 - 18 illustrate the result images from using adaptive local thresholding.

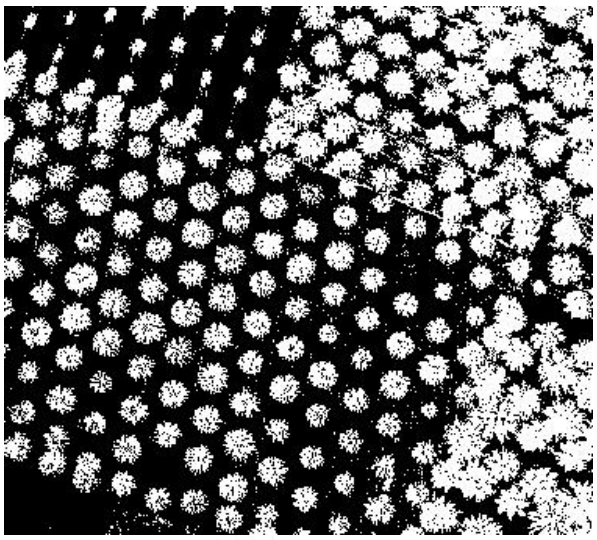

Figure 17 Binary image of an aerial image that was captured from far distance

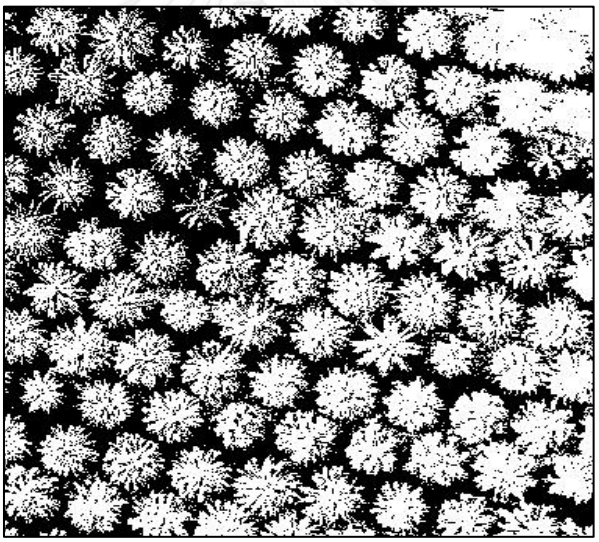

Figure 18 Binary image of an aerial image that was captured from near distance

2.5 Connected component labeling

Connected component labeling is one of the most fundamental operations in pattern recognition and is widely used in image processing for connected component analysis, blob extraction or region extraction. An algorithm relates to the graph theory that studies about graphs for modeling the relations between components.

These components are called nodes or vertices. These nodes are connected by edges. An example of a graph is illustrated in Figure 19. In graph theory, subsets of connected components are uniquely labeled based on a given problem. The graph in Figure 20 illustrates three connected components.

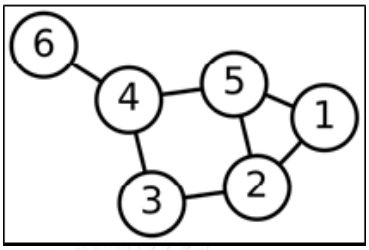

Figure 19 A graph with six vertices or nodes and seven edges

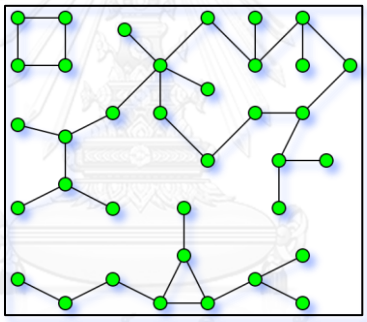

Figure 20 A graph with three connected components

A graph contains vertices and connecting edges, which is constructed from relevant input data. An algorithm traverses the graph and label vertices based on the connectivity and relative values of their neighborhood vertices. The connectivity is determined by either 4-connectivity in Figure 21 or 8-connectivity as shown in Figure 22. This algorithm can be applied to two-dimensional binary or gray scale image using two-scan algorithm. Figures 23 - 24 show the result images from applying 8-connected connectivity to aerial images of oil palm plantation.

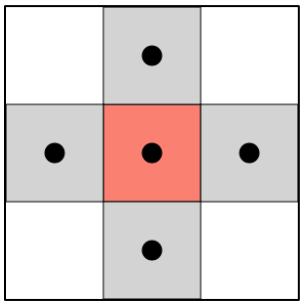

Figure 21 4 –connected connectivity

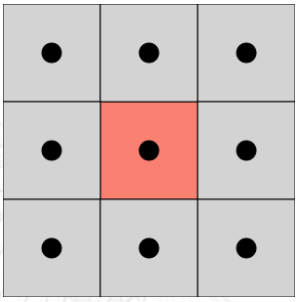

Figure 22 8 – connected connectivity

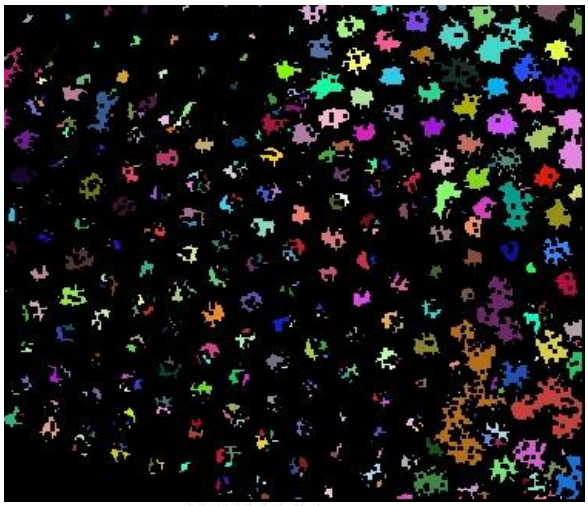

Figure 23 The result of connected component labeling performed on the result binary image from Figure 16 including the component of oil palms

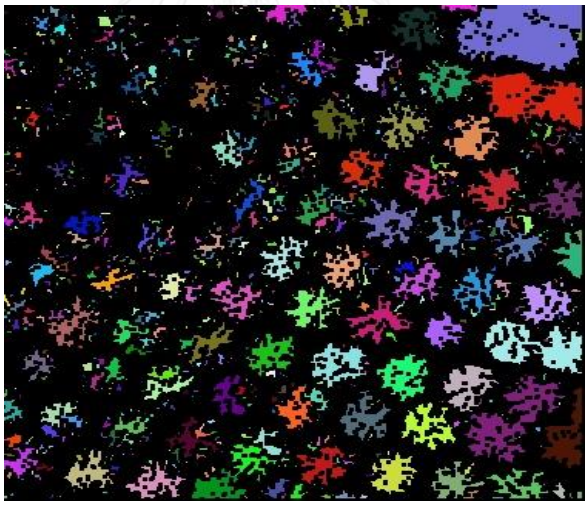

Figure 24 The result of connected component labeling performed on the result binary image from Figure 17 including the component of oil palms

2.6 Erosion

Morphology in image processing is a collection of non-linear operations, e.g., erosion and dilation, that relates to shape feature in images. The operations can be applied to both gray scale and binary images. Erosion is an operation that removes pixels along the boundary of a component in an image using a structuring element which causes the size of a component to be smaller. In our case, it is used to separate individual oil palms from a tree stand.

Morphological operation operates pixels on a binary image according to the correlative ordering of pixel values. The operation probes an image with a structuring element that scans pixels one by one where each pixel will be compared with the corresponding neighborhood pixels. The structuring element is a small matrix of pixels with various sizes specified by matrix dimension where pixel value in matrix is either zero or one. Examples of structuring elements are shown in Figures 25 – 27.

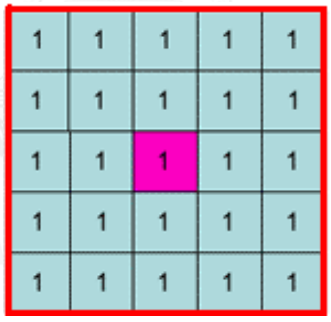

Figure 25 5 x 5 square structuring element

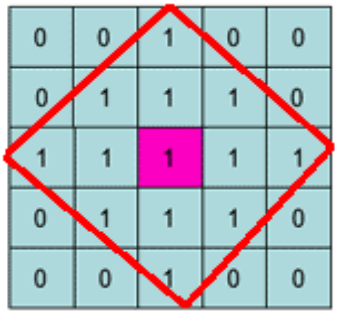

Figure 26 5 x 5 diamond-shaped structuring element

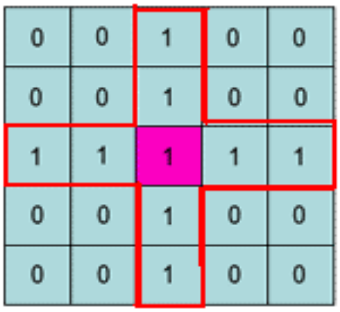

Figure 27 5 x 5 cross-shaped structuring element

Figure 28 illustrates the morphological operations that probe an image with a structuring element and check whether the structuring element fits within the neighborhood pixels, and whether the element hits or intersects the neighborhood pixels or not. Region A in Figure 28 shows the structuring element that fits a component, region B shows the structuring element that hits or intersects a component, and region C shows the structuring element that neither fits, nor hits a component.

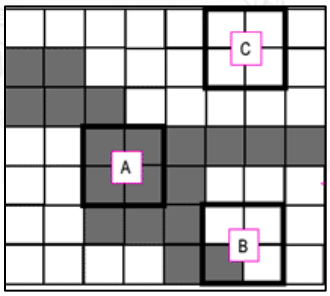

Figure 28 Probing an image with three structuring elements (https://www.cs.auckland.ac.nz/courses/compsci773s1c/lectures/ImageProcessing-html/topic4.htm 2015:Online)

The erosion of a binary image f in 2-dimensional Euclidean space E^2 where f is considered as a subset of E^2, by using a structuring element s, is defined as follow:

$$f \ominus s = \{z \in E^2 | (z + q) \in f, \forall q \in s\} \tag{7}$$

where z is the set of coordinates (x, y) in Euclidean space E^2 of binary image f, and q is the value under the structuring element s

Figure 29 is the color aerial image that was captured from near distance by the digital camera and the results from erosion Figure 29 with one-iteration by different structuring elements are shown in Figures 30 – 32.

(a) (b)

Figure 29 Original image and binary image

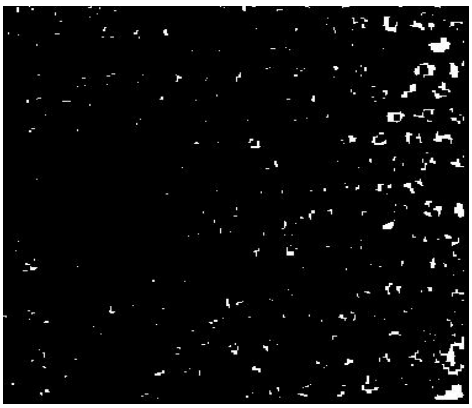

Figure 30 Result from using 5 x 5 square structuring element

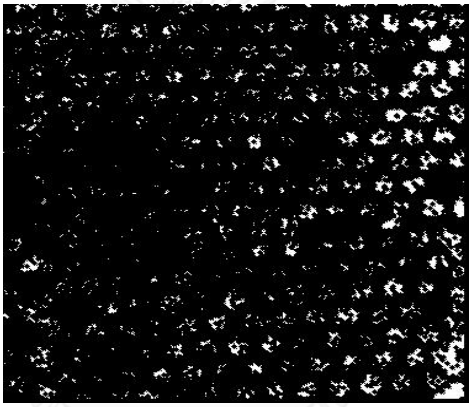

Figure 31 Result from using 5 x 5 diamond-shaped structuring element

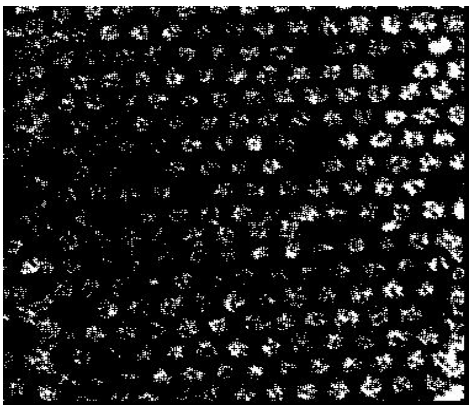

Figure 32 Result from using 5 x 5 cross-shaped structuring element

Figure 33 is the color aerial image that was captured from near distance by the digital camera and the results from erosion Figure 33 with one-iteration by different structuring elements are shown in Figures 34 – 36.

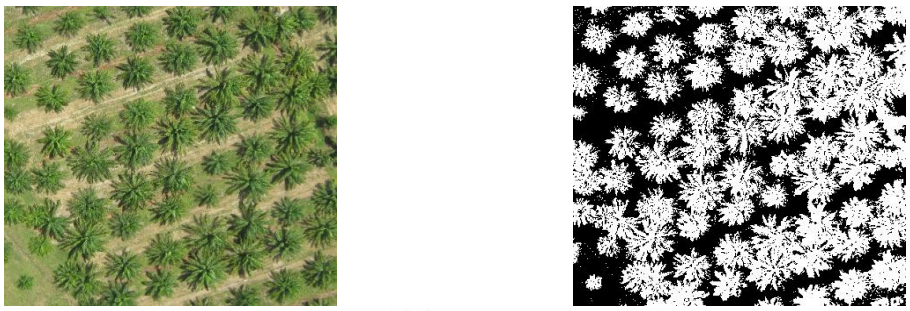

(a) (b)

Figure 33 Original image and binary image

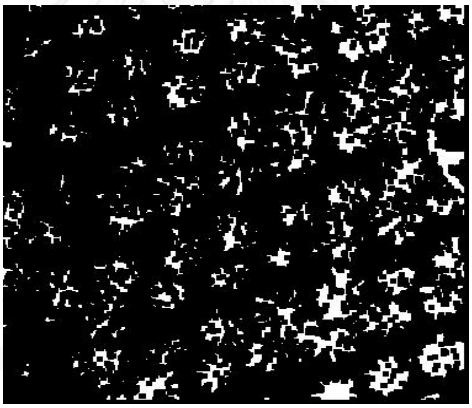

Figure 34 Result from using 5 x 5 square structuring element

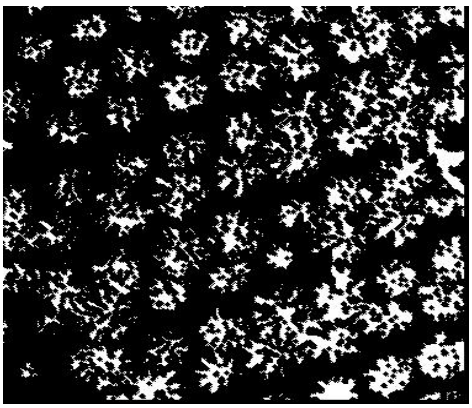

Figure 35 Result from using 5 x 5 diamond-shaped structuring element

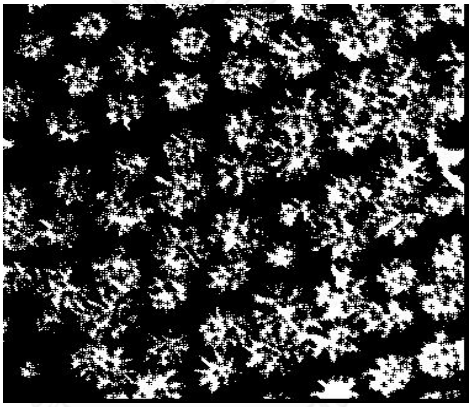

Figure 36 Result from using 5 x 5 cross-shaped structuring element

2.7 Normalized cross correlation for template matching

Template matching has been used for object recognition. It is widely used to locate and recognize objects of interest in the scene with the method of searching for the most similar pattern within the original image by using template images to perform scanning to all pixels within the original image. Each pixel in the original image is compared to the overlapped pixel of the template image and the degree of similarity is computed using normalized cross correlation. This is the exhaustive searching method to detect the existence of templates within a given image. A component is similar to a template if the correlation value is high and vice versa.

Convolution and cross correlation in image processing are quite similar in the way that they both apply a kernel (template) over pixels within the original input image one by one. They extract information from an image by the use of shift invariant operation to calculate the new values through all the pixels of an image with the same operation and replace every pixel with a linear combination of its neighborhood pixels to form a new image. In practice, cross correlation is used for matching the original gray scale image f against a template t, which can be calculated as follows:

$$f(x,y) \circ t(x,y) = \sum_{i=0}^{W-1} \sum_{j=0}^{H-1} f\,(x+i, y+j) t(i,j) \tag{8}$$

where W and H are width and height of the template t, respectively.

The cross correlation find components that are similar to a template by placing a template over an image starting from the top-left corner of an image then calculating the normalized cross correlation between pixels of a template and pixels of an image that are under the template.

The correlation is calculated from the sum of the product between the values of pixels in t and f over the overlapped region. Any region with high correlation coefficient is considered to be similar to the template. An example of template matching by cross correlation is shown in Figure 37.

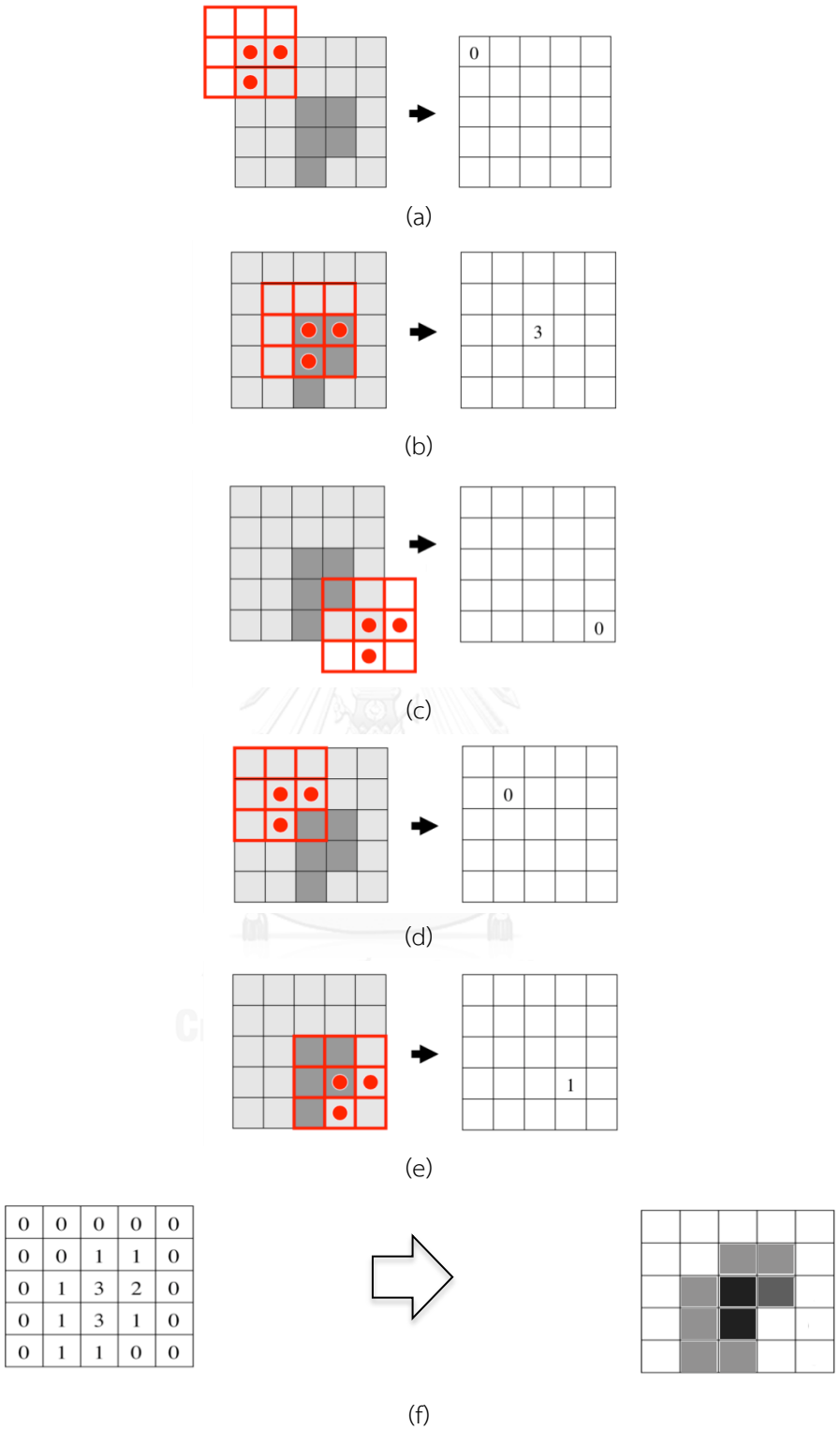

Figure 37 The process of template matching using cross correlation to find the region in an image I that matches a template t which pictures (a) – (e) has the 3 × 3 template that placed over a region of an image and (f) is the final result

For image-processing, if we use cross correlation, the matching result might not be correct because the brightness of the image and the template can vary due to lighting and exposure conditions. Thus the image should be first normalized. In such case, normalized cross correlation is one of the most effective methods used for matching. It measures the similarity between an image and a template under different lighting conditions by computing the normalized cross correlation between a template t and any region within an image f. Template should not be set larger than image.

The result matrix r contains the correlation coefficients range from -1.0 to 1.0. The technique can be easily performed on a grey scale image with small changes in rotation and scaling between two images. The normalized cross correlation can be computed as follows:

$$r(x,y) = \frac{\sum_{i=0}^{W-1}\sum_{j=0}^{H-1}(t(i,j) \times f(x+i,y+j))}{\sqrt{\sum_{i=0}^{W-1}\sum_{j=0}^{H-1} t(i,j)^2 \times \sum_{i=0}^{W-1}\sum_{j=0}^{H-1} f(x+i,y+j)^2}} \quad (10)$$

where f is a gray scale input image and t is the template with $W \times H$ pixels.

The normalized cross correlation calculates the summation of numerator and denominator in equation (10). The correlation is calculated from the sum of the product between the values of pixels in t and f over the overlapped region. Any region with high correlation coefficient is considered to be similar to the template as shown in Figure 38.

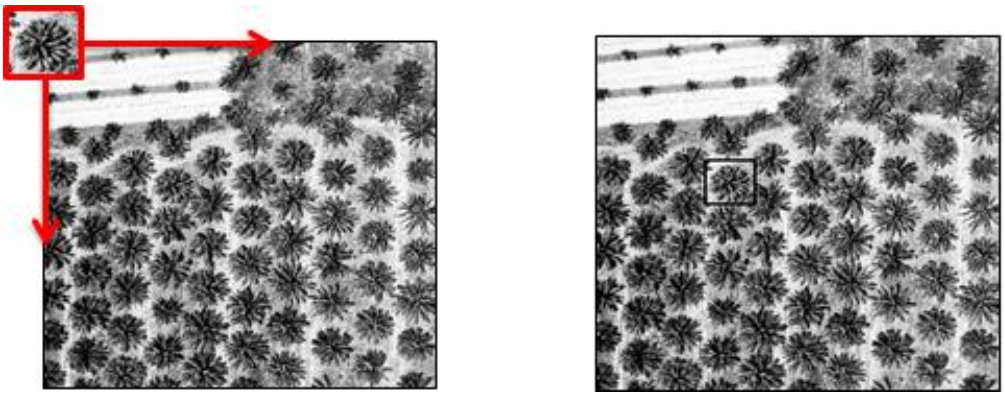

(a) (b)

Figure 38 An example of template matching by cross correlation

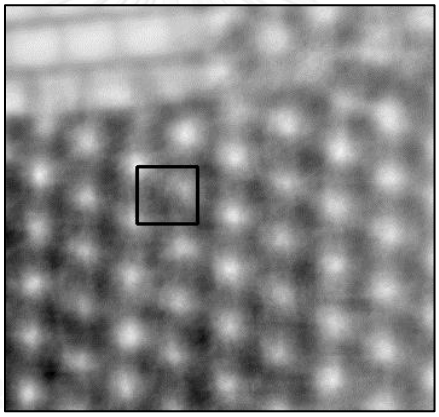

Figure 39 The best match region after performing template matching using normalized cross correlation from Figure 38

Chapter III

Proposed Method and Implementation

This chapter describes the proposed method to estimate the population of oil palms from high resolution aerial images that were captured by digital camera mounted to the remote-control airplane that was controlled to fly over oil palm plantations. The proposed method consists of four steps as shown in Figure 40.

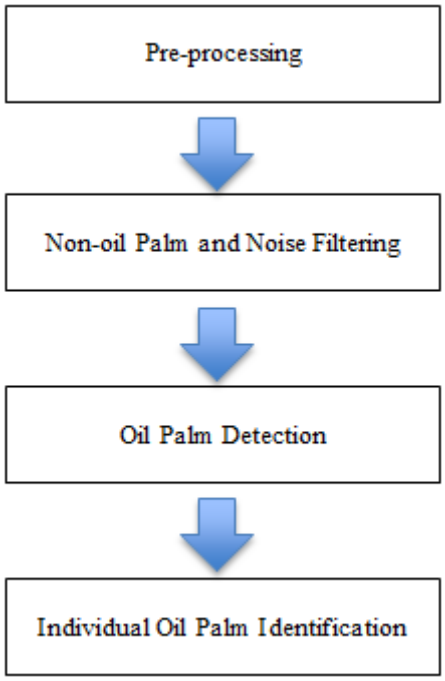

Figure 40 The process of oil palm detection and identification

3.1 Preprocessing

The first step begins with preprocessing that accepts color images as input. Each input image is resized to 912x684 pixels and is then converted to a gray scale image. To improve the quality of an image, the contrast of an image is enhanced by histogram equalization. The global histogram equalization is used to increase the global contrast of an image by remapping intensities using probability distribution of an input image. The overall process is shown in Figure 41.

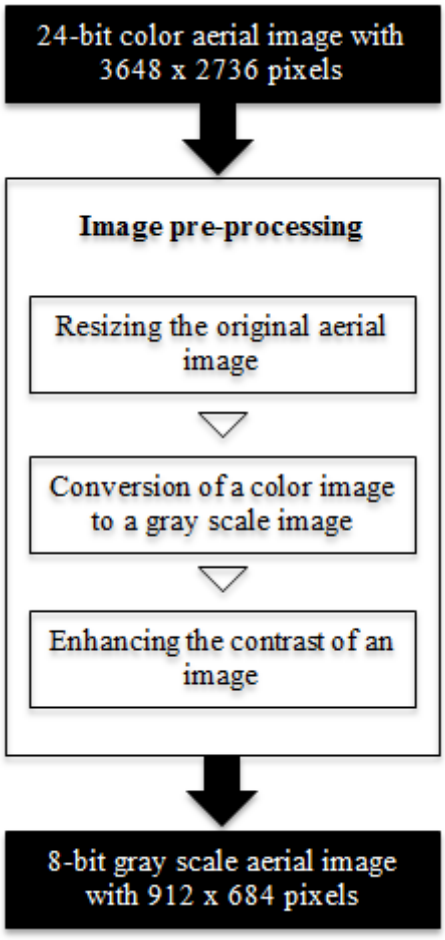

Figure 41 The operation of image pre-processing

Figure 42(a) shows a 24-bit color image while Figure 42(b) shows the 8-bit gray scale image after the image in Figure 42 (a) is converted to a gray scale image. Figures 42 (c) – (e) are histograms of each color channel and Figure 42(f) is the histogram of the gray scale image. The values along the x-axis represent intensities and the values along the y-axis represent frequency of these intensities.

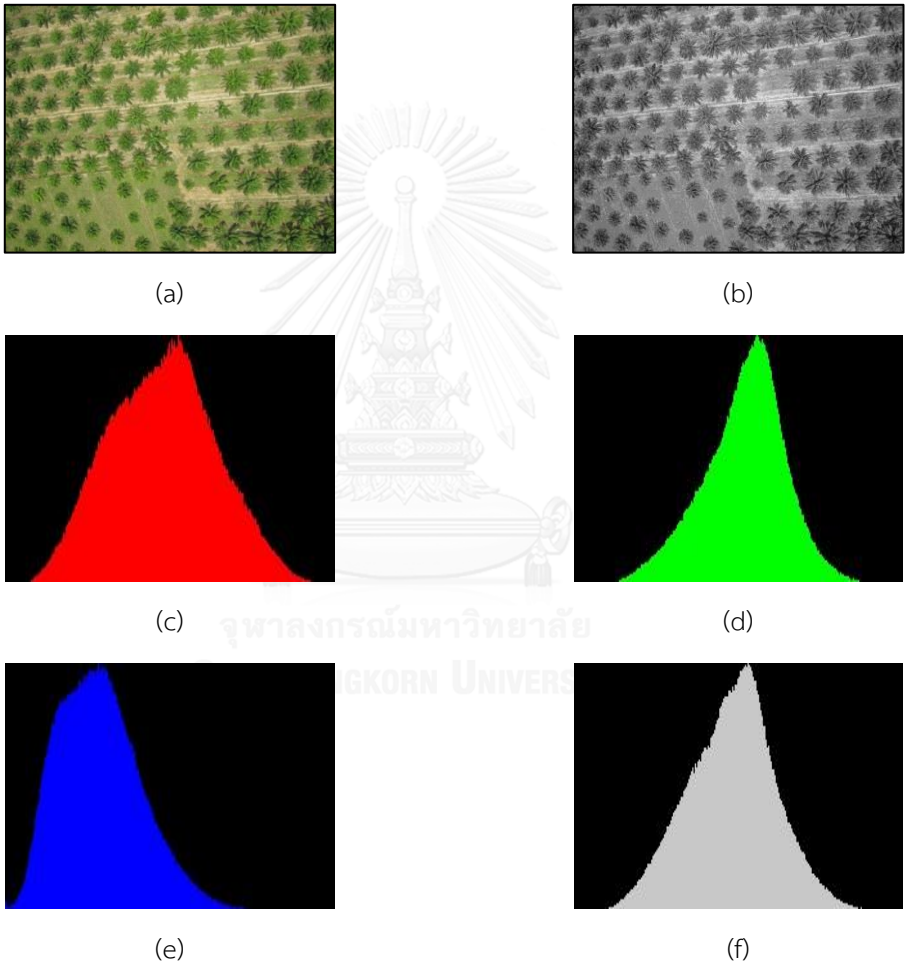

Figure 42 (a) the original image, (b) the gray scale image of (a), (c)-(e) the histograms of red, green, and blue channels, respectively, (f) the histogram of a gray scale image

The contrast of the gray scale image in Figure 42(a) is enhanced by histogram equalization. The output image is shown in Figure 43(a) and the representative of the equalized histogram is shown in Figure 43(b).

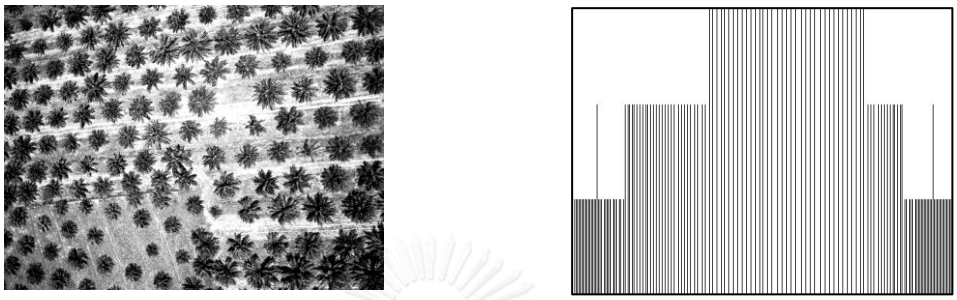

(a) The equalized image (b) The equalized histogram

Figure 43 (a) the result image from histogram equalization and (b) the histogram of the equalized image

3.2 Non-oil palm and noise filtering

Figure 44 shows the non-oil palm and noise filtering step. In this step, each enhanced image is smoothed by convolving each pixel in an image with 15 x 15 average filter. This size of a filter is chosen because it can blend all the leaves together to form a tree and it can also remove most of the noises in an image. Larger filter size makes an image more blur and individual oil palms cannot be seen. Whereas, smaller filter size cannot remove noises in an image and individual oil palms are hard to identify.

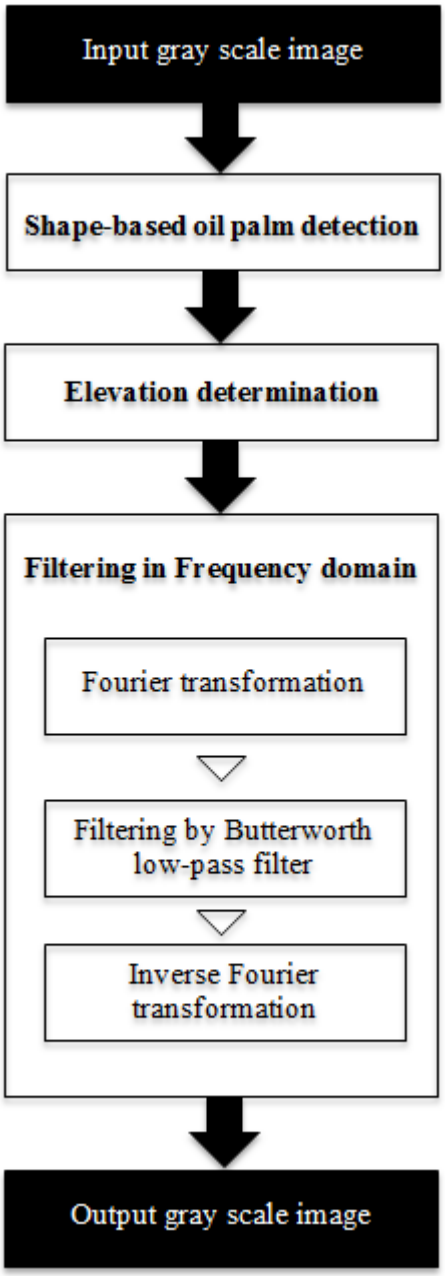

Figure 44 The operation of non-oil palm and noise filtering

The image smoothing function using an average filter is expressed by the following equation:

$$g(x,y) = \frac{1}{P} \sum_{(i,j) \in K} f(x,y) H_{Average}(i,j) \quad (11)$$

where P is the total number of pixels in a neighborhood K, K is a set of neighbor pixels of $H_{Average}(i,j)$, and $H_{Average}(i,j)$ is a $k \times k$ average filter whose coefficients are set to 1.

Next, individual oil palms of each smoothed image is identified by applying the shape-based method as explained below:

For each component of an image

- Check the shape of a component

If the shape of a component is square

Specify this component as individual oil palm

Else

Specify this component as non-individual oil palm

- Repeat the process for all the components

3.2.1 Elevation Determination

After that, the gray scale aerial images are categorized into two groups of near- and far- distance images by using the average and the standard deviation of the size of oil palms. From each image, all individual oil palms are sorted in ascending order and the median size is selected. All 21 median-size oil palms are used to calculate the average size of oil palms and standard deviation. The threshold value for categorizing near- or far-distance is set to the average size plus standard

deviation. If the median size of an image is smaller than the threshold value, this image is categorized as a far-distance image; otherwise, it is categorized as a near-distance image.

Figure 45 shows the far-distance aerial image with individual oil palms marked with green boxes and the median-size oil palm marked with red box. Figure 46 shows the near-distance aerial image with individual oil palms marked with green boxes and the median-size oil palm marked with red box.

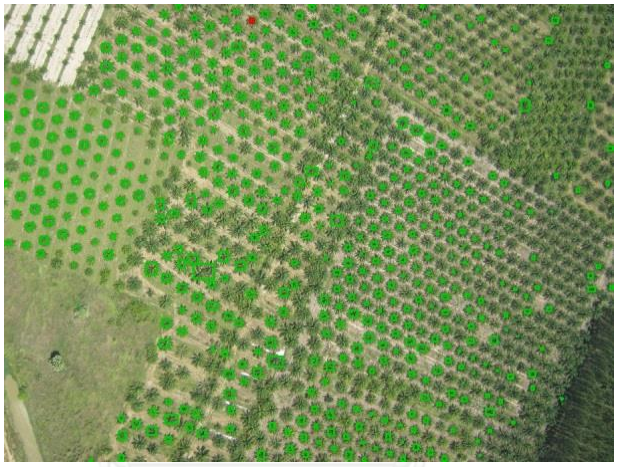

Figure 45 The aerial image including all individual oil palms (green) and the median-size oil palm (red)

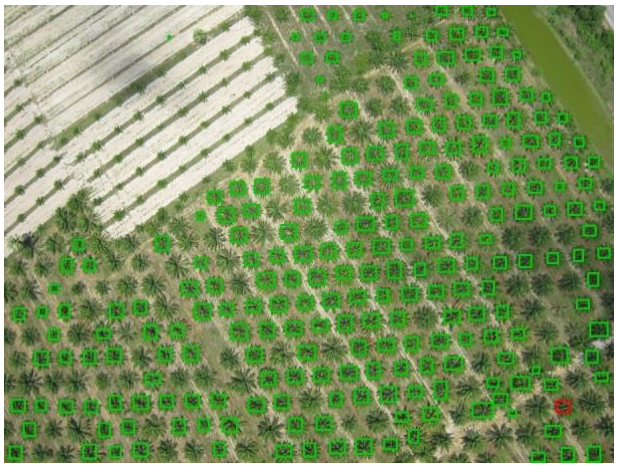

Figure 46 The aerial image including all individual oil palms (green) and the median-size oil palm (red)

3.2.2 Filtering in Frequency Domain

Finally, an image is smoothed and the leaves of each tree are connected by using Butterworth low-pass filter in frequency domain. In order to filter noise in frequency domain, an equalized image, $f\ (x, y)$, of size $M \times N$ in spatial domain in preprocessing step is transformed to Fourier spectrum, $F\ (u, v)$, in frequency domain using Fast Fourier transform. Butterworth low-pass filter, $H_{low-pass}(u, v)$, with cut-off, D, is then applied to smooth an image. The size of the cut-off depends on the elevation of the airplane. The higher the elevation is, the larger the cut-off will be. The filtered image, $G_{filtered}(u, v)$, can be obtained from

$$G_{filtered}(u, v) = H_{low-pass}(u, v)F(u, v) \tag{12}$$

$$H_{low-pass}(u, v) = \frac{1}{1 + (D(u, v)/D)^{2n}} \tag{13}$$

$$D(u, v) = [\left(u - \frac{M}{2}\right)^2 + (v - \tfrac{N}{2})^2]^{1/2} \tag{14}$$

where $u = 0,1,2, \dots, M - 1$, $v = 0,1,2, \dots, N - 1$, M is the height, N is the width, and $D(u, v)$ is the distance from any pixel (u, v) to the origin.

Figure 48 is the enhanced image of the original aerial image in Figure 47 which includes most of the oil palms that are distinguishable from the background.

Figure 47 Original aerial image

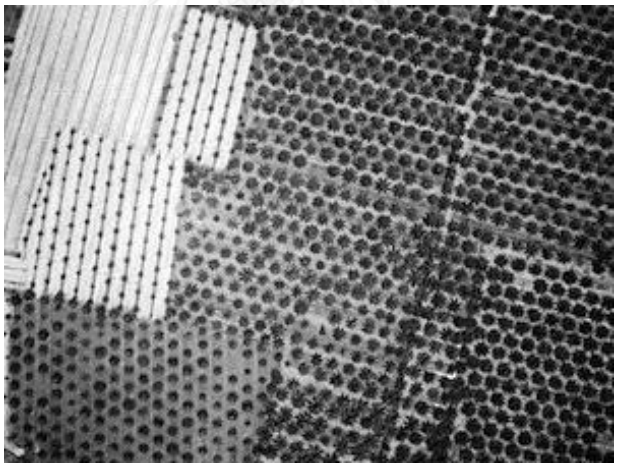

Figure 48 The output of equalized image

Figure 49 shows the spectrum of the image in Figure 48 and Figure 50 shows the Butterworth low-pass filter with $D = 75$. The cut-off radius depends on the elevation of the airplane. For a near-distance image, it contains large components with lots of leaves with high frequency, thus the cut-off radius is set to small value in order to blur the edges of leaves and other non-oil palm components. For a far-

distance image, the cut-off radius is set to large value because an image contains small components with wide range of intensities.

The spectrum after performing Butterworth low-pass filter is shown in Figure 51 and its corresponding image in spatial domain is shown in Figure 52. Figure 53 shows the final result of oil palm detection from an aerial image that is smoothed by Butterworth low-pass filter while Figure 54 shows the final result of oil palm detection from an aerial image without smoothing. It can be seen that smoothing an image with Butterworth low-pass filter can improve the detection rate.

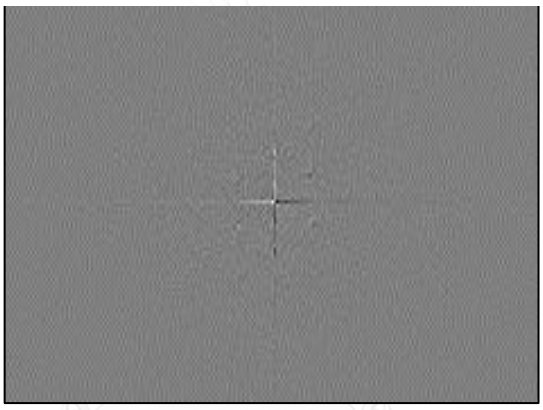

Figure 49 The output of Fourier spectrum image

Figure 50 The Butterworth low pass filter

Figure 51 The result of Fourier spectrum image after filtering

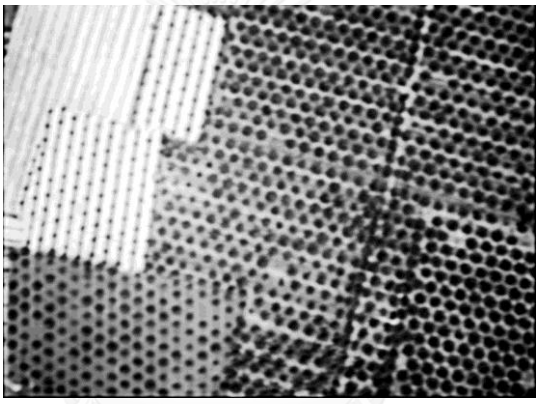

Figure 52 The final output of filtered image on spatial domain

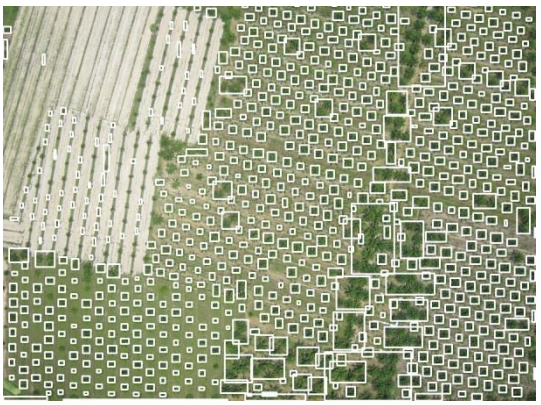

Figure 53 The result of detected oil palms from filtered image

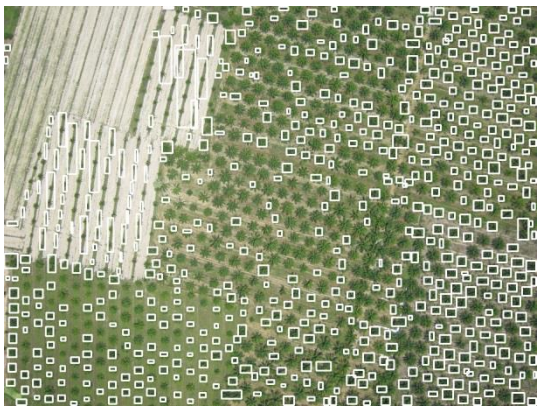

Figure 54 The result of detected oil palms from enhanced image

After smoothing, an image is converted back to an image in spatial domain by using inverse Fourier transform:

$$\tilde{f}(x,y) = \frac{1}{MN}\sum_{u=0}^{M-1}\sum_{v=0}^{N-1} G_{filtered}(u,v)e^{2\pi i(\frac{ux}{M}+\frac{vy}{N})} \quad (15)$$

3.3 Oil palm detection

Figure 55 shows oil palm detection step. In this step, a filtered image, $\tilde{f}(x,y)$, is converted to a binary image using adaptive local thresholding with the mask of initial size 3 x 3 and the threshold value is set equal to the average of intensities under the mask.

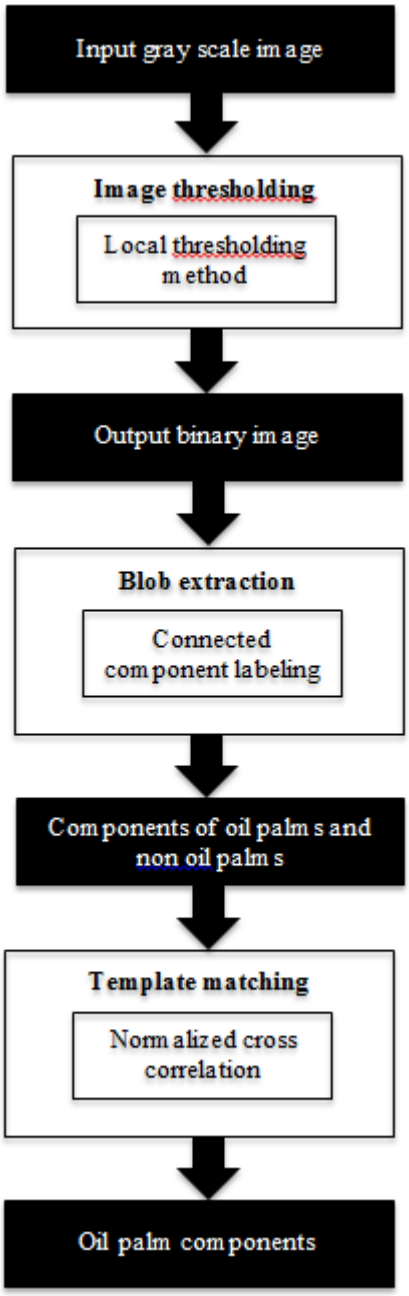

Figure 55 The operation of oil palm detection

This adaptive local thresholding is used to convert grass, footpath, and roads to background. A binary image can be obtained from:

$$\tilde{f}_2(x,y) = \begin{cases} 1 & if\ \tilde{f}(x,y) > T(x,y) \\ 0 & otherwise \end{cases} \quad (16)$$

where $T(x,y)$ is the average of intensities under the mask and $\tilde{f}(x,y)$ be the intensity at (x,y).

Figure 56 (a)-(d) are the results from the filtering step which still contain grass, roads, and footpath. These non-oil palm components can be removed by our proposed adaptive local thresholding. The results of binary images after performing adaptive local thresholding are shown in Figures 57 (a) – (d). However, there are some non-oil palm components that have not been removed, such as pond, swamp, shrub, thick grass – weed, and other trees as shown in Figure 57 (d).

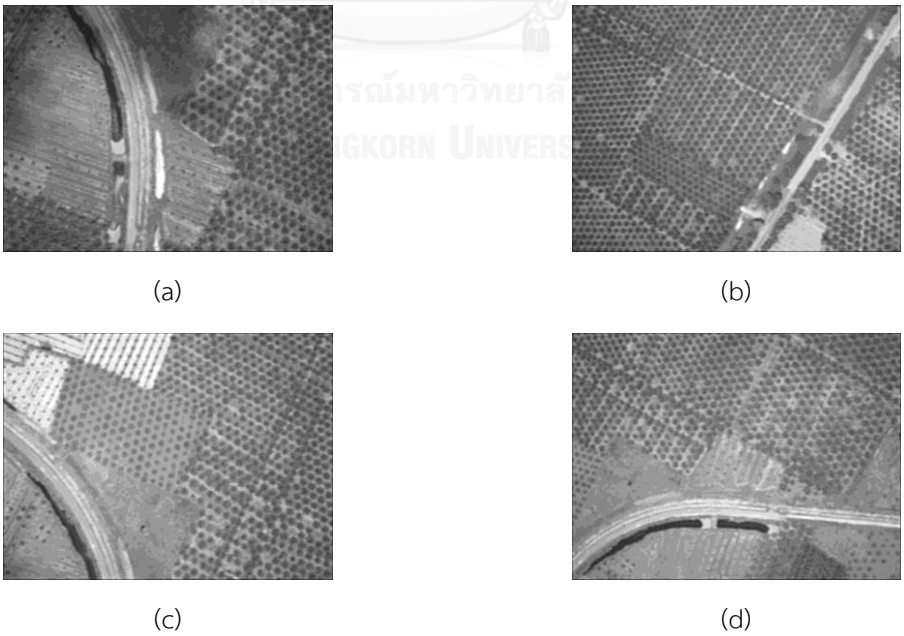

(a) (b)

(c) (d)

Figure 56 Examples of aerial images from different view

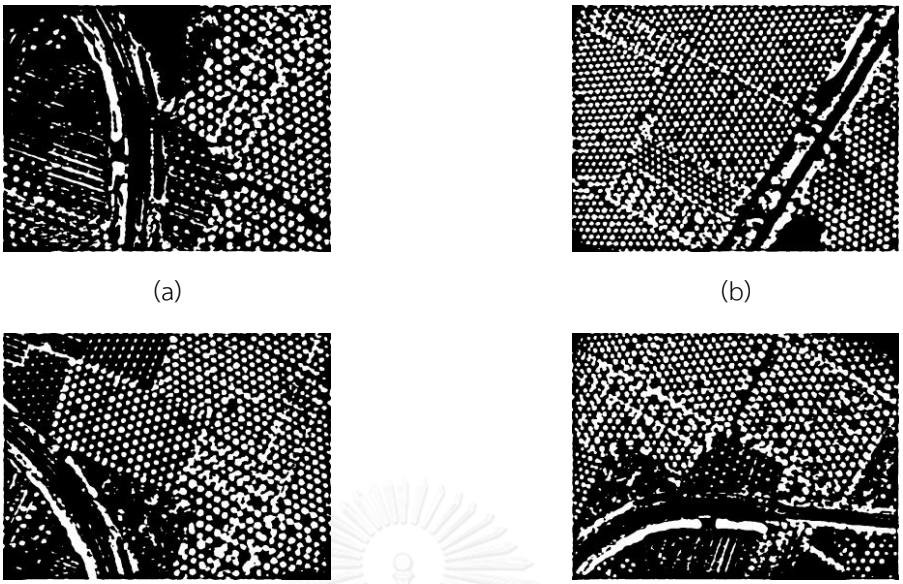

(a) (b)

(c) (d)

Figure 57 The results of binary images after applying adaptive local thresholding method on images in Figures 56 (a) – (d)

If the proposed oil palm detection method is applied directly to Figures 57 (a)-(d), the oil palm detection results are shown in Figures 58 (a) – (d). It can be seen that some non-oil palm components are detected as oil palms. Thus, the normalized cross correlation is applied to remove these non-oil palm components before performing oil palm detection.

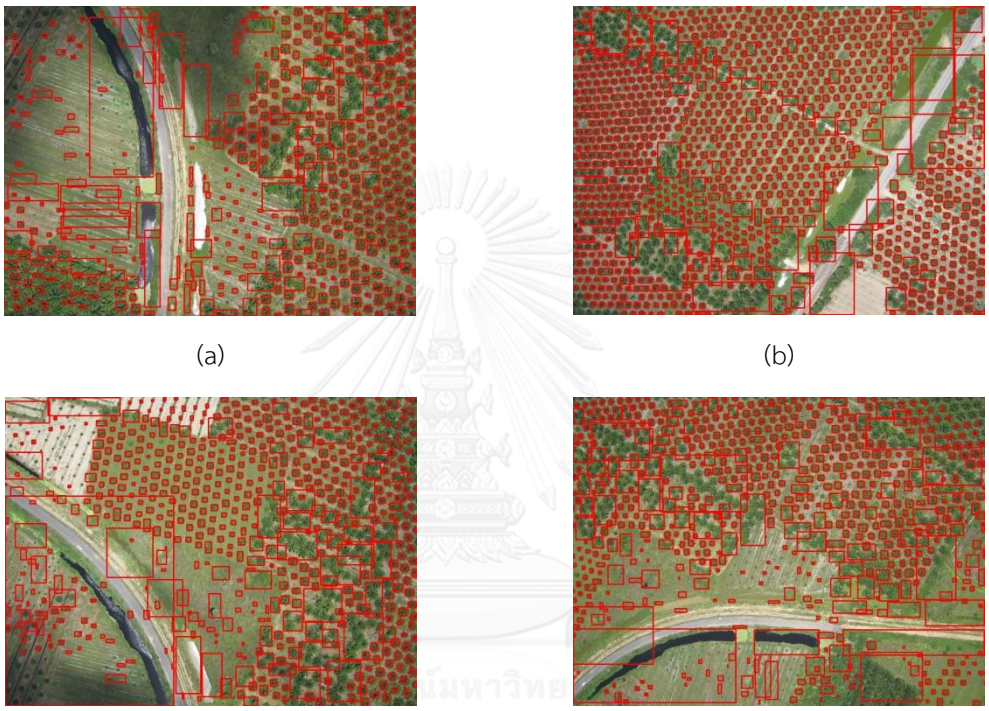

(a) (b)

(c) (d)

Figure 58 The detection results from using the proposed oil palm detection method on a set of binary images in Figures 57 (a)-(d)

After that, the 8-neighbor connected component labeling is applied on a binary image, $\tilde{f}_2(x,y)$. It is used to identify each component in an image. If $\tilde{f}_2(x,y)$ represents a binary image with size $M \times N$ where M is the height of an image and N is the width of an image then each component in a binary image consists of pixels that belong to the same connected component that is identified by a unique label assigning to them from the two-scan algorithm[11]. The two-scan algorithm is used for labeling operation by scanning all the pixels one by one within a binary image using the mask with 8-connected connectivity as shown in Figure 59.

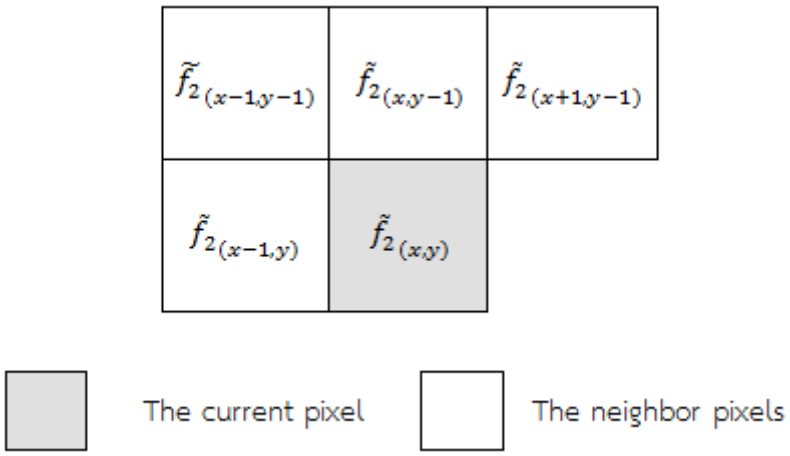

Figure 59 An example of mask with 8-connected connectivity

Figure 60 shows an example of a binary image size 7 x 7 pixels which contains two connected components. The pixels of foreground and background are represented by 1s and 0s, respectively. The foreground pixels will be labelled by the mask with 8-connected connectivity in the first scanning of two-scan algorithm.

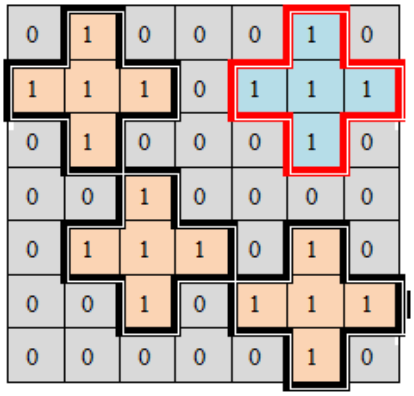

Figure 60 An example of a binary image containing foreground and background components represented by 1s and 0s, respectively

In the two-scan algorithm, if the intensity, $\tilde{f}_2(x,y)$, of the current pixel at (x,y) is 0 then there is no change to the intensity. On the other hand, if the intensity, $\tilde{f}_2(x,y)$ of the current pixel at (x,y) is 1 then that current pixel requires labeling operation. The labeling operation is as follows:

Let $L(x,y) = l$ be the labeling number, l =1 be the initial labeling number, and $E(x,y)$ be neighbor pixels of (x,y).

In the first scan, if all neighbor pixels under the mask of (x, y) have intensities equal to 0 then that current pixel is labeled with the new number. Otherwise, it will be labeled with the same number as its neighbor; i.e.,

$$l = \begin{cases} l+1 & \forall (s,t) \in E(x,y) |\, \tilde{f}_2(s,t) = 0 \\ L(s,t) & otherwise \end{cases}, \tag{17}$$

$$L(x, y) = l$$

For the case where the neighbor pixels of (x, y) have more than one label numbers, our algorithm selects any one of the numbers, usually the minimum number. This process is repeated until all pixels are scanned.

Figure 61 (a) shows the first scanning of two-scan algorithm of two pixels in the first row of a binary image $\tilde{f}_2$, whose neighbor pixels under the mask have intensities equal to 0 as shown in Figure 61 (a), therefore, they are assigned by the new number, e.g., 2 and 3, respectively. The initial label number is set to 1, $l = 1$.

For example, the pixel at the second column on the first row, (x_1, y_1), whose neighbor pixels, $\forall\, (s,t)$ under the mask, E, of the current pixel at (x_1, y_1) are equal to 0, $\forall\, (s,t) \in E\, (x_1, y_1) | f_2(s,t) = 0$. Therefore, the intensity, $\tilde{f}_2(x_1, y_1)$, of the current pixel at (x_1, y_1) is labeled by the new number, $L(x_1, y_1) = l$+1 as shown in Figure 61 (b).

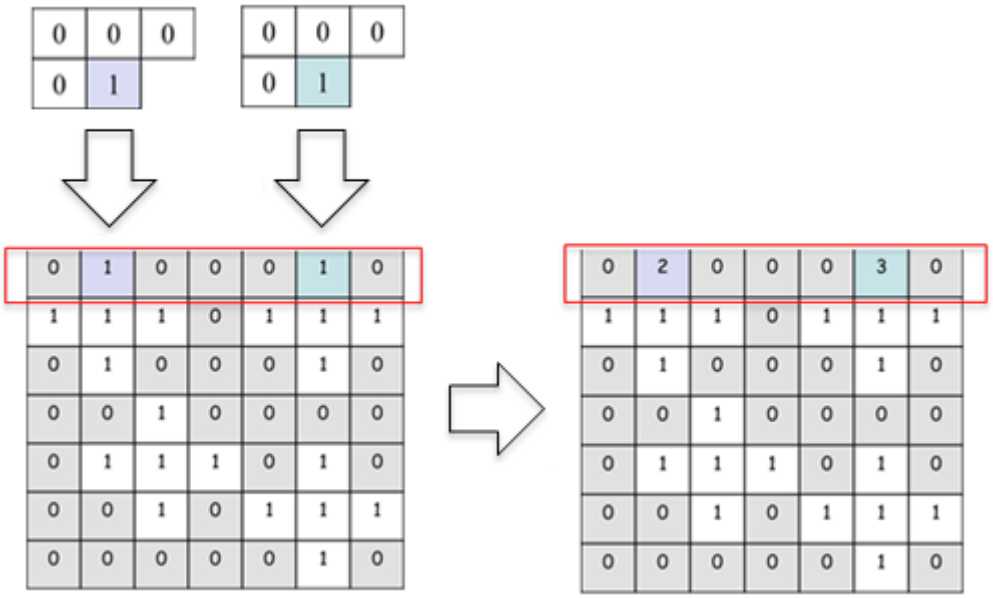

(a) (b)

Figure 61 (a) all pixels under the mask of current pixel at (x, y) of the second and the sixth columns in the first row have intensities equal to 0. Then, those pixels are labeled by the new number, e.g., 2 and 3 as the output image shown in (b)

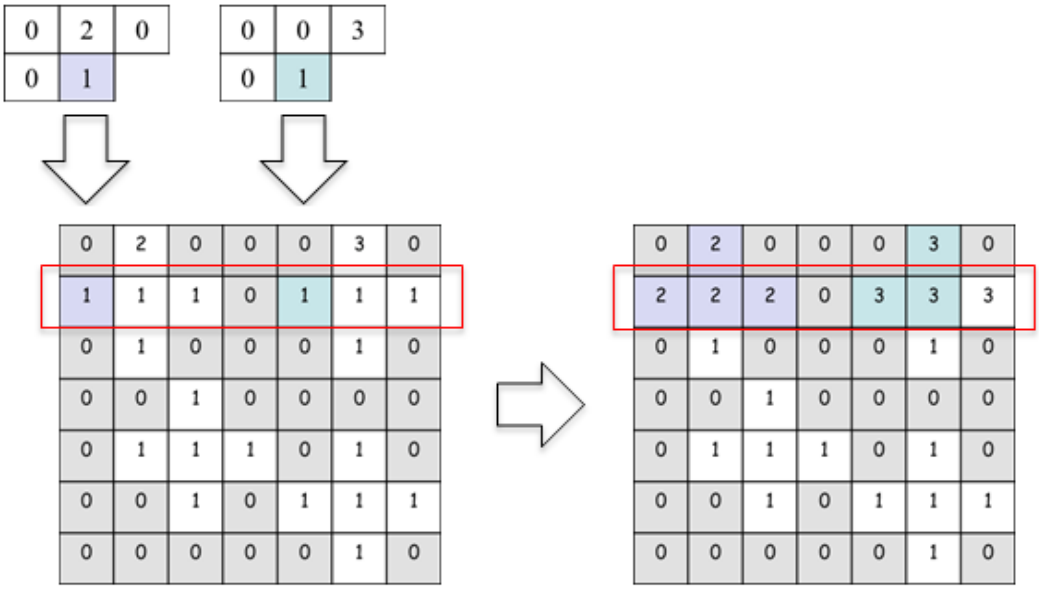

(a) Labeling operation on the second row of a binary image

(b) The result of labeling in the second row

Figure 62 (a) the current pixel at (x, y) in the second row of the first column contains some pixels under the mask whose intensities are not equal to 0, so that pixel is labeled by the same number as its neighbor pixel, e.g., 2 as shown in Figure (b)

Figure 62 (a) shows the first scanning of two-scan algorithm on the second row of a binary image. A given example of current pixel at (x_1, y_1) in the first column of the second row has some neighbor pixels, $\exists\,(s,t)$, under the mask E, whose intensities are not equal to 0, $\exists\,(s,t) \in E\,(x_1, y_1) | f_2(s,t) \neq 0$. Then, the intensity, $\tilde{f}_2(x_1, y_1)$ of the current pixel at (x_1, y_1) was labeled by the same number as its neighbors,$L(x_1, y_1) = L\,(s,t)$, where L is the labels of any pixels in the neighborhood under the mask of the current pixel. If the neighbor pixels under the mask have more than one labelling numbers, the labelling number of the current pixel is set equal to the minimum number. The labeling results are shown in Figure 62 (b).

After the first scan of two-scanning algorithm is finished, all foreground pixels are labeled by the new numbers as shown in Figure 63. As the result of the first scanning of two-scan algorithm includes two components such that one of them has more than one labeling numbers in the same component, e.g., 2 and 4. This problem can be resolved by applying the second scanning of the two-scanning algorithm.

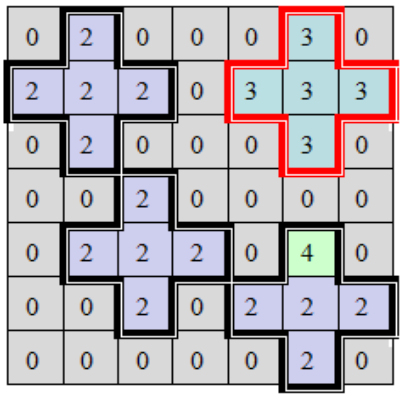

Figure 63 The process of first scanning is repeated until all the first pixels are scanned

In the second scanning, if the current pixel at (x, y) has more than one neighbor pixels under the mask with different labeling numbers then the different labeling numbers are connected together and the minimum labelling number is assign to this component.

For example, the current pixel at (x_2, y_2) in the fifth column of the sixth row as shown in Figure 64 (a) has two neighbor pixels under the mask with two different labelling numbers; i.e., 2 and 4, these pixels must be connected to the same component and the minimum labelling number is assigned to them. In this example, the minimum labelling number is 2 as shown in Figure 64 (b).

0	2	0	0	0	3	0
2	2	2	0	3	3	3
0	2	0	0	0	3	0
0	0	2	0	0	0	0
0	2	2	2	0	4	0
0	0	2	0	2	2	2
0	0	0	0	0	2	0

(a) The result of the first scanning

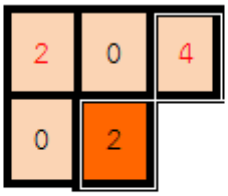

{2, 4}, the minimum label is 2

(b) The current pixel at (x_2, y_2) and its neighbors

Figure 64 During the second scanning, if there are different labeling numbers of the pixels under the mask, they should belong to the same component as shown in picture (b)

During the second scanning, all pixels of the same component will be labelled by the minimum labelling number of that component. Thus, labelling number 4 in Figure 65 is replaced by labelling number 2 as shown in Figure 66.

0	2	0	0	0	3	0
2	2	2	0	3	3	3
0	2	0	0	0	3	0
0	0	2	0	0	0	0
0	2	2	2	0	4	0
0	0	2	0	2	2	2
0	0	0	0	0	2	0

Figure 65 There are two different labeling numbers in the same component

0	2	0	0	0	3	0
2	2	2	0	3	3	3
0	2	0	0	0	3	0
0	0	2	0	0	0	0
0	2	2	2	0	2	0
0	0	2	0	2	2	2
0	0	0	0	0	2	0

Figure 66 The result of the second scanning of two-scan algorithm

The results from applying the two-scan algorithm are shown in Figures 67 (a) – (d). All components of oil palms and non-oil palms are shown by colors.

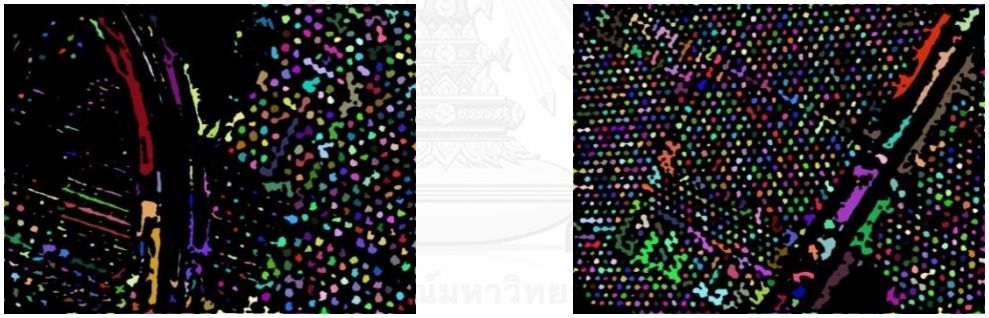

(a) (b)

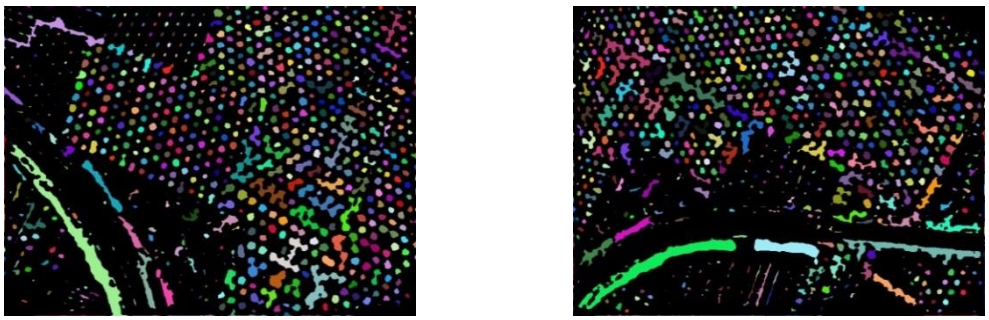

(c) (d)

Figure 67 The result images from 8-neighbor connected component labeling using the two-scan algorithm on binary images in Figures 57 (a) – (d)

However, there is still a problem with a binary image obtained from the previous step. There are pond, swamp, shrub, thick grass and weed in some images as shown in Figures 68 (a) – (d) which cannot be removed from an image because their intensity values are very close to the intensities of the trees. This problem can be solved by using normalized cross correlation template matching to match the texture of a template with each component as expressed in Equation (18).

$$R(x,y) = \frac{\sum_{i=0}^{W-1}\sum_{j=0}^{H-1}(t(i,j) \times C(x+i,y+j))}{\sqrt{\sum_{i=0}^{W-1}\sum_{j=0}^{H-1} t(i,j)^2 \times \sum_{i=0}^{W-1}\sum_{j=0}^{H-1} C(x+i,y+j)^2}} \quad (18)$$

where $t\ (i,j)$ represents a template of non-oil palm of size $W \times H$ and $C(x,y)$ represents each component.

If the size of a component is not equal to the size of a template, its size will be scale down to $W \times H$. While sliding the template on each pixel over a component, a matrix, $R(x,y)$, is calculated to represent the similarity between the template and the particular area of the component. Any component with similarity greater than 0.99 is considered as non-oil palm.

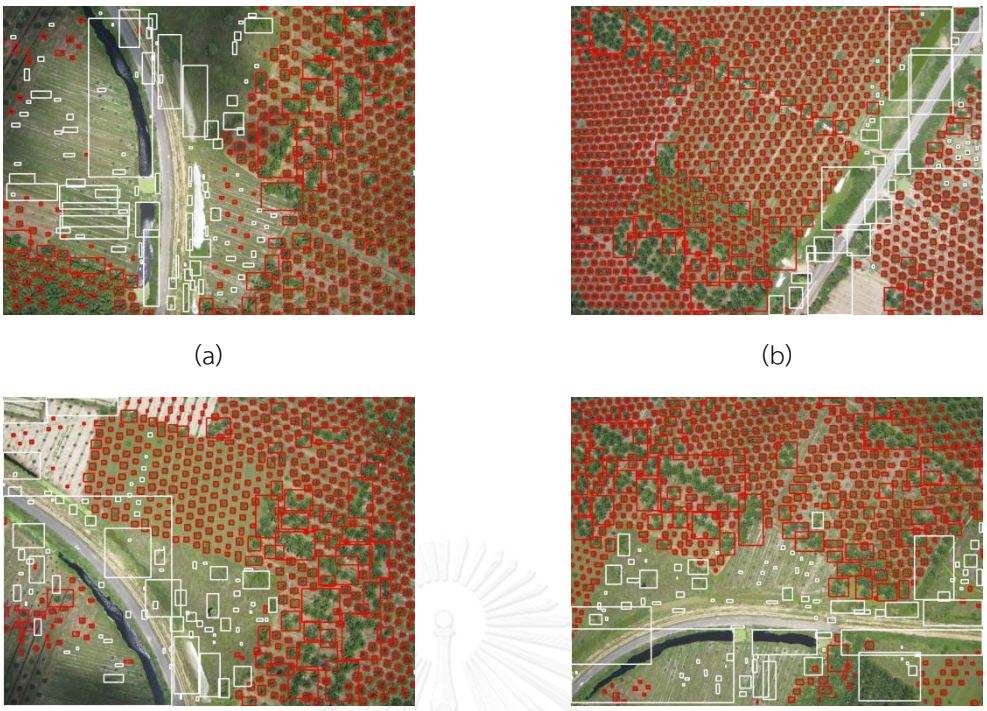

(a) (b)

(c) (d)

Figure 68 Some components of non-oil palm have been detected during the process of oil palm detection, such as pond, swamp, thick grass and weed. These components are marked by red color

However, there are some oil palms that are similar to the template and are removed from an image when applying normalized cross correlation because their intensities are close to those of non-oil palm templates as shown in Figures 68 (a) – (d).

(a) (b)

(c) (d)

Figure 69 the results of removing the components of none oil palm from an image in Figures 68 (a) – (d)

And there are also some non-oil palm components that have not been removed from an image after applying normalized cross correlation because their intensities are quite different from the non-oil palm templates as shown in Figures 69 (a) – (d).

3.4 Individual oil palm identification

The final step is to identify individual oil palms. The last problem that is needed to be solved is the oil palm stand. Even though the oil palm cultivation has a standard pattern, some oil palms are very close to each other. Instead of seeing individual oil palms from an aerial image, we see stands of oil palms. A stand of oil palm is generally a group of several oil palms that looks like a single oil palm, thus we have to separate them into individual oil palms.

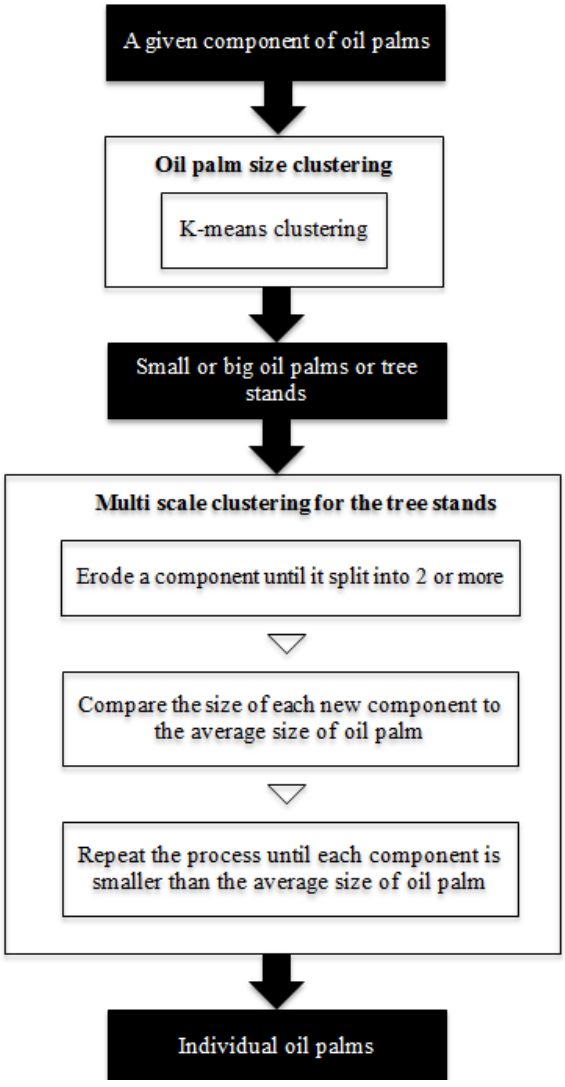

Figure 70 The process of individual oil palm identification

Figure 70 shows the individual oil palm identification. At first, K-means clustering is used to classify oil palms in an image into three clusters due to the fact that the sizes of oil palms in most of the images are different. Some are large and some are small. Thus, these three clusters represent small trees, large trees, and tree stands. The seed points for these three clusters are set to 30, 60, and 95 percentiles of the component's size, respectively.

Figures 71 (a) – (d) show the results of applying K-means clustering to the images in Figures 69 (a) – (d). The clusters of small and large oil palms are marked on the original image as single trees (individual oil palms), while the cluster of tree stands is needed to be forward to the proposed multi-scale clustering method which is used to separate individual oil palms from each tree stands.

(a) (b)

(c) (d)

Figure 71 The results from applying K-means clustering to separate oil palms into three clusters of small trees (green), big trees (yellow), and tree stands (red)

In the multi-scale clustering, each tree-stand component is passed to the multi-scale clustering algorithm in order to identify individual oil palms in a tree stand. The proposed multi-scale clustering for separating individual trees from each tree stand is as follows:

For each component of tree stands

- *Erode a component until it splits into two or more components or until the size of a component is smaller than the average oil palm size*
- *Compare the size of each new component to the average size of an oil palm*

  If it is smaller than the average oil palm

  Mark each component as a single oil palm on the original image

  Else

  Go back to the beginning
- *Repeat the process until each component is smaller than the average oil palm*

Firstly, the region of each tree stand from clustering with K-means from a binary image, $\tilde{f}$, is input into the multi-scale clustering. The region is eroded until it is split in two or more components or until the size of the region is smaller than the average oil palm. Each component's size is compared to the average oil palm. If the component's size is larger than the average oil palm, the component is input into the multi-scale clustering and the process is repeated until the size of each component is smaller than the average oil palm. This component is identified as an individual oil palm. The algorithm is repeated until all regions and components are smaller than the average oil palm. Figure 72 show an example of tree stands and its binary image and Figures 73(a)-(f) are the results of erosion and identification from the multi-scale clustering.

(a) the tree stands

(b) The region of tree stands on a binary image, $\tilde{f}$

Figure 72 An example of tree stands obtained from Figure 71 (a)

(a) The result of first erosion from Figure 72 (b) is on the left and the result of identification of individual oil palm is on the right

(b) The result of second erosion from Figrue 73 (a) is on the left and the result of identificaiton of individual oil palm is on the right

(c) The result of third erosion from Figrue 73 (b) is on the left and the result of identificaiton of individual oil palm is on the right

(d) The result of third erosion from Figrue 73 (c) is on the left and the result of identificaiton of individual oil palm is on the right

(e) The result of third erosion from Figrue 73 (d) is on the left and the result of identificaiton of individual oil palm is on the right

Figure 73 The process of erosion and identification in multi-scale clustering from Figure 72(a)

Figure 74 shows an example of a near-distance image with regions of tree stands. These regions are extracted from Figure 74 and are shown in Figures 75(a)-(d).

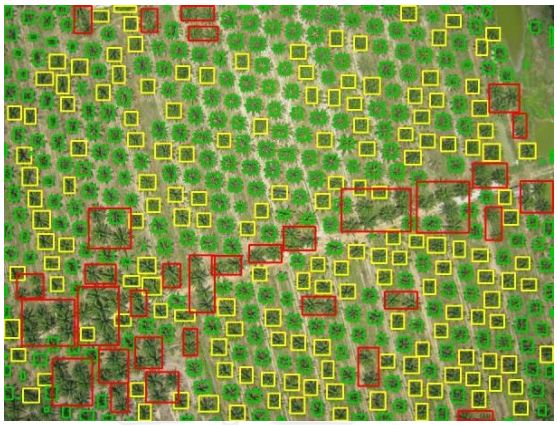

Figure 74 K-means clustering result of an aerial image

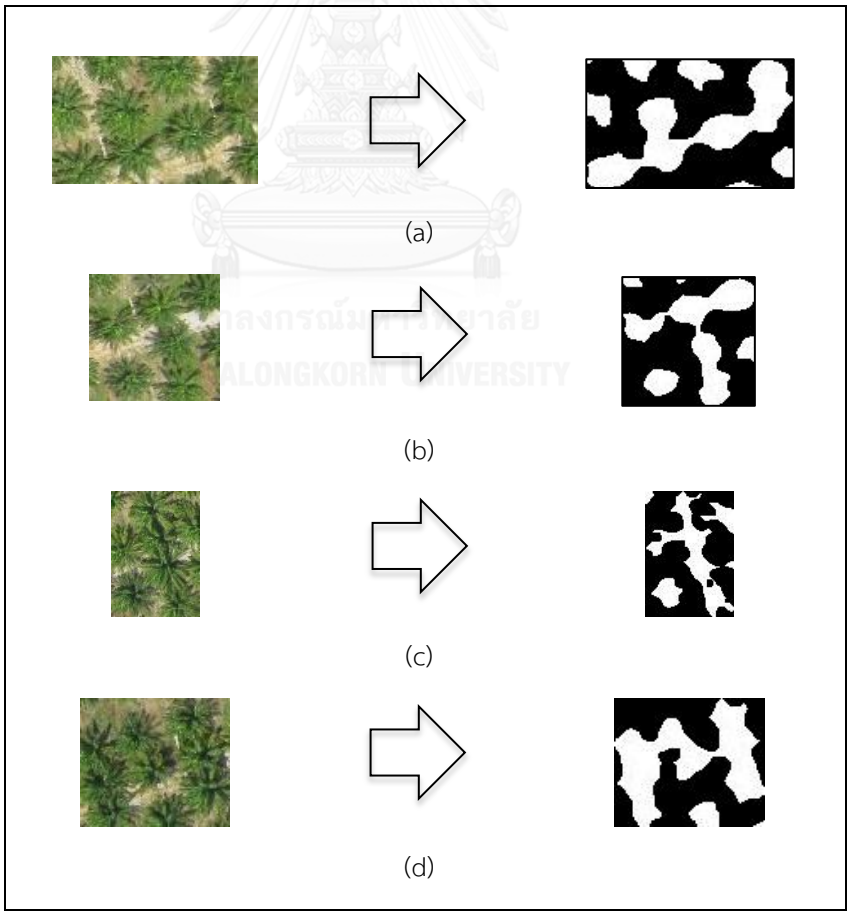

Figure 75 Example of tree stands obtained from K-means clustering and its regions obtained from a binary image, $\tilde{f}$

Figures 76(a)-(e) are the results of erosion and identification from the multi-scale clustering of tree stands obtained from Figure 75 (a). The tree stands from Figure 75 (a) is eroded until it splits to two or more components. Each component's size is compared to the average size of an oil palm. If the size is larger than the average, that component is input into the multi-scale clustering. This process is repeated until the size of a component is smaller than an oil palm. The results are shown in Figures 76(a)-(e).

(a) The result of first erosion from Figure 75 (a) is on the left and the result of identification of individual oil palm is on the right

(b) The result of second erosion from Figrue 76 (a) is on the left and the result of identificaiton of individual oil palm is on the right

(c) The result of third erosion from Figrue 76 (b) is on the left and the result of identificaiton of individual oil palm is on the right

(d) The result of forth erosion from Figrue 76 (c) is on the left and the result of identificaiton of individual oil palm is on the right

(e) The result of fifth erosion from Figrue 76 (d) is on the left and the result of identificaiton of individual oil palm is on the right

Figure 76 The process of erosion and identification in multi-scale clustering from Figure 75(a)

Finally, the results from the multi-scale clustering are shown in Figures 77 and 78.

Figure 77 The result of multi-scale clustering from Figure 74

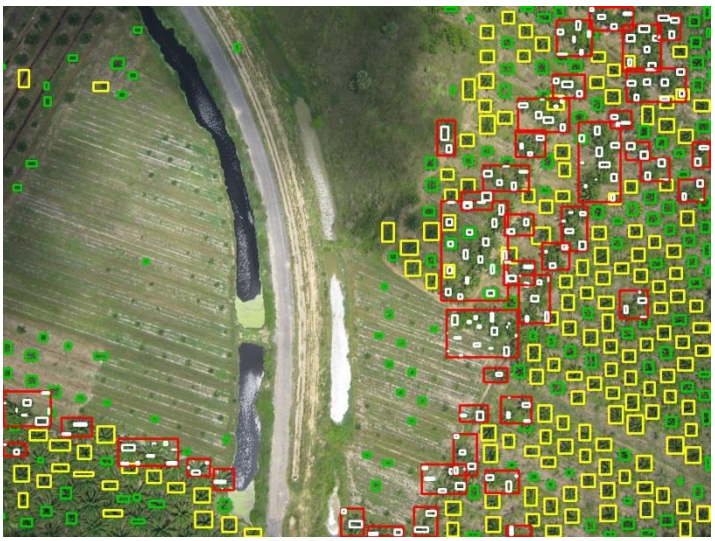

(a)

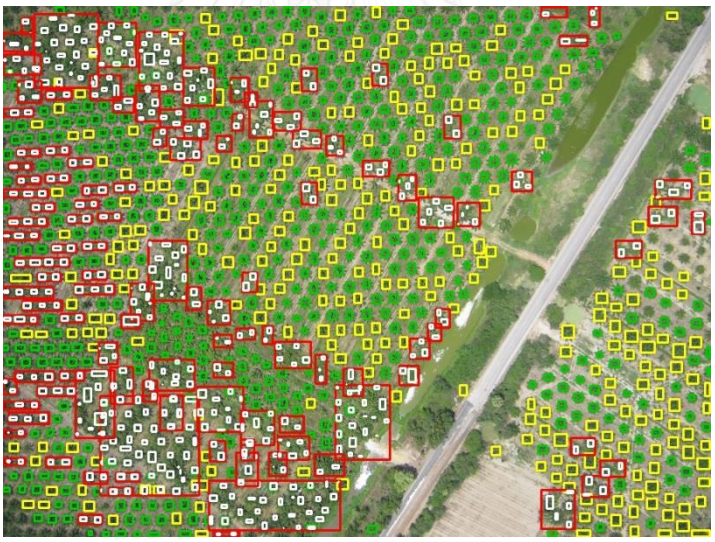

(b)

(c)

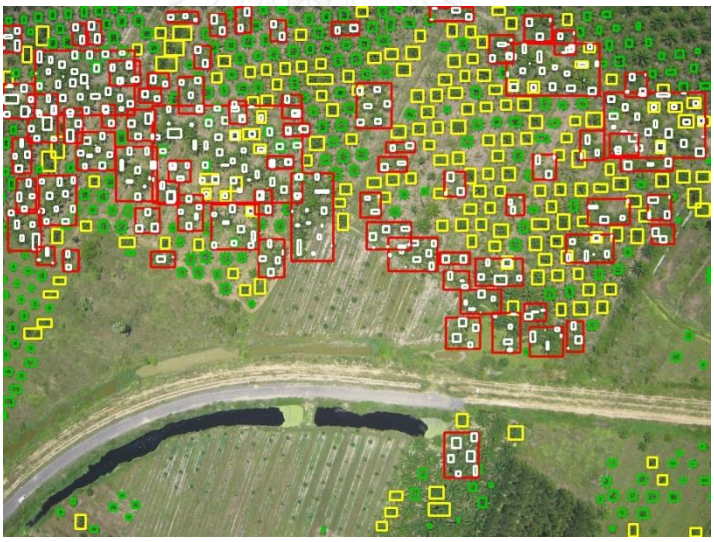

(d)

Figure 78 The results of multi-scale clustering from Figures 71 (a)-(d)

Chapter IV

Experimental Results and Discussion

The proposed methods for detecting and identifying individual oil palms were evaluated on a set of 21 digital aerial images captured by digital video camera mounted on the model airplane that was controlled to fly over the oil palm plantations with various elevation. Some images were taken from far distance and some images were taken from near distance. The location of the plantations are situated in the southern part of Thailand. The actual resolution of all aerial images is 3648×2736 pixels which were then converted to gray scale and were resized to 912×684 pixels. Most of the images do not contain only oil palms but also non-oil palm components, such as road, footpath, shrub, grass, weed, pond and swamp.

Table 1 shows the median sizes of oil palms obtained from 21 aerial images as shown in Figures 79 – 99. These median sizes are used to calculate the average size of the oil palms, $\bar{x}$, which is equal to 102.10 with standard deviation SD equals to 104.77.

Table 1: the median sizes of oil palms obtained from 21 aerial images

# Of aerial image	Figures	Sizes (Pixels)
1	79	55
2	80	53
3	81	57
4	82	65
5	83	50
6	84	72
7	85	63
8	86	41
9	87	33
10	88	32
11	89	41
12	90	77
13	91	72
14	92	60
15	93	56

# Of aerial image	Figures	Sizes (Pixels)
16	94	60
17	95	115
18	96	132
19	97	249
20	98	293
21	99	468

Figures 79 - 99 show the median-size oil palms that are marked by red rectangle. An image is determined as near- or far-distance by comparing the median-size oil palm of each image with the threshold size. The threshold size is set equal to the average-size oil palm plus standard deviation. If the median-size oil palm is larger than the threshold size then an image is determined as a near-distance image and vice versa. For example, the median-size oil palm of the aerial image in Figure 87 is 468 which is larger than the threshold size which means that most of the oil palms are larger than the threshold size; therefore, this image is determined as a near-distance image. Whereas the median-size oil palm in Figure 67 is smaller than the threshold size, thus, this image is determined as a far-distance image.

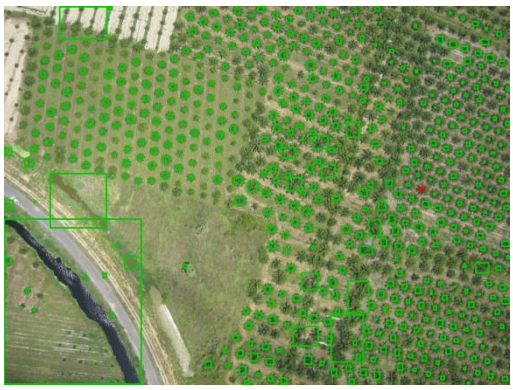

Figure 79 The far-distance aerial image with median-size oil palm smaller than the threshold size

Figure 80 The far-distance aerial image with median-size oil palm smaller than the threshold size

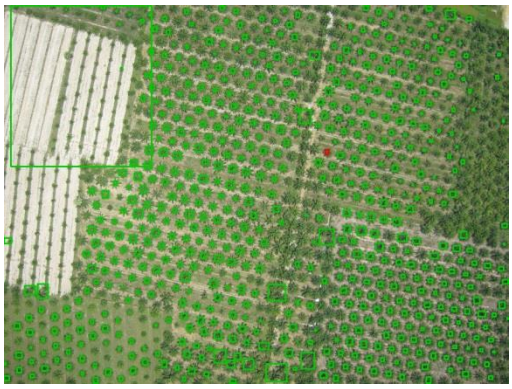

Figure 81 The far-distance aerial image with median-size oil palm smaller than the threshold size

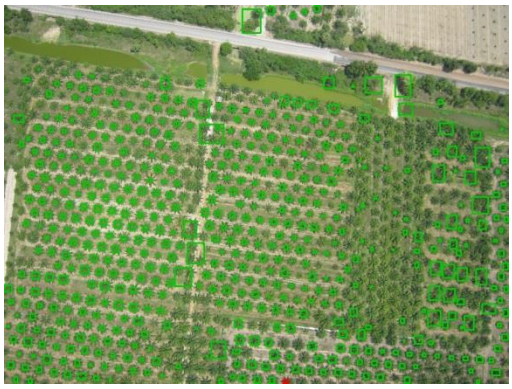

Figure 82 The far-distance aerial image with median-size oil palm smaller than the threshold size

Figure 83 The far-distance aerial image with median-size oil palm smaller than the threshold size

Figure 84 The far-distance aerial image with median-size oil palm smaller than the threshold size

Figure 85 The far-distance aerial image with median-size oil palm smaller than the threshold size

Figure 86 The far-distance aerial image with median-size oil palm smaller than the threshold size

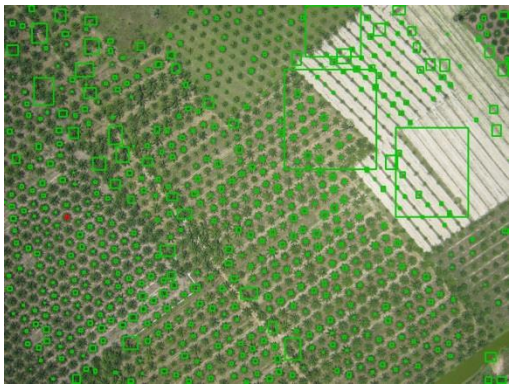

Figure 87 The far-distance aerial image with median-size oil palm smaller than the threshold size

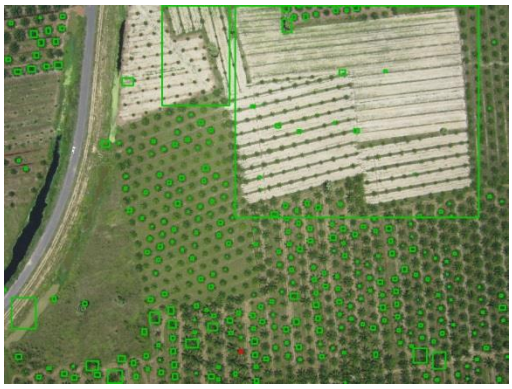

Figure 88 The far-distance aerial image with median-size oil palm smaller than the threshold size

Figure 89 The far-distance aerial image with median-size oil palm smaller than the threshold size

Figure 90 The far-distance aerial image with median-size oil palm smaller than the threshold size

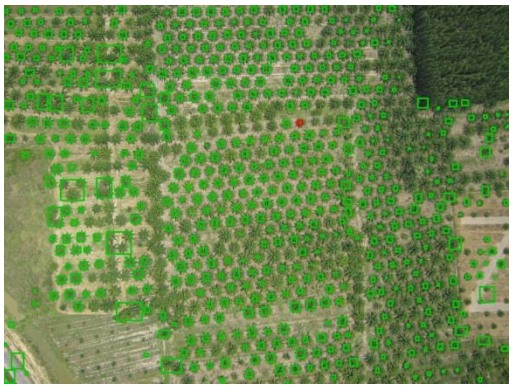

Figure 91 The far-distance aerial image with median-size oil palm smaller than the threshold size

Figure 92 The far-distance aerial image with median-size oil palm smaller than the threshold size

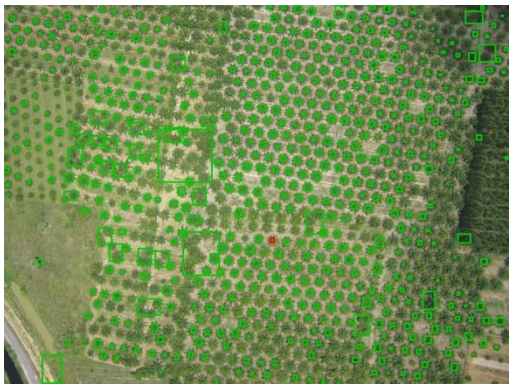

Figure 93 The far-distance aerial image with median-size oil palm smaller than the threshold size

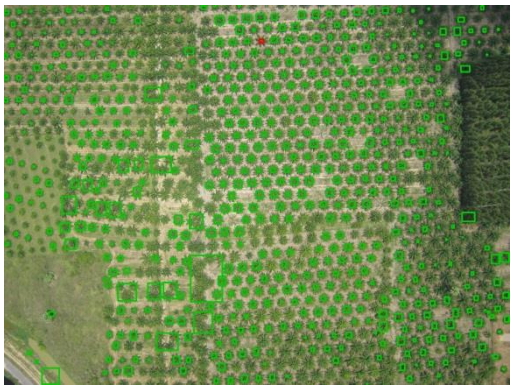

Figure 94 The far-distance aerial image with median-size oil palm smaller than the threshold size

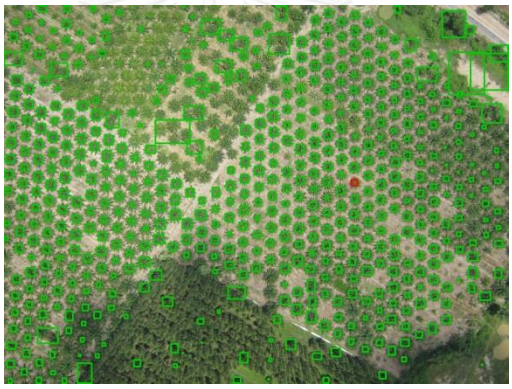

Figure 95 The near-distance aerial image with median-size oil palm larger than the threshold size

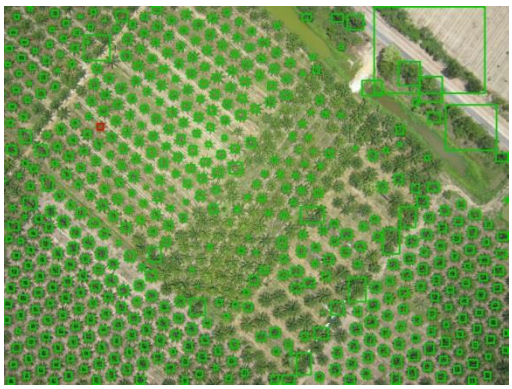

Figure 96 The near-distance aerial image with median-size oil palm larger than the threshold size

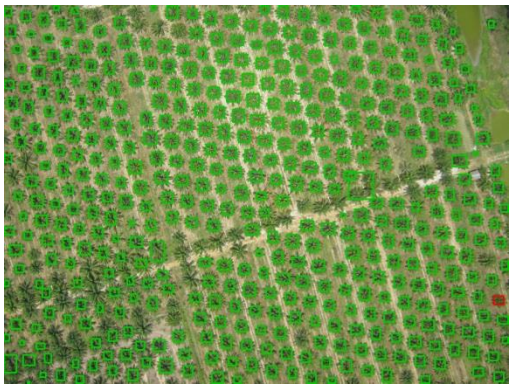

Figure 97 The near-distance aerial image with median-size oil palm larger than the threshold size

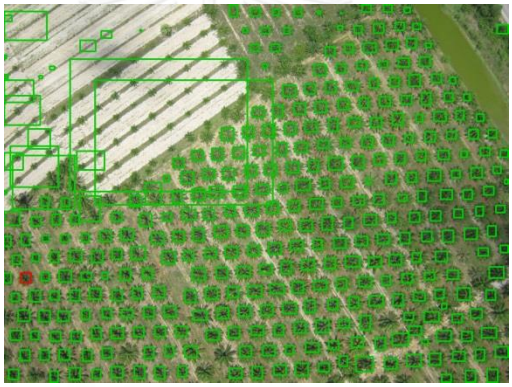

Figure 98 The near-distance aerial image with median-size oil palm larger than the threshold size

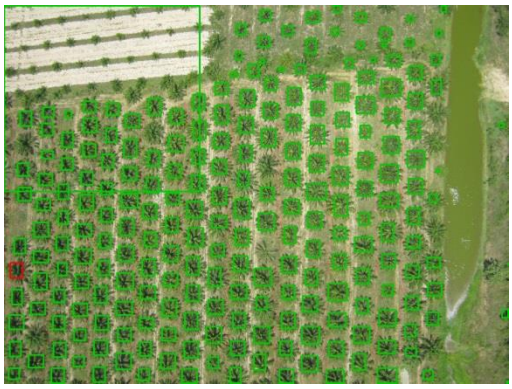

Figure 99 The near-distance aerial image with median-size oil palm larger than the threshold size

After each image is classified as either near- or far-distance image, the next step is to detect oil palms from each image. However, the results from oil palm detection detect not only individual oil palms but also oil palm stands, and other non-oil palm components as shown in Figure 100 (a)-(l).

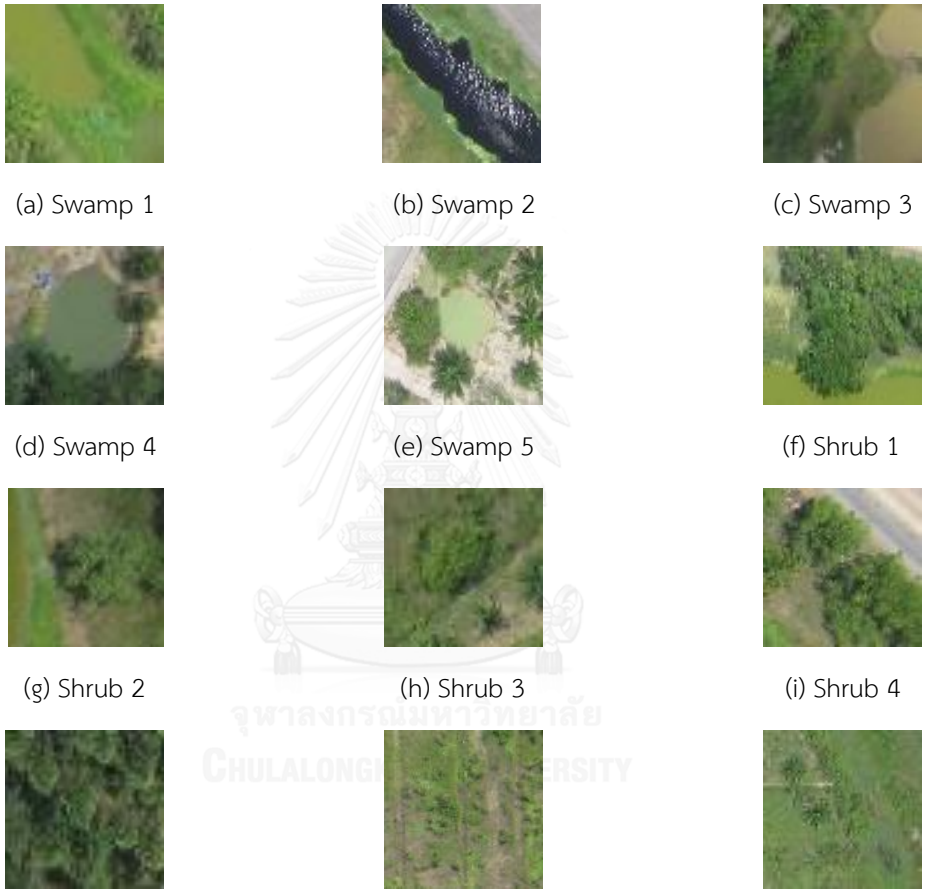

(a) Swamp 1 (b) Swamp 2 (c) Swamp 3

(d) Swamp 4 (e) Swamp 5 (f) Shrub 1

(g) Shrub 2 (h) Shrub 3 (i) Shrub 4

(j) Other trees (k) Weed (l) Thick grass

Figure 100 The appearance of all kinds of components in plantation areas

There are five kinds of non-oil palm components in plantation area as shown in Figure 100 that are detected as oil palms. They are pond or swamp, shrub, other trees, weed, and thick grass. A color or intensity of a swamp (as shown in Figures 100(a)-(5)) might or might not be similar to an oil palm but it is always detected as an oil palm. The second kind of non-oil palm component is a shrub that looks similar to an oil palm and its color or intensity is very close to an oil palm (as shown in Figures 100(f)-(i)) is always detected as an oil palm. The third kind of non-oil palm components are other trees as shown in Figure 100(j). They are also detected as oil palms because their color or intensities and shapes are similar to an oil palm. The forth non-oil palm component is a bunch of weeds (as shown in Figure 100(k)) that is also detected as an oil palm because of its shape and color. The last kind of non-oil palm component is thick grass (as shown in Figure 100(l)) that may be detected as an oil palm if it is dense.

In order to remove these non-oil palm components, normalized cross correlation is applied to the detection results by using Figures 100(a)-(l) as the templates. Any component that are correlated with the templates are removed from an image. However, Figures 101 (a) – 105 (a) show some of the non-oil palm components surrounded by purple boxes that cannot be removed and they are also identified as oil palms from using K-means clustering in oil palm identification. The K-means clustering classifies identified components into three clusters: small tree(green box), big tree(yellow box), and tree stand(red box). Figures 101(a)-105(a) show images that contain non-removable non-oil palm components which are passed to the K-means clustering to classify the size of each component. The oil palms are classified correctly, while the non-oil palm components are also classified as small oil palms which lead to false detection as shown in Figure 101(b)-105(b).

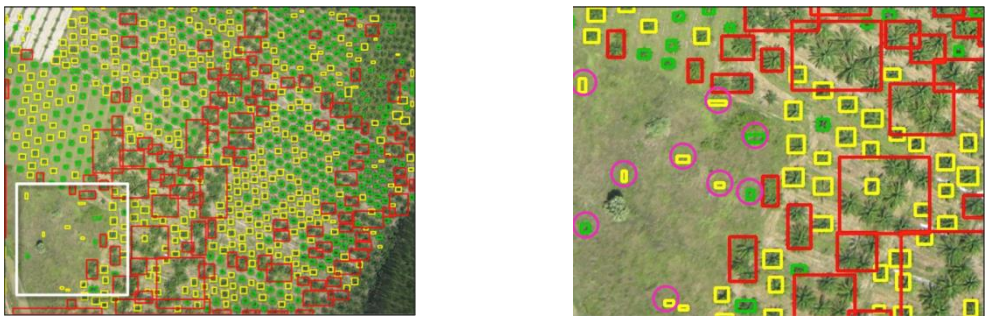

(a) Identification results (b) Enlarged region of the white box in (a)

Figure 101 The results from oil palm identification: (a) the result of using K means clustering to classify small tree, big tree and tree stands; (b) enlarged region where false detection occurs from non-removable non-oil palm components

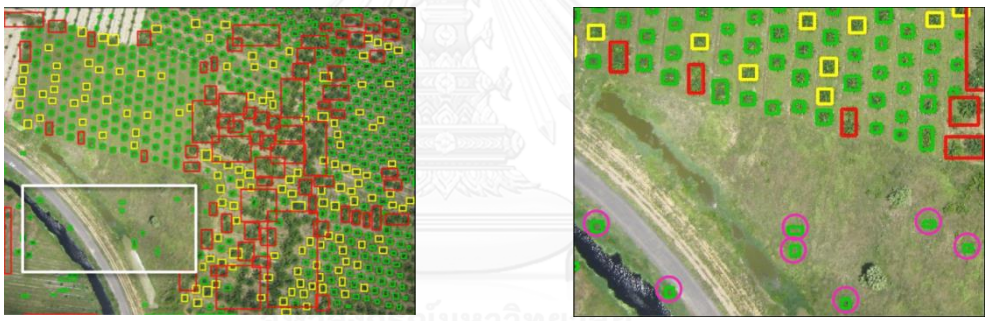

(a) Identification results (b) Enlarged region of the white box in (a)

Figure 102 The results from oil palm identification: (a) the result of using K means clustering to classify small tree, big tree and tree stands; (b) enlarged region where false detection occurs from non-removable non-oil palm components

(a) Identification results (b) Enlarged region of the white box in (a)

Figure 103 The results from oil palm identification: (a) the result of using K means clustering to classify small tree, big tree and tree stands; (b) enlarged region where false detection occurs from non-removable non-oil palm components

(a) Identification results (b) Enlarged region of the white box in (a)

Figure 104 The results from oil palm identification: (a) the result of using K means clustering to classify small tree, big tree and tree stands; (b) enlarged region where false detection occurs from non-removable non-oil palm components

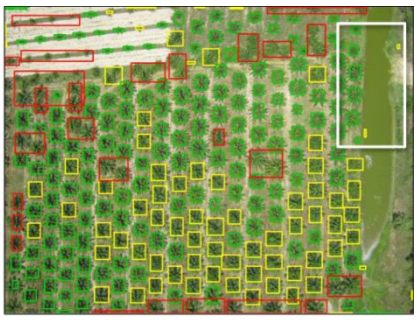

(a) Identification results

(b) Enlarged region of the white box in (a)

Figure 105 The results from oil palm identification: (a) the result of using K means clustering to classify small tree, big tree and tree stands; (b) enlarged region where false detection occurs from non-removable non-oil palm component**s**

Because tree stands obtained from the previous step consist of several oil palms which are needed to be separated into individual oil palms before counting the total number of oil palms; therefore, the multi-scale clustering is applied to each tree stand in these images. The results after applying the multi-scale clustering are shown in Figures 106 – 110. Figures 106(b)-110(b) show the enlarged images of Figures106 (a)-110(a) where each tree stand (red box) is separated into individual oil palms (white box).

(a) The result from applying multi-scale clustering to Figure 101 (a)

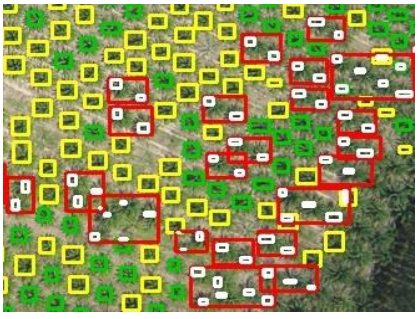

(b) Enlarged image of (a)

Figure 106 (a) The result from using multi-scale clustering to separate individual oil palms from tree stands

(a) The result from applying multi-scale clustering to Figure 102 (a)

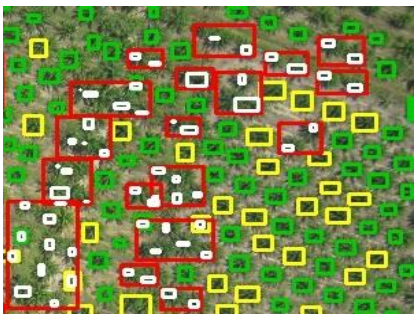

(b) Enlarged image of (a)

Figure 107 (a) The result from using multi-scale clustering to separate individual oil palms from tree stands

(a) The result from applying multi-scale clustering to Figure 103 (a)

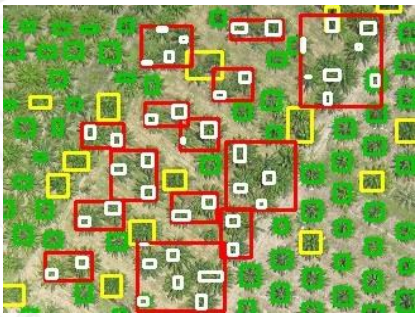

(b) Enlarged image of (a)

Figure 108 (a) The result from using multi-scale clustering to separate individual oil palms from tree stands

(a) The result from applying multi-scale clustering to Figure 104 (a)

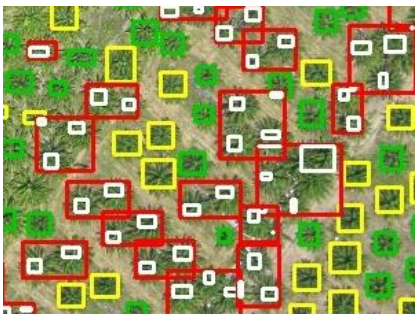

(b) Enlarged image of (a)

Figure 109 (a) The result from using multi-scale clustering to separate individual oil palms from tree stands

(a) The result from applying multi-scale clustering to Figure 105 (a)

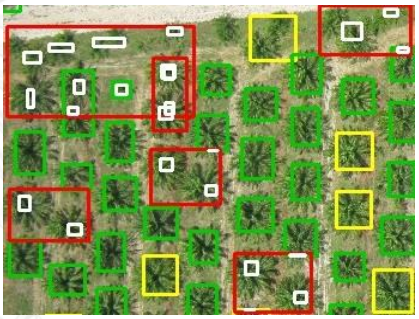

(b) Enlarged image of (a)

Figure 110 (a) The result from using multi-scale clustering to separate individual oil palms from tree stands

In order to evaluate the proposed method, the population of oil palms is counted manually by marking each oil palms using any drawing tools as shown in Figure 111. In Figure 111(b), there are some uncounted oil palms(marked by red) along the edges of the image because they are not perfect. There are also young oil palms(marked by orange and blue) that are not counted because they are too young.

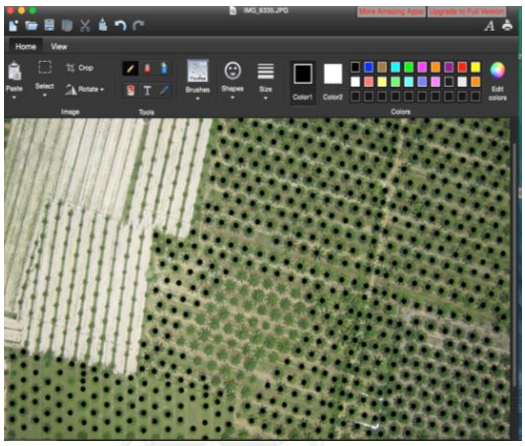

(a) Manually counted oil palms

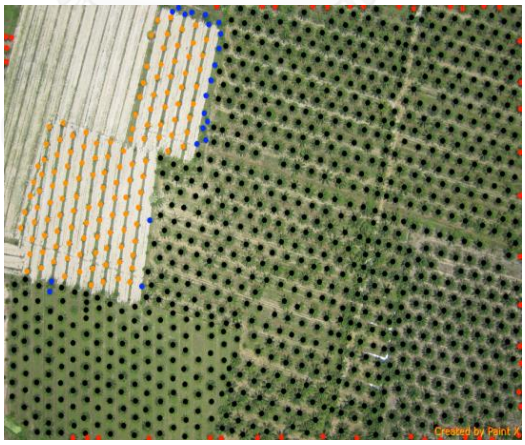

(b) Some uncountable oil palms

Figure 111 Manually counted oil palms: (a) counted oil palms and (b) some uncountable oil palms

Table 2 shows the total numbers of oil palms counted by the proposed method and the total numbers of oil palms that were manually counted from 21 images. There are two types of errors: the errors from false detection and the errors from false identification. The errors from false detection are caused during oil palm detection when non-oil palm components are detected as oil palms, thus, they are counted as oil palms. On the other hand, the errors from false identification are caused during oil palm identification when performing erosion in multi-scale clustering, some small trees in a tree stand disappear. Figure112 contains an example of false detection when non-oil palm components, such as small thick grass and weed (pink circles), are detected as oil palms; whereas, Figures 113 shows an example of false identification when two or more oil palms are detected as one oil palm (orange circles).

Table 2 The results for oil palm detection and identification using multi-scale clustering

Image no.	# of oil palms counted by the proposed method	# of oil palms counted manually	Errors from false detection	Errors from false identification	# of all errors	%Acc.	%Err.	Image types
1	1,117	1,168	12	20	32	97.13	2.86	Far
2	871	836	19	13	32	96.32	3.67	Far
3	961	1001	11	7	18	98.12	1.87	Far
4	936	966	8	20	28	97.00	2.99	Far
5	825	848	17	2	19	97.69	2.30	Far
6	547	573	12	8	20	96.34	3.65	Far
7	736	722	18	15	33	95.51	4.48	Far
8	1,094	1,103	16	18	34	96.89	3.10	Far
9	1,056	1,038	15	19	34	96.78	3.21	Far
10	880	850	19	13	32	96.36	3.63	Far
11	966	992	12	17	29	96.99	3.00	Far
12	755	757	10	23	33	95.62	4.37	Far
13	830	820	16	20	36	95.66	4.33	Far
14	920	940	20	24	44	95.21	4.78	Far
15	1,016	1,021	12	16	28	97.24	2.75	Far

Image no.	# of oil palms counted by the proposed method	# of oil palms counted manually	Errors from false detection	Errors from false identification	# of all errors	%Acc.	%Err.	Image types
16	996	1,002	17	18	35	96.48	3.51	Far
17	719	729	15	14	29	95.96	4.03	Far
18	761	742	6	18	24	96.84	3.15	Near
19	600	537	5	16	21	96.50	3.50	Near
20	467	421	7	16	23	95.07	4.92	Near
21	324	297	8	13	21	93.51	6.48	Near
				Average		96.34	3.64	

Figure 112 An example of false detection from K-means clustering

Figure 113 An example of false identification from multi-scale clustering

For false detection (pink circles) in Figure 112, the small thick grass and weed are detected as oil palms because their gray scale and texture are similar to oil palms; thus, they are kept during noise removal using low-pass filtering and they are identified as oil palms as the result. For false identification(orange circles) in Figure 113, the errors occur during multi-scale clustering when a tree stand is eroded until the size of the remaining tree stand is smaller than the average oil palm size. Some of these remaining tree stands contain two or more small oil palms that are smaller than the average oil palm, thus the erosion stops and these remaining tree stands are count as individual oil palms.

Figure 114(a)-(j) show the results obtained after each iteration of erosion. Figure 114(a) shows the result from the first erosion where the component in a circle is detached from the large component in the center of a region but it is not marked as an oil palm yet because its size is larger than the average size. Figure 114(b) shows the result from the second erosion where the component in a circle is detached from the large one and it is marked as an oil palm since its size is very close to the average. Figure 114(e) shows that after the fifth erosion, the size of the component in a circle is very close to the average size, thus it is marked as an oil palm. Figure 114(f) shows that the largest components is separated into two smaller component but they are not marked as oil palms because their sizes are larger than the average size. The erosion is repeated until the remaining components are smaller than the average size and thus causes the iteration to stop.

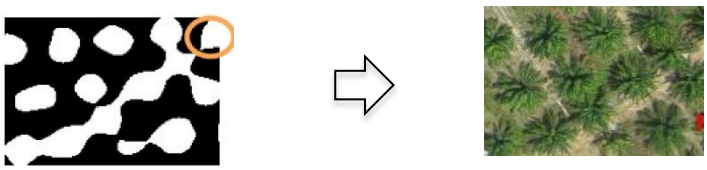

(a) The first erosion

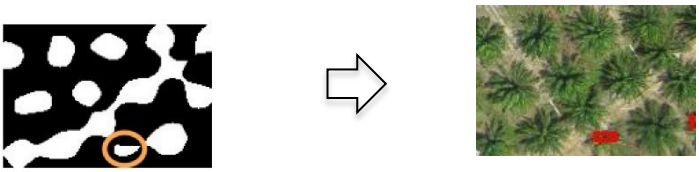

(b) The second erosion

(c) The third erosion

(d) The forth erosion

(e) The fifth erosion

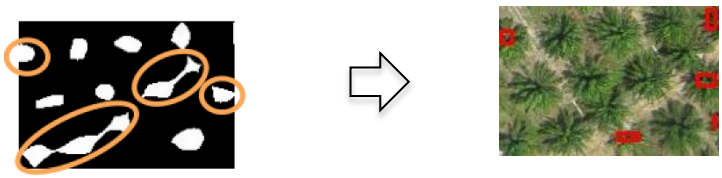

(f) The sixth erosion

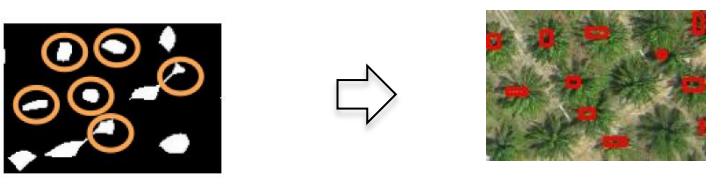

(g)The seventh erosion

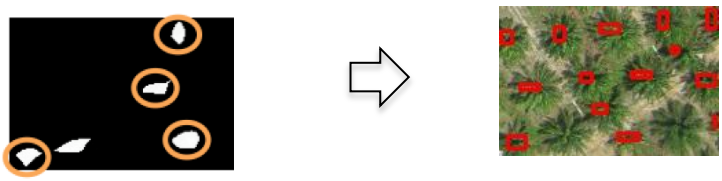

(h) The eighth erosion

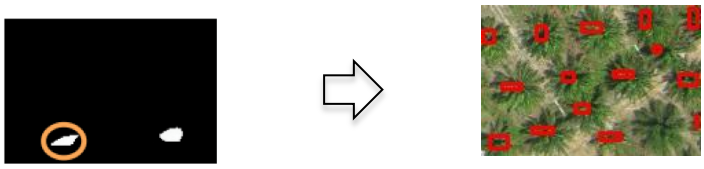

(i) The nine erosion

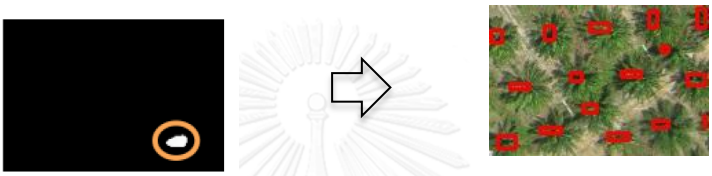

(j) The tenth erosion

Figure 114 Examples of multi-scale clustering results of tree stands from Figure 113 (blue circle)

Chapter V
Conclusion

This thesis presents new methods for oil palm detection and identification from aerial images using the multi-scale clustering and normalized cross correlation. The proposed methods are applied on 21 aerial images that were taken from near and far-distances. It can be seen that most of the images contain not only oil palms but also other non-oil palm components, such as other trees, shrubs, swamps, roads, weed and thick grass. These non-oil palm components have to be removed by using adaptive local thresholding, and template matching. Many different techniques are used to remove these non-oil palm components because they have different characteristics. Adaptive local thresholding is used to remove non-oil palm components that have different gray scale from oil palms. Template matching is used to remove non-oil palm components by matching each component in an image with non-oil palm templates using normalized cross correlation to calculate similarity. Finally, tree stands that contains two or more oil palms that are separated into individual oil palms using multi-scale clustering.

Table 2 from chapter 4 reveals there are two types of errors: false detection and false identification. The false detection occurs when small thick grass and weed in plantation areas are detected as oil palms because their intensity scales are very similar to oil palms. The adaptive local thresholding, and template matching techniques might not be able to completely remove all non-oil palm components, however, the average error from false detection of near-distance images is 1.40% and the average error from false detection of far-distance images is 1.68% which make the overall average error from false detection of 1.62% which is acceptable.

On the other hand, the false identification happens when two or more oil palms are identified as a single oil palm in multi-scale clustering method and when a single oil palm is identified as two or more individual oil palms. This false identification is the result from overlapped oil palms in tree stands that cannot be

separated into individual oil palms correctly. Some of the small oil palms are disappeared from an image during erosion; therefore, the total numbers of oil palms counted by our proposed methods are always less than the total numbers of oil palms counted manually. The average error from false identification of near-distance images is 1.68% and the average error from false identification of far-distance images is 1.76% which make the overall average error from false identification of 2.02% which is also acceptable. Thus, the total average error from false detection and false identification is 3.64% which is quite promising.

As the conclusions, the proposed methods work well when the images are near-distance images and the density of oil palms in tree stands is sparse.

The proposed method of oil palm detection and identification can be applied to aerial images which are in the color coded .jpg format. The method can classify the near and far distance images automatically based on the thresholding of the median size of oil palm extracted from the image.

This enhance the capability of detection and identification oil palms from many variation altitudes of the aerial images. It is clear that on the results of the proposed method, not only the variation of the altitudes of the captured images, but also oil palm of different sizes can be detected and identified correctly. This is because the proposed method does not rely only on the shape and size of oil palms, but the proposed method algorithm utilizes the texture of the preprocessed images for oil palm classification.

In addition, the proposed algorithm can also separate individual oil palms from oil palm stands using multi-scale clustering technique in order to count the number of oil palm in oil palm plantation.

In the future, we are trying to distinguish oil palms from the remaining non-oil palm components (e.g., small thick grass and weed) that cannot be removed by our proposed methods and to improve oil palm detection method in order to obtain better results. Most of the false detection errors are from identifying thick grass and weeds because there are small and contain fine details that is difficult for

normalization cross correlation to identify. We are trying to find other features that can be used to detect and identify oil palms which can be apply to both near- and far-distance images. Next, we would like to estimate the age of oil palms and to stich all the aerial images together to view the whole plantation area.

REFERENCES

1. Chen, G. and A. Zakhor. *2D tree Detection in Large Urban Landscapes using Aerial LiDar Data*. in *Image Processing (ICIP), 2009 16th IEEE International Conference*. 2009. Cairo: IEEE.
2. Forlani, G., et al., *Complete classification of raw LIDAR data and 3D reconstruction of buildings.* Pattern Analysis and Applications, 2006. **8**(4): p. 357-374.
3. Arasato, L.S., S. Amaral, and C.D. Rennó, *Detecting individual palm trees (Arecaceae family) in the Amazon rainforest using high resolution image classification*. 2011.
4. Charaniya, A.P., R. Manduchi, and S.K. Lodha, *Supervised Parametric Classification of Aerial LiDAR Data*, in *Computer Vision and Pattern Recognition Workshop*. 2004, IEEE. p. 30.
5. Yang, L., et al. *Tree detection from aerial imagery*. in *the 17th ACM SIGSPATIAL International Conference on Advances in Geographic Information Systems*. 2009.
6. Malek, S., et al., *Efficient Framework for Palm Tree Detection in UAV Images.* Selected Topics in Applied Earth Observations and Remote Sensing, 2014(12): p. 4692 - 4703.
7. Lowe, D.G., *Distinctive Image Features from Scale-Invariant Keypoints.* International Journal of Computer Vision, 2004. **60**(2): p. 91-110.
8. Huang, G.-B., L. Chen, and C.-K. Siew, *Universal approximation using incremental constructive feedforward networks with random hidden nodes.* Neural Networks, IEEE Transactions on Neural Networks, 2006. **17**(4): p. 879 - 892.
9. Huang, G.-B., et al., *Extreme Learning Machine for Regression and Multiclass Classification.* Systems, Man, and Cybernetics, Part B: Cybernetics, IEEE Transactions on Systems, Man, and Cybernetics, Part B: Cybernetics focuses on cybernetics, including communication and control across humans,

machines and organizations at the structural or neural level, 2011. **42**(2): p. 513 - 529.

10. Huang, G.-B., Q.-Y. Zhu, and C.-K. Siew, *Extreme learning machine: Theory and applications.* Neurocomputing - Selected Papers from the 7th Brazilian Symposium on Neural Networks (SBRN '04), 2006. **70**(1-3): p. 489-501.

APPENDIX

Appendix A

(a) (b)

Figure 115 (a) original aerial image and (b) the result from applying K-means clustering

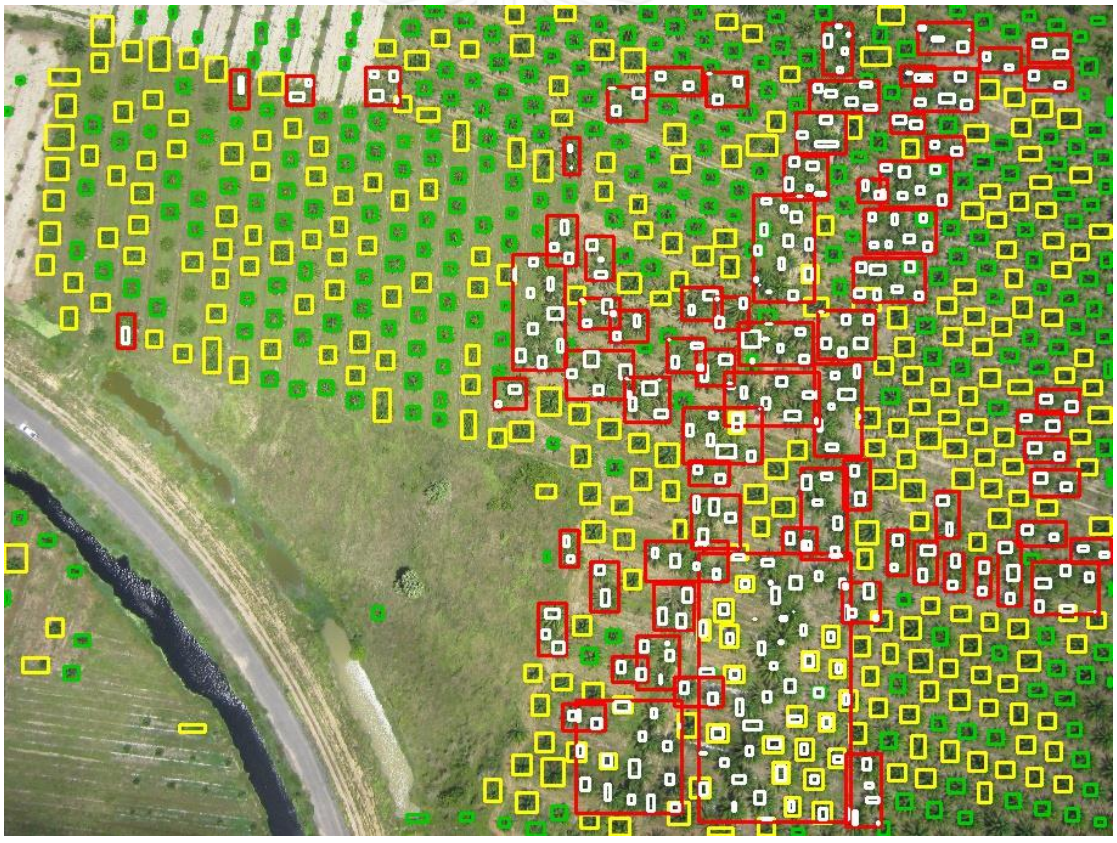

Figure 116 The result of multi-scale clustering from Figure 115 (b) including 272 small trees, 285 big trees, and 74 tree stands consist of 330 individual oil palms

(a) (b)

Figure 117 (a) original aerial image and (b) the result from applying K-means clustering

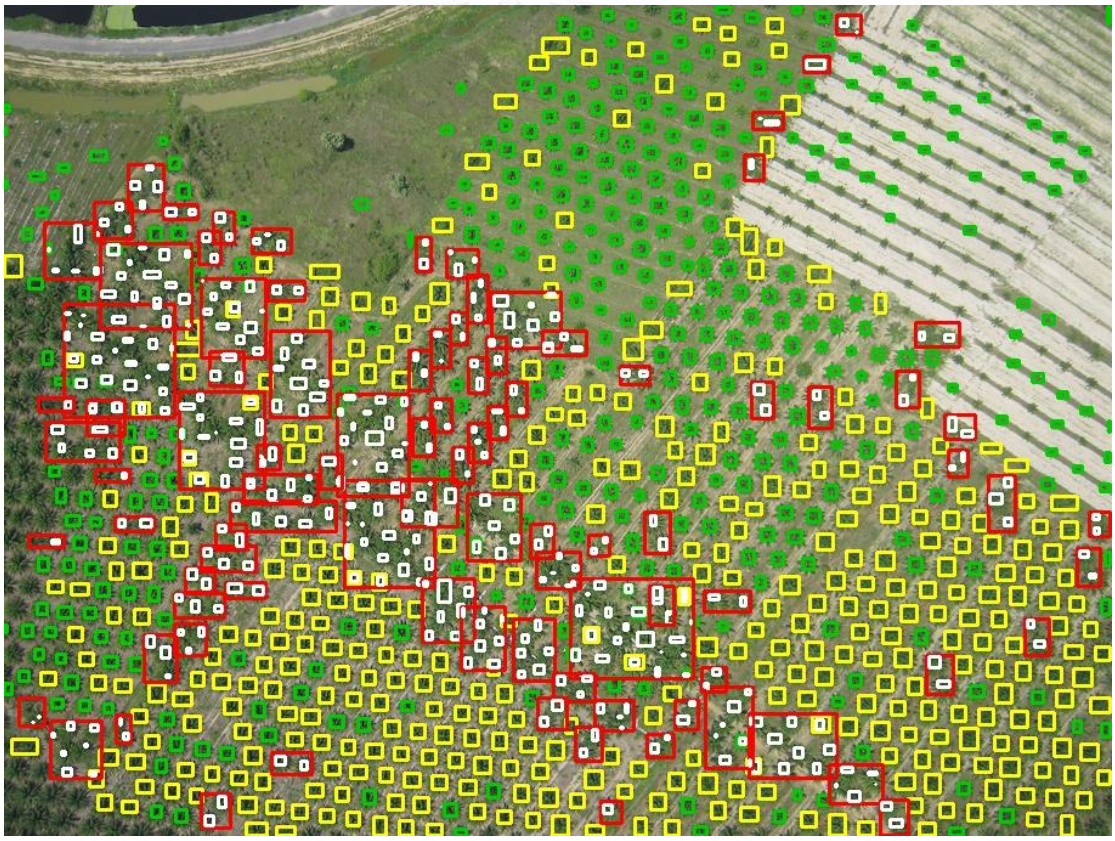

Figure 118 The result of multi-scale clustering from Figure 117 (b) including 383 small trees, 383 big trees, and 95 tree stands consist of 397 individual oil palms

(a) (b)

Figure 119 (a) original aerial image and (b) the result from applying K-means clustering

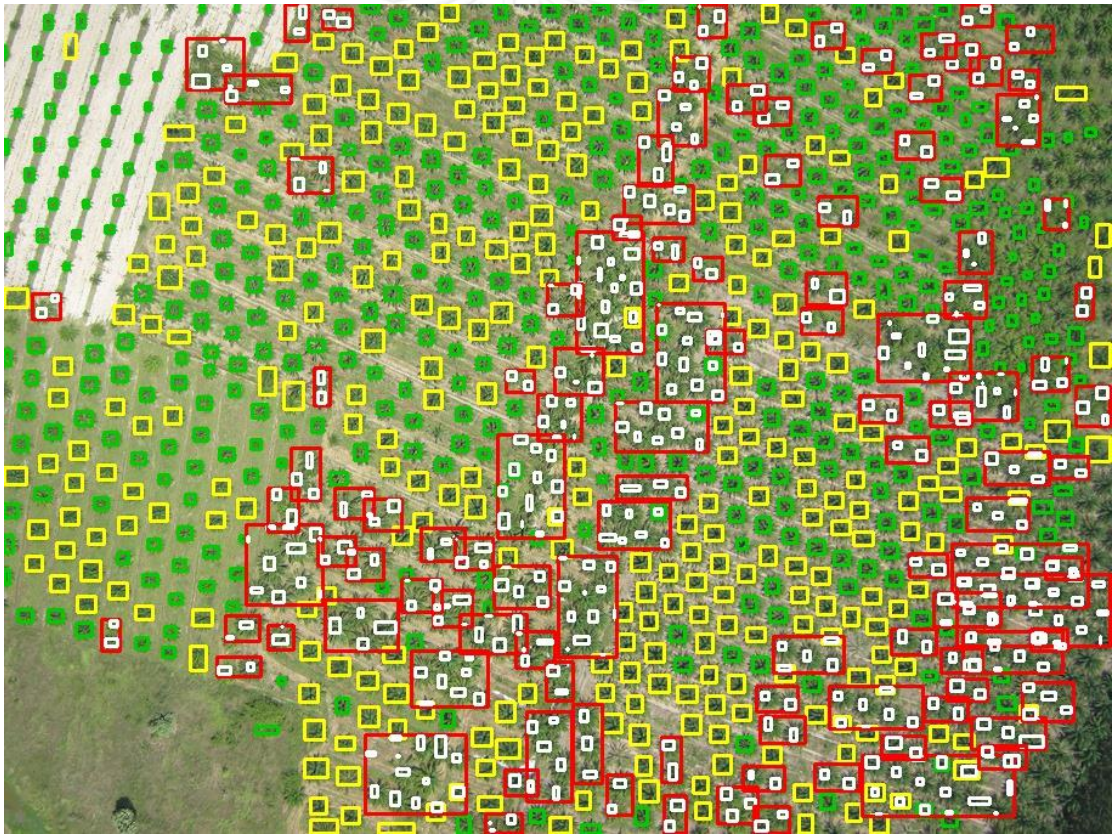

Figure 120 The result of multi-scale clustering from Figure 119 (b) including 403 small trees, 302 big trees, and 113 tree stands consist of 468 individual oil palms

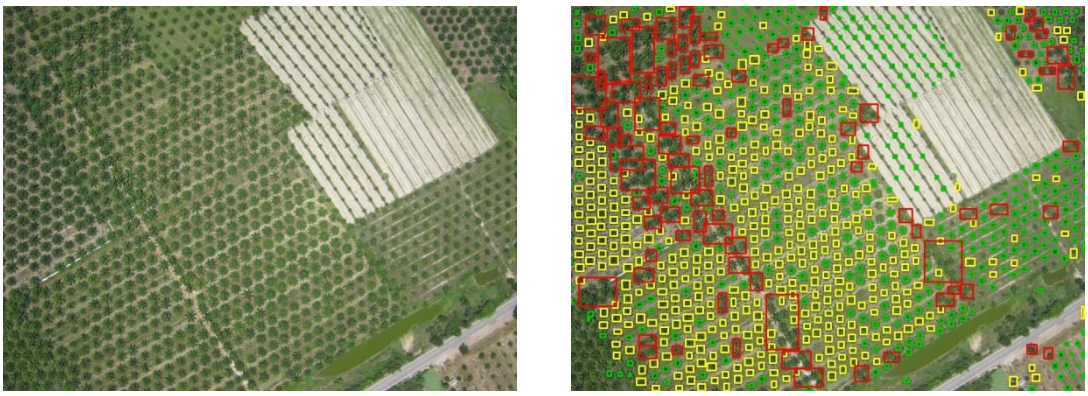

(a) (b)

Figure 121 (a) original aerial image and (b) the result from applying K-means clustering

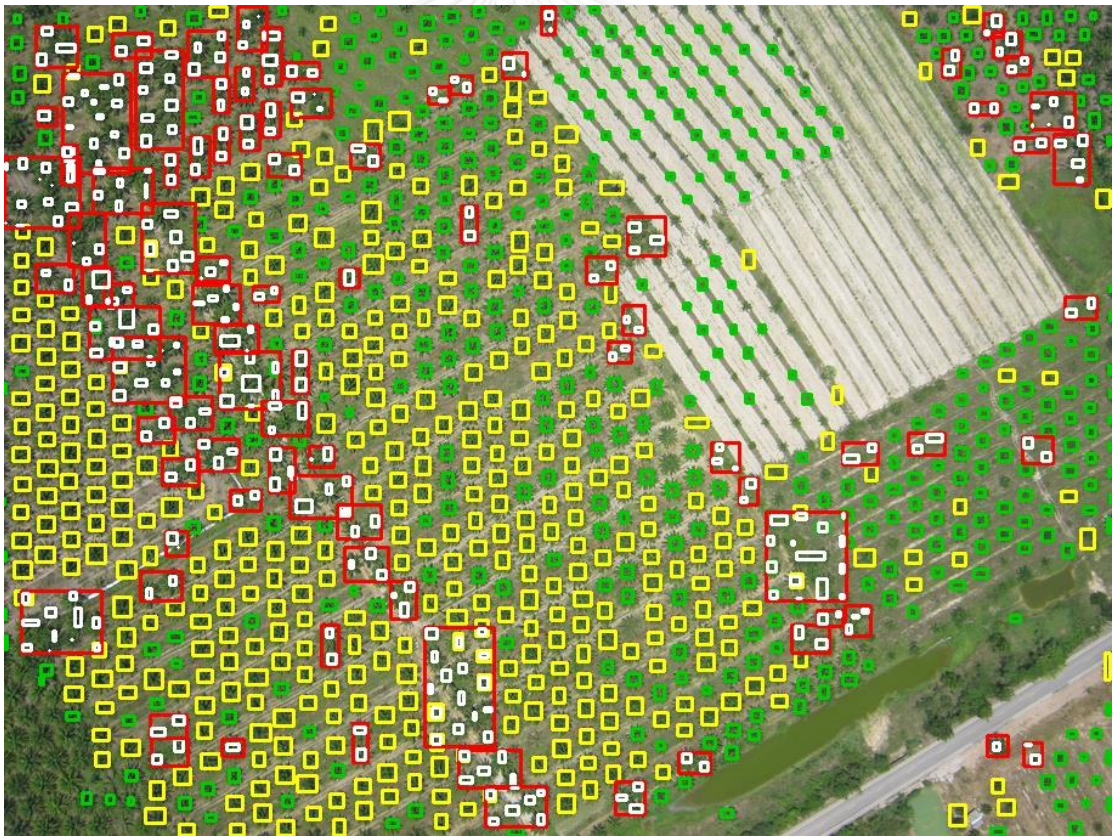

Figure 122 The result of multi-scale clustering from Figure 121 (b) including 428 small trees, 414 big trees, and 91 tree stands consist of 314 individual oil palms

(a) (b)

Figure 123 (a) original aerial image and (b) the result from applying K-means clustering

Figure 124 The result of multi-scale clustering from Figure 123 (b) including 241 small trees, 224 big trees, and 63 tree stands consist of 228 individual oil palms

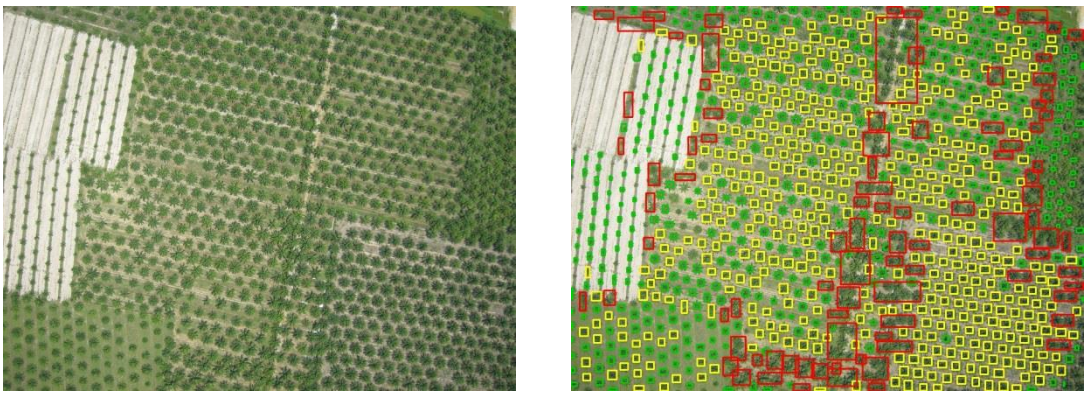

(a) (b)

Figure 125 (a) original aerial image and (b) the result from applying K-means clustering

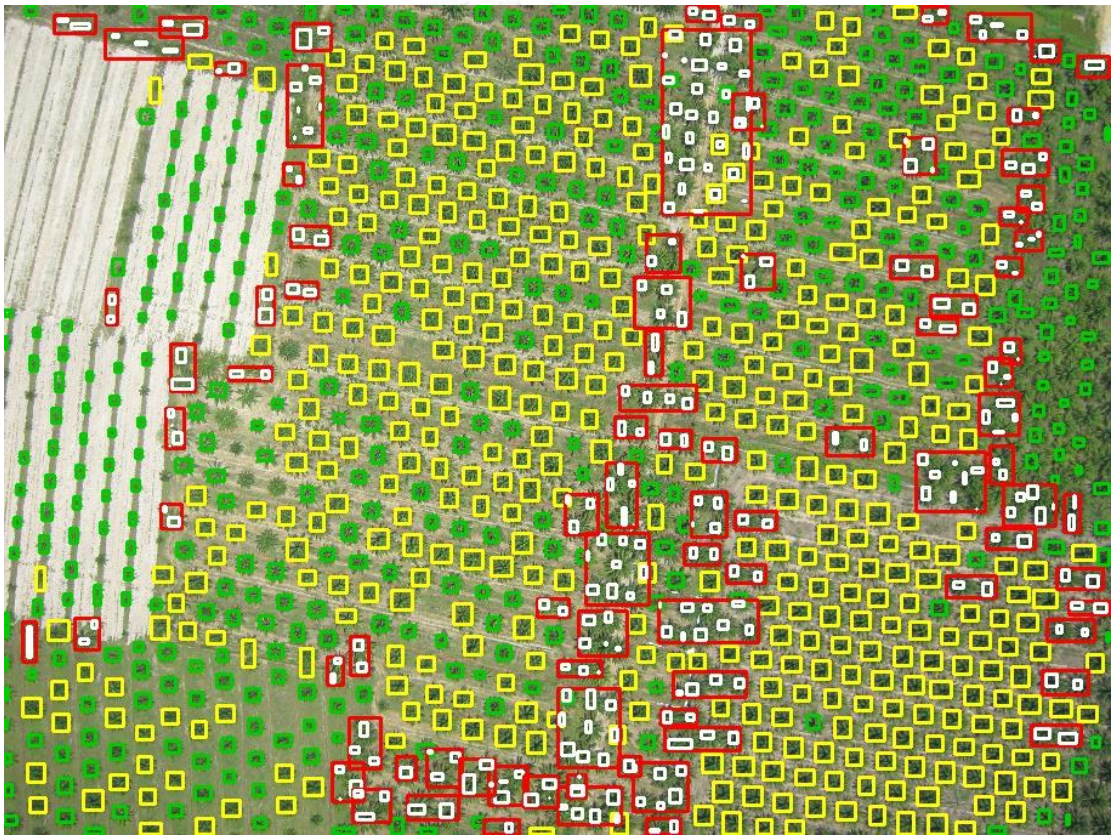

Figure 126 The result of multi-scale clustering from Figure 125 (b) including 382 small trees, 443 big trees, and 91 tree stands consist of 285 individual oil palms

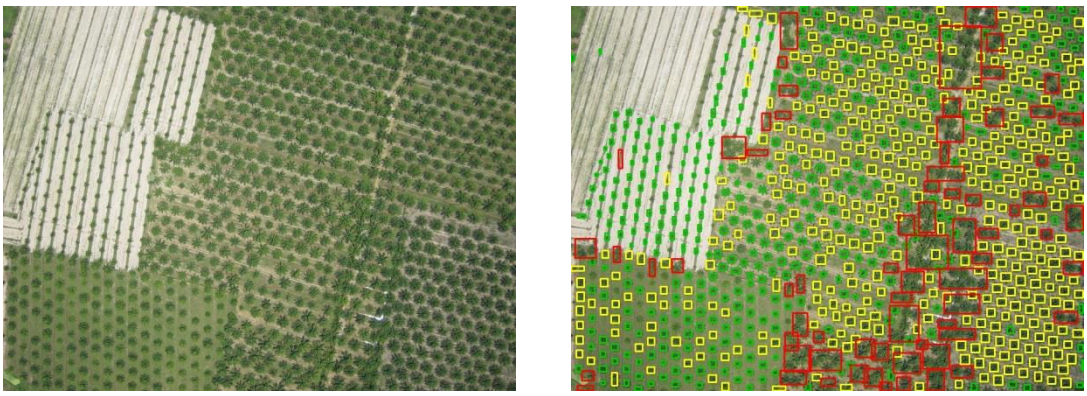

(a) (b)

Figure 127 (a) original aerial image and (b) the result from applying K-means clustering

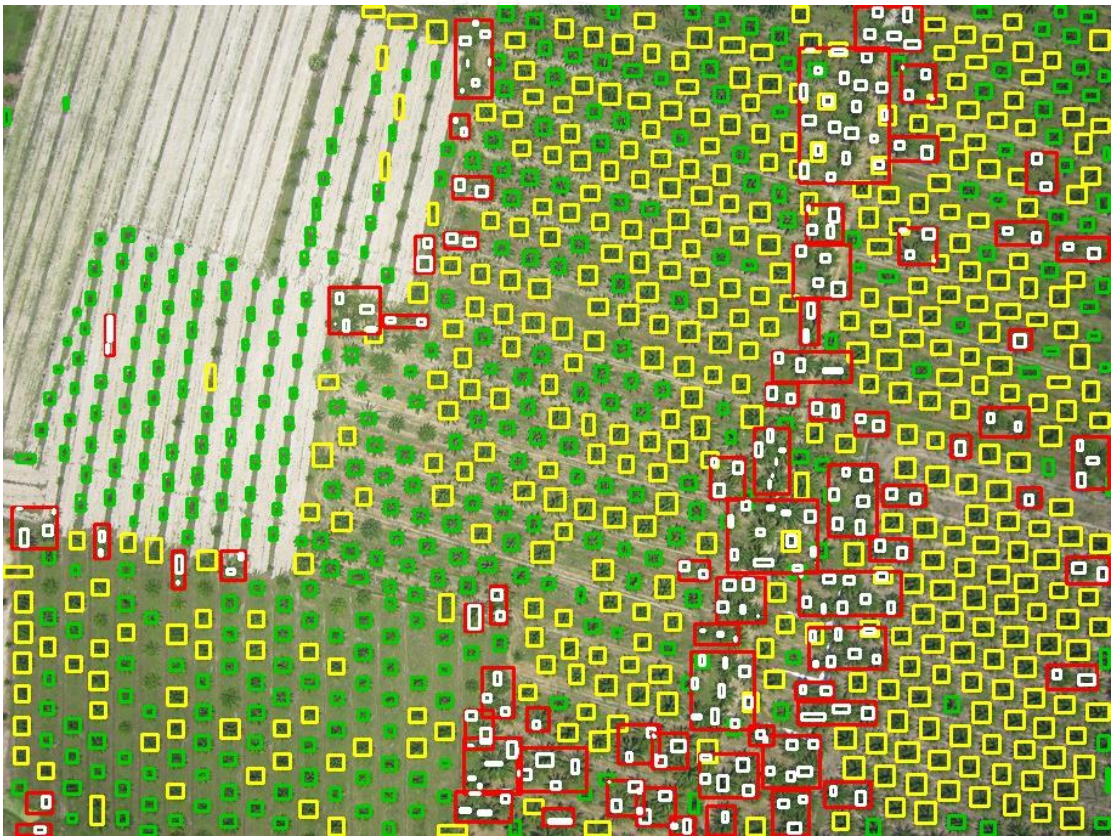

Figure 128 The result of multi-scale clustering from Figure 127 (b) including 373 small trees, 402 big trees, and 71 tree stands consist of 241 individual oil palms

(a) (b)

Figure 129 (a) original aerial image and (b) the result from applying K-means clustering

Figure 130 The result of multi-scale clustering from Figure 129 (b) including 328 small trees, 302 big trees, and 79 tree stands consist of 352 individual oil palms

(a) (b)

Figure 131 (a) original aerial image and (b) the result from applying K-means clustering

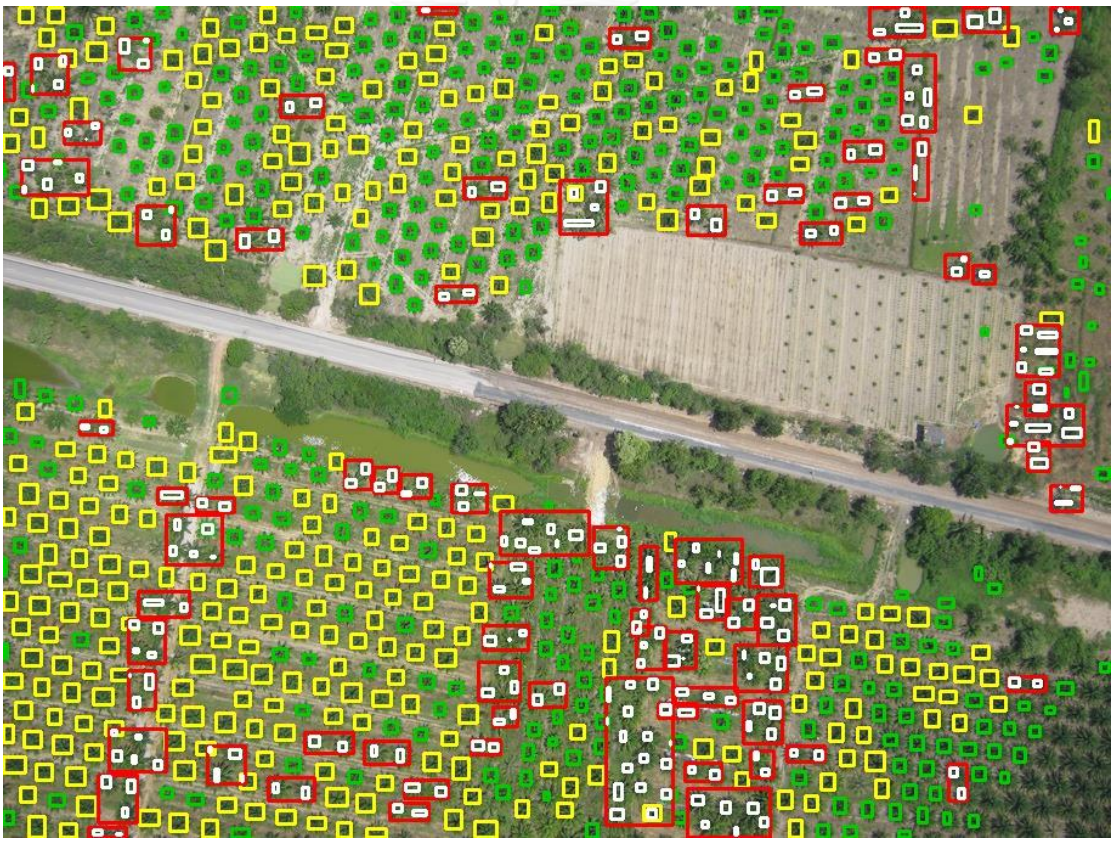

Figure 132 The result of multi-scale clustering from Figure 131 (b) including 322 small trees, 308 big trees, and 81 tree stands consist of 243 individual oil palms

(a) (b)

Figure 133 (a) original aerial image and (b) the result from applying K-means clustering

Figure 134 The result of multi-scale clustering from Figure 133 (b) including 335 small trees, 313 big trees, and 66 tree stands consist of 213 individual oil palms

(a) (b)

Figure 135 (a) original aerial image and (b) the result from applying K-means clustering

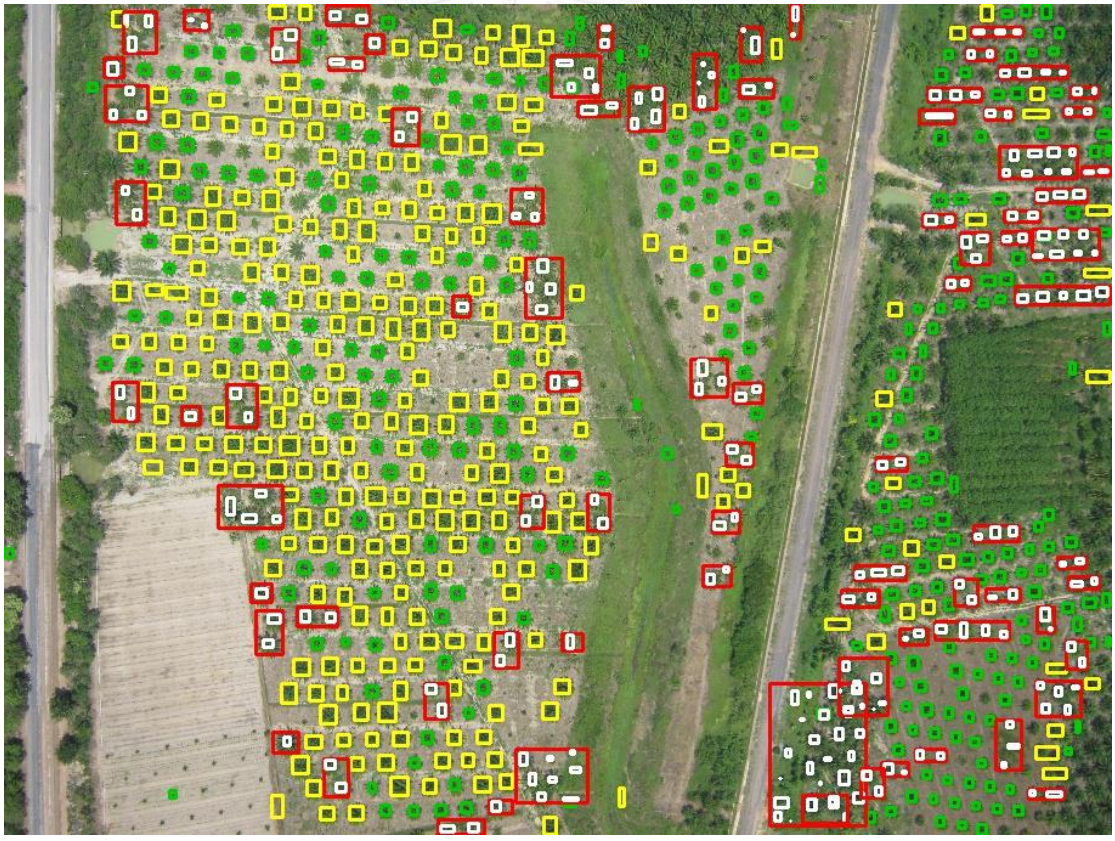

Figure 136 The result of multi-scale clustering from Figure 135 (b) including 313 small trees, 287 big trees, and 84 tree stands consist of 235 individual oil palms

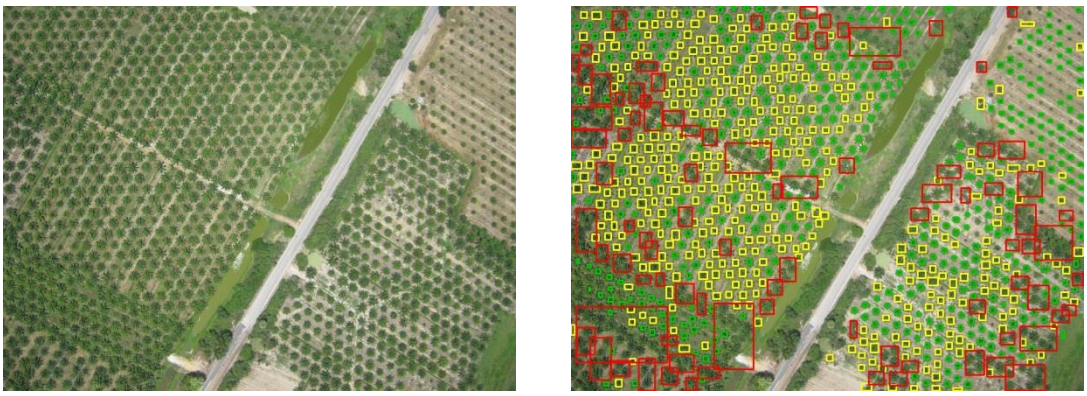

(a) (b)

Figure 137 (a) original aerial image and (b) the result from applying K-means clustering

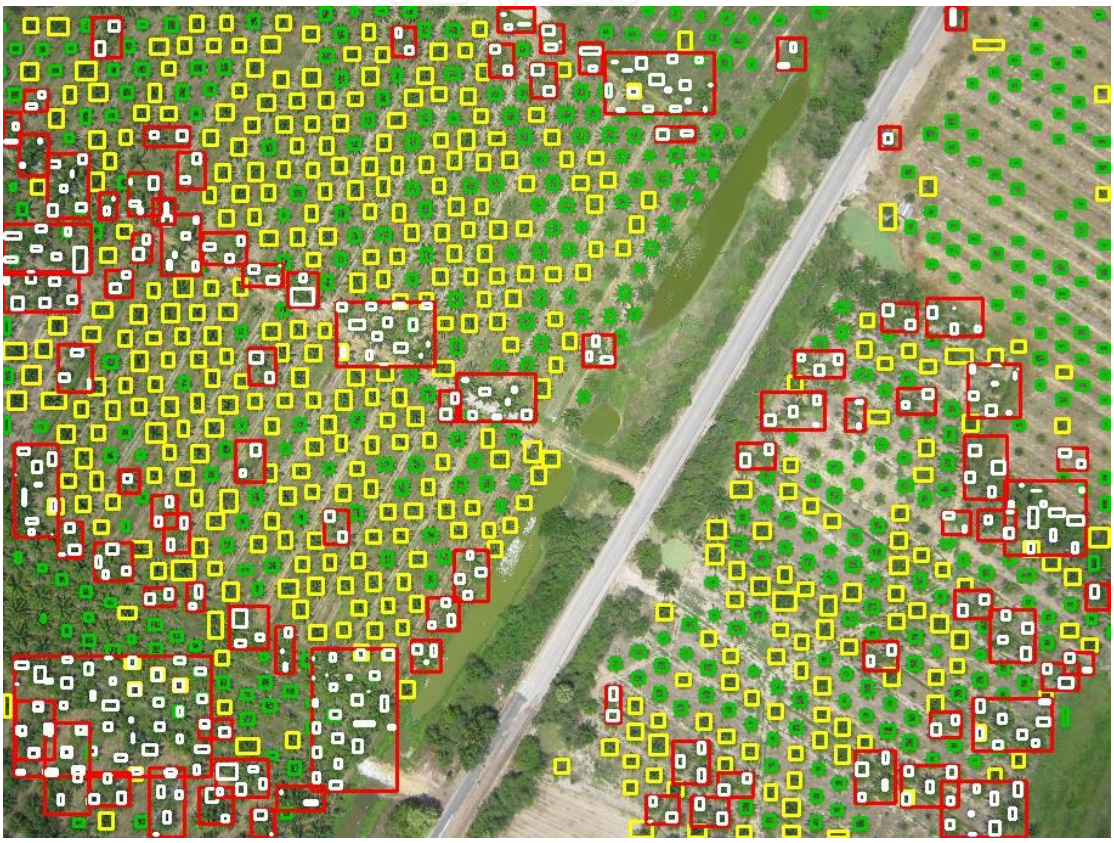

Figure 138 The result of multi-scale clustering from Figure 137 (b) including 525 small trees, 413 big trees, and 117 tree stands consist of 476 individual oil palms

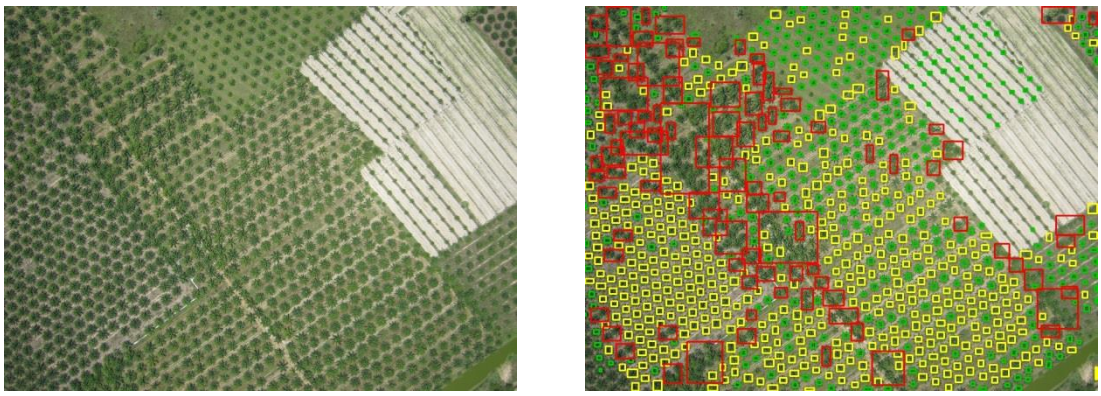

(a) (b)

Figure 139 (a) original aerial image and (b) the result from applying K-means clustering

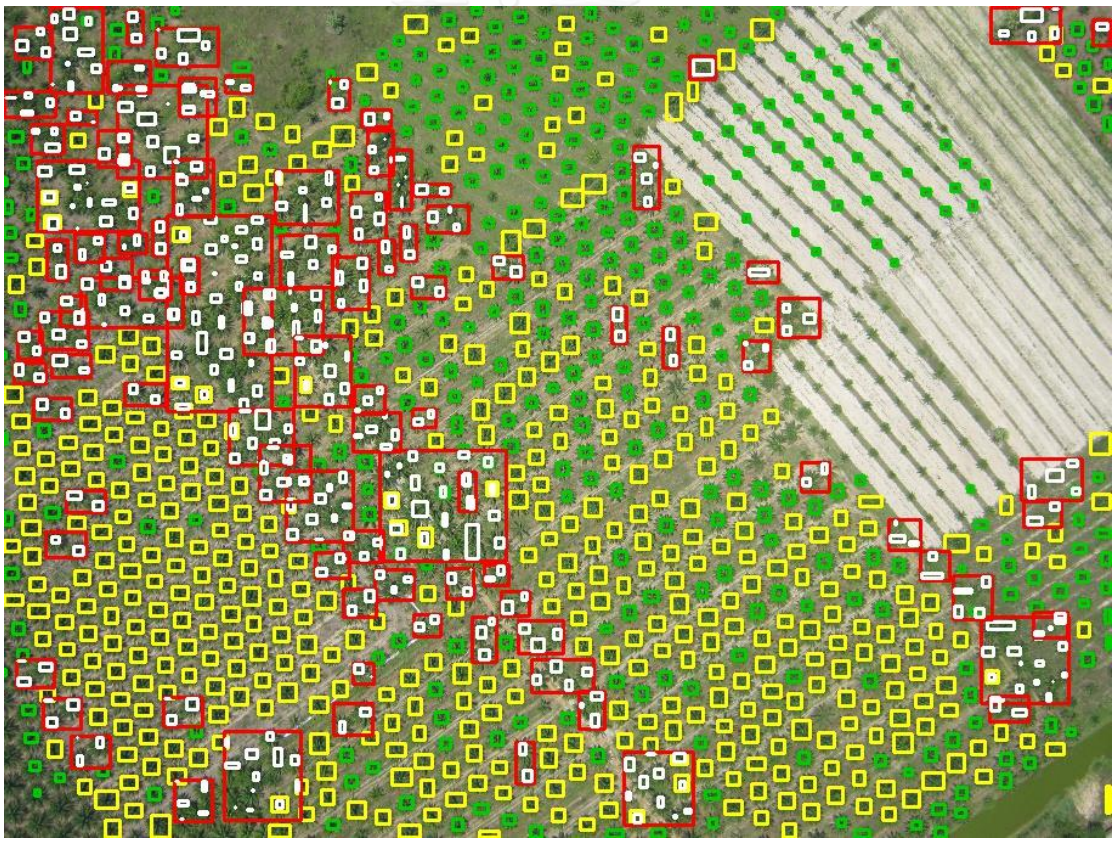

Figure 140 The result of multi-scale clustering from Figure 139 (b) including 358 small trees, 455 big trees, and 97 tree stands consist of 428 individual oil palms

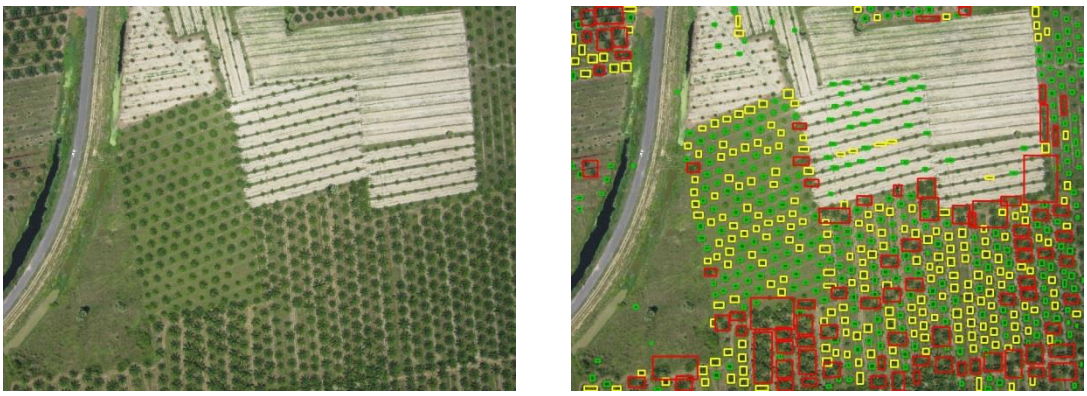

(a) (b)

Figure 141 (a) original aerial image and (b) the result from applying K-means clustering

Figure 142 The result of multi-scale clustering from Figure 141 (b) including 307 small trees, 224 big trees, and 84 tree stands consist of 222 individual oil palms

(a) (b)

Figure 143 (a) original aerial image and (b) the result from applying K-means clustering

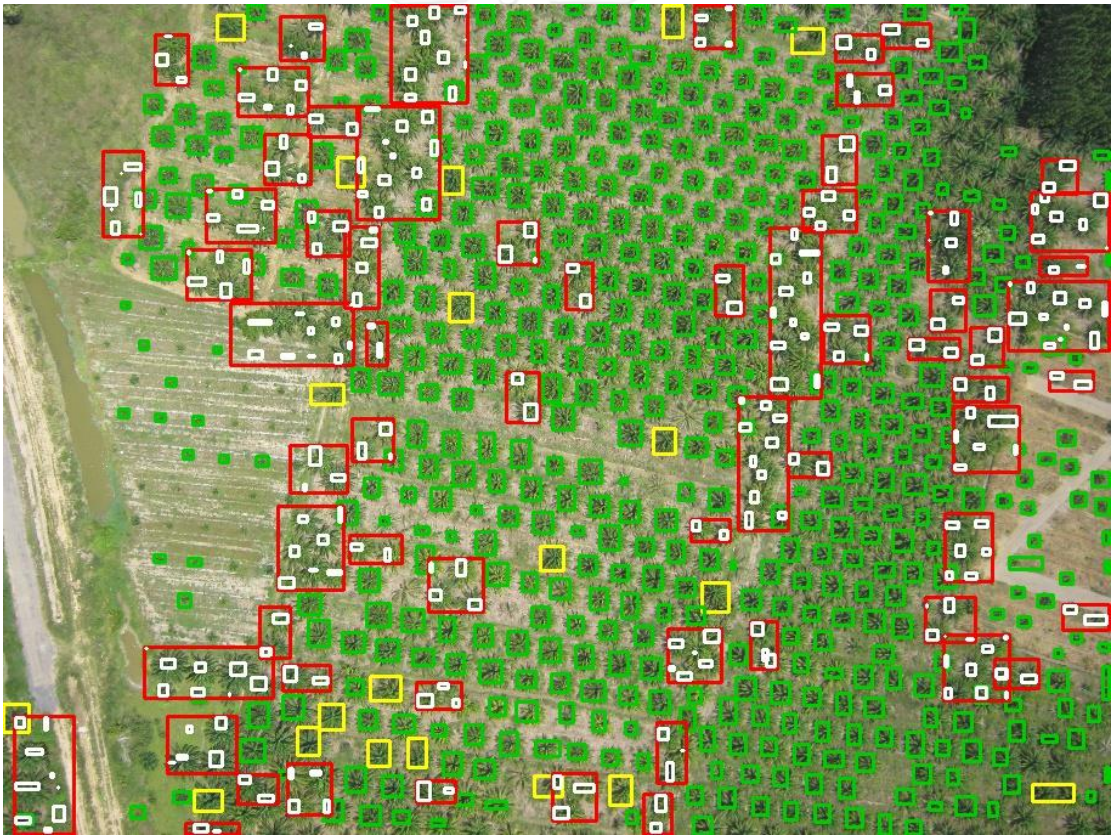

Figure 144 The result of multi-scale clustering from Figure 143 (b) including 498 small trees, 21 big trees, and 66 tree stands consist of 277 individual oil palms

(a) (b)

Figure 145 (a) original aerial image and (b) the result from applying K-means clustering

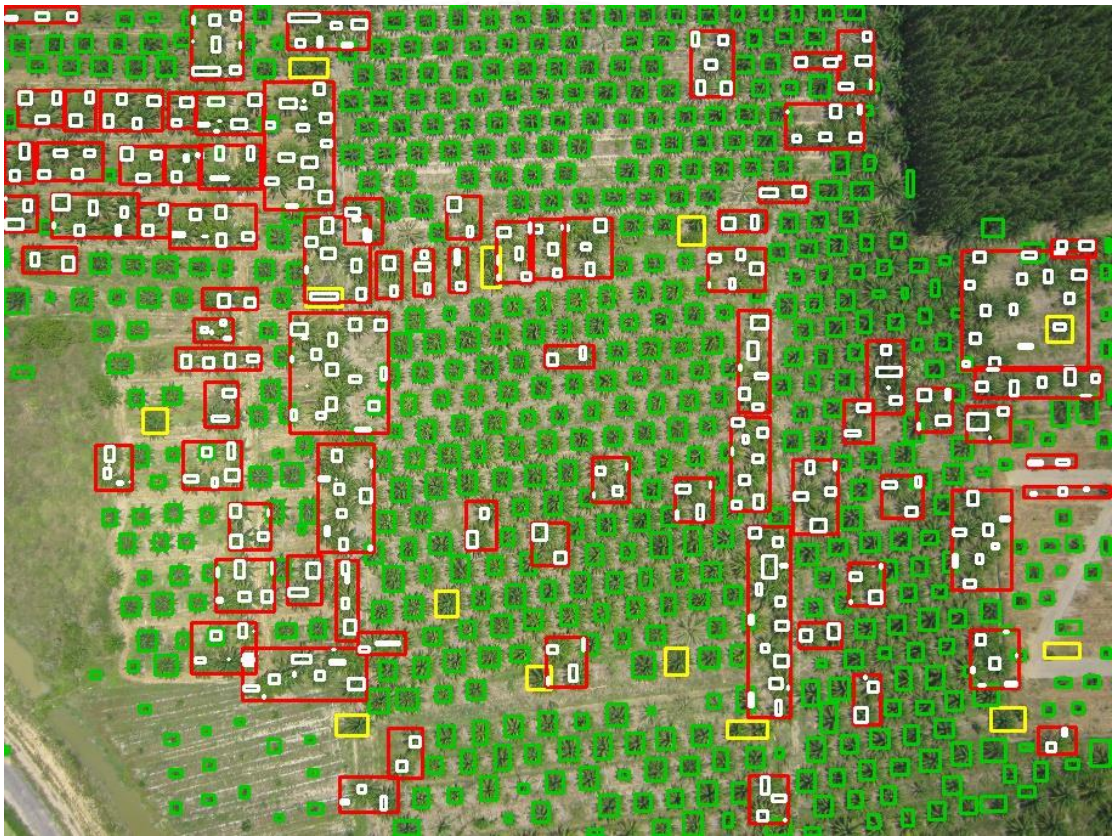

Figure 146 The result of multi-scale clustering from Figure 145 (b) including 550 small trees, 14 big trees, and 80 tree stands consist of 362 individual oil palms

(a) (b)

Figure 147 (a) original aerial image and (b) the result from applying K-means clustering

Figure 148 The result of multi-scale clustering from Figure 147 (b) including 344 small trees, 314 big trees, and 90 tree stands consist of 397 individual oil palms

(a) (b)

Figure 149 (a) original aerial image and (b) the result from applying K-means clustering

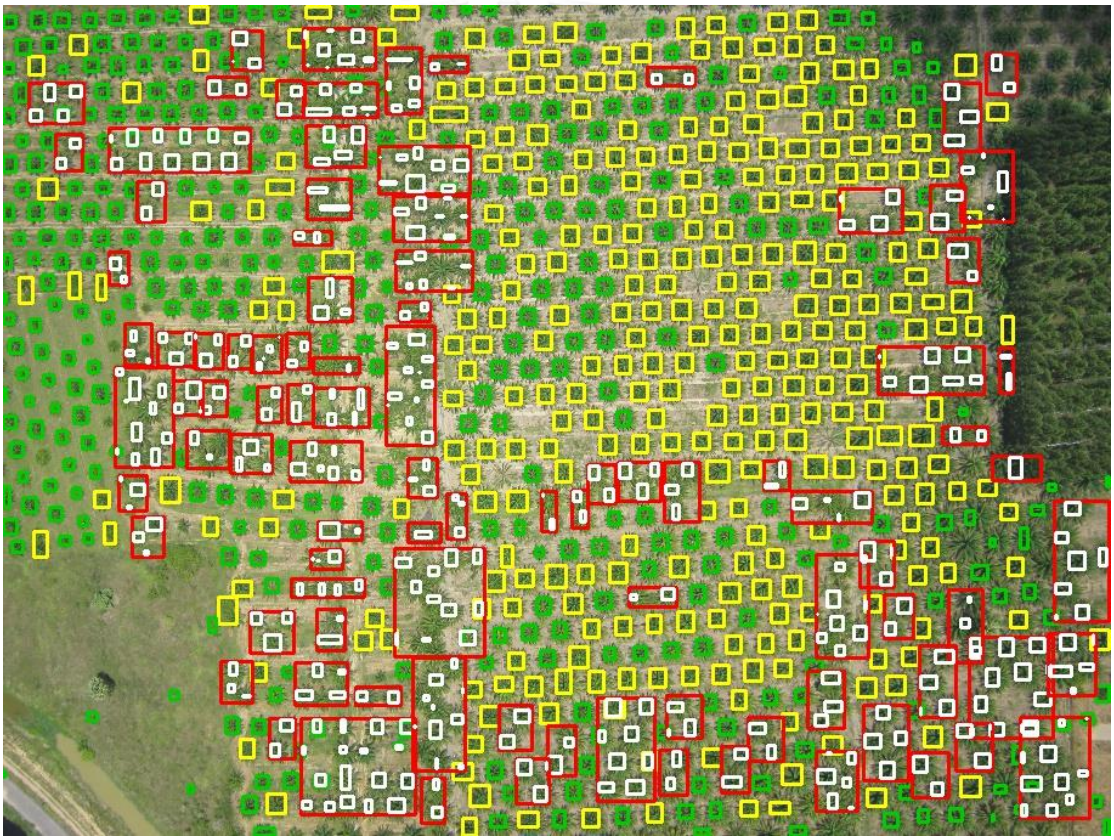

Figure 150 The result of multi-scale clustering from Figure 149 (b) including 354 small trees, 313 big trees, and 97 tree stands consist of 379 individual oil palms

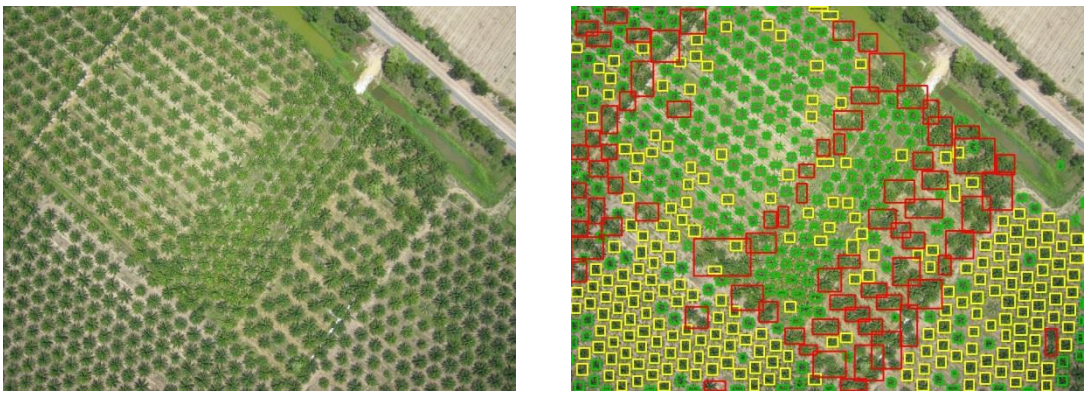

(a) (b)

Figure 151 (a) original aerial image and (b) the result from applying K-means clustering

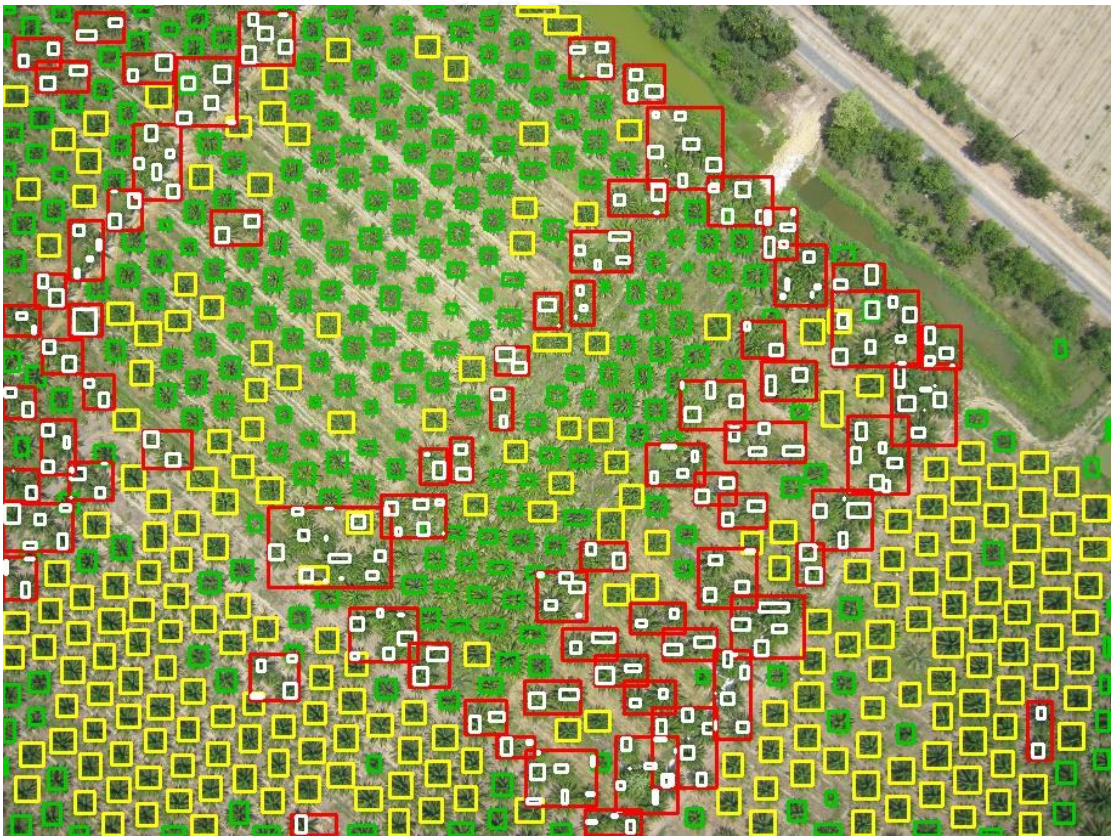

Figure 152 The result of multi-scale clustering from Figure 151 (b) including 281 small trees, 227 big trees, and 75 tree stands consist of 271 individual oil palms

(a) (b)

Figure 153 (a) original aerial image and (b) the result from applying K-means clustering

Figure 154 The result of multi-scale clustering from Figure 153 (b) including 133 small trees, 294 big trees, and 30 tree stands consist of 167 individual oil palms

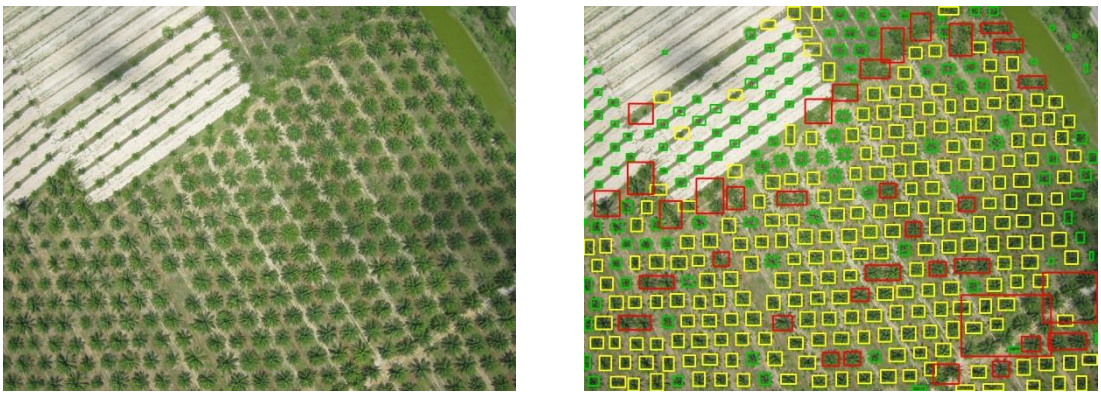

(a) (b)

Figure 155 (a) original aerial image and (b) the result from applying K-means clustering

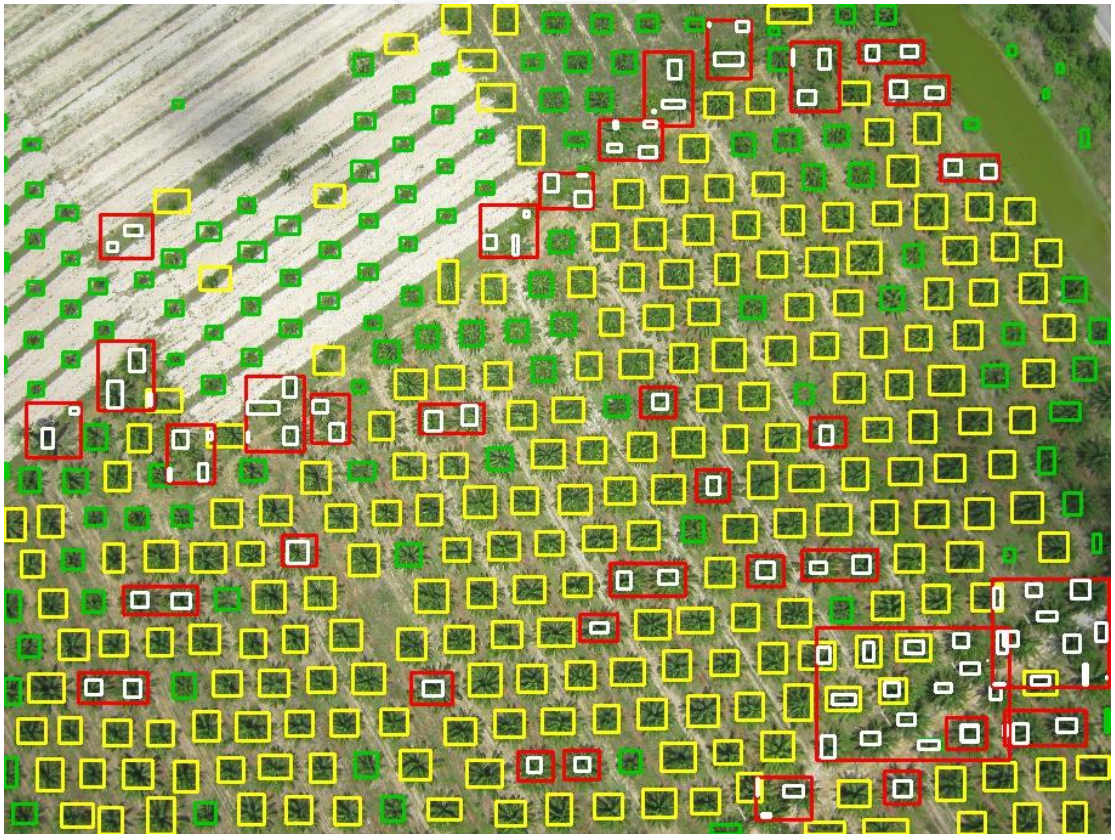

Figure 156 The result of multi-scale clustering from Figure 155 (b) including 132 small trees, 227 big trees, and 36 tree stands consist of 97 individual oil palms

VITA

Mr.Teerawut Wong-in was born on January 27th, 1982, in Nan, Thailand. He has got a Bachelor degree in Business Administration from Lampang Rajabhat University in 2004.